REPORT NO. FAA-RD-76-20 - II - A

AN ANALYSIS OF RADIO FREQUENCY SURVEILLANCE SYSTEMS FOR AIR TRAFFIC CONTROL
Volume II: Appendixes

Louis A. Kleiman

FEBRUARY 1976
FINAL REPORT

DOCUMENT IS AVAILABLE TO THE PUBLIC THROUGH THE NATIONAL TECHNICAL INFORMATION SERVICE, SPRINGFIELD, VIRGINIA 22161

Prepared for
U.S. DEPARTMENT OF TRANSPORTATION
FEDERAL AVIATION ADMINISTRATION
Systems Research and Development Service
Washington DC 20591

TECHNICAL REPORT STANDARD TITLE PAGE

1. Report No. 19

18 FAA-RD-76-20-Vol-2

2. Government Accession No.

3. Recipient's Catalog No.

4. Title and Subtitle

6 AN ANALYSIS OF RADIO FREQUENCY SURVEILLANCE SYSTEMS FOR AIR TRAFFIC CONTROL*

Volume II. Appendixes

5. Report Date

11 Feb[redacted]76

6. Performing Organization Code

7. Author(s)

10 Louis A. Kleiman

8. Performing Organization Report No.

14 [redacted]~~TSC~~-FAA-75-10-Vol-2

9. Performing Organization Name and Address

U.S. Department of Transportation
Transportation Systems Center
Kendall Square
Cambridge MA 02142

10. Work Unit No.

~~FA510/R6117~~

11. Contract or Grant No.

12. Sponsoring Agency Name and Address

U.S. Department of Transportation
Federal Aviation Administration
Systems Research and Development Service
Washington DC 20591

13. Type of Report and Period Covered

9 Final Report.
Sep[redacted]74 - May [redacted]75

14. Sponsoring Agency Code

15. Supplementary Notes

*This report is a doctoral thesis by the author.

12 75p.

16. Abstract

Performance criteria that afford quantitative evaluation of a variety of current and proposed configurations of the Air Traffic Control Radar Beacon System (ATCRBS) are described in detail. Two analytic system models are developed to allow application of these performance criteria. A simple system model, based on the assumption of a flat earth, enables closed-form analytic expressions for some of the performance criteria to be developed for a wide range of desired areas of coverage. An extremely accurate complex system model provides a tool for simulation of operating characteristics that would be observed in the course of actual flight tests. The complex model includes a new solution for the grazing angle of radiation over a spherical earth that is shown to be more accurate than the commonly-used solution of Fishback. Applications and limitations of both models in the evaluation of four new ATCRBS antennas and of the proposed receiver side-lobe suppression feature are discussed. Both numerical results and a computer-generated representation of an air traffic controller's display are presented.

17. Key Words

ATCRBS, Air Traffic Control, Radar Beacons, Surveillance, Radar, Propagation, Simulation

18. Distribution Statement

DOCUMENT IS AVAILABLE TO THE PUBLIC THROUGH THE NATIONAL TECHNICAL INFORMATION SERVICE, SPRINGFIELD, VIRGINIA 22161

19. Security Classif. (of this report)	20. Security Classif. (of this page)	21. No. of Pages	22. Price
Unclassified	Unclassified	76	

Form DOT F 1700.7 (8-69)

APPENDIX A

PROCEDURE TO DETERMINE A LEAST-SQUARES FIT FOR ANTENNA PATTERNS

In this appendix a procedure to fit a third-order polynomial to the voltage pattern $v(\theta)$ of an antenna is derived and described. Given the arbitrary pattern $v(\theta)$, the procedure determines those values of a, b, c, and d that minimize the sum of the squares of the differences between the actual value $v(\theta)$ and the value of the polynomial approximation

$$v'(\theta) = a + b\theta + c\theta^2 + d\theta^3 \tag{A.1}$$

at every point specified.

The value $v(\theta_i)$ of an antenna voltage pattern at an angle θ_i can be determined from its corresponding power pattern expressed in dB, $A_f(\theta_i)_{dB}$, by use of the following equation:

$$v(\theta_i) = \left\{10^{.1[A_f(\theta_i)_{dB}]}\right\}^{1/2} = 10^{.05[A_f(\theta_i)_{dB}]} \tag{A.2}$$

Since most antenna patterns with which this thesis is concerned are generally available in the form of $A_f(\theta_i)_{dB}$, equation (A.2) must generally be applied to obtain the voltage pattern required by Chapter 4.

Each row of the augmented matrix[22] contains the coefficients

of the unknowns a, b, c, and d, for a particular value of θ and for the corresponding value of $v(\theta)$:

$$\begin{bmatrix} 1 & \theta_1 & \theta_1^2 & \theta_1^3 & v(\theta_1) \\ 1 & \theta_2 & \theta_2^2 & \theta_2^3 & v(\theta_2) \\ & & \vdots & & \\ 1 & \theta_n & \theta_n^2 & \theta_n^3 & v(\theta_n) \end{bmatrix} \tag{A.3}$$

The n specified values of the antenna pattern to which the fit is to be made are generally chosen at equal intervals along the region of interest. The normal equations then become

$$n\,a + \sum_{i=1}^{n} \theta_i b + \sum_{i=1}^{n} \theta_i^2 c + \sum_{i=1}^{n} \theta_i^3 d = \sum_{i=1}^{n} v(\theta_i) \tag{A.4}$$

$$\sum_{i=1}^{n} \theta_i a + \sum_{i=1}^{n} \theta_i^2 b + \sum_{i=1}^{n} \theta_i^3 c + \sum_{i=1}^{n} \theta_i^4 d = \sum_{i=1}^{n} \theta_i v(\theta_i) \tag{A.5}$$

$$\sum_{i=1}^{n} \theta_i^2 a + \sum_{i=1}^{n} \theta_i^3 b + \sum_{i=1}^{n} \theta_i^4 c + \sum_{i=1}^{n} \theta_i^5 d = \sum_{i=1}^{n} \theta_i^2 v(\theta_i) \tag{A.6}$$

$$\sum_{i=1}^{n} \theta_i^3 a + \sum_{i=1}^{n} \theta_i^4 b + \sum_{i=1}^{n} \theta_i^5 c + \sum_{i=1}^{n} \theta_i^6 d = \sum_{i=1}^{n} \theta_i^3 v(\theta_i) \tag{A.7}$$

By making the substitutions

$$r_j = \sum_{i=1}^{n} \theta_i^j \tag{A.8}$$

and

$$s_k = \sum_{i=1}^{n} \theta_i^k v(\theta_i) \tag{A.9}$$

one arrives at the following normal equations:

$$n\,a + r_1 b + r_2 c + r_3 d = s_0 \tag{A.10}$$

$$r_1 a + r_2 b + r_3 c + r_4 d = s_1 \tag{A.11}$$

$$r_2 a + r_3 b + r_4 c + r_5 d = s_2 \tag{A.12}$$

$$r_3 a + r_4 b + r_5 c + r_6 d = s_3 \tag{A.13}$$

The determinant D of the matrix of coefficients of a, b, c, and d is

$$D = n\begin{vmatrix} r_2 & r_3 & r_4 \\ r_3 & r_4 & r_5 \\ r_4 & r_5 & r_6 \end{vmatrix} - r_1\begin{vmatrix} r_1 & r_3 & r_4 \\ r_2 & r_4 & r_5 \\ r_3 & r_5 & r_6 \end{vmatrix} + r_2\begin{vmatrix} r_1 & r_2 & r_4 \\ r_2 & r_3 & r_5 \\ r_3 & r_4 & r_6 \end{vmatrix} - r_3\begin{vmatrix} r_1 & r_2 & r_3 \\ r_2 & r_3 & r_4 \\ r_3 & r_4 & r_5 \end{vmatrix}$$

$$= n\left[r_2\,(r_4 r_6 - r_5^2) - r_3\,(r_3 r_6 - r_4 r_5) + r_4\,(r_3 r_5 - r_4^2)\right]$$

$$-r_1\left[r_1\,(r_4 r_6 - r_5^2) - r_3\,(r_2 r_6 - r_3 r_5) + r_4\,(r_2 r_5 - r_3 r_4)\right]$$

$$+r_2\left[r_1\,(r_3 r_6 - r_4 r_5) - r_2\,(r_2 r_6 - r_3 r_5) + r_4\,(r_2 r_4 - r_3^2)\right]$$

$$-r_3\left[r_1\,(r_3 r_5 - r_4^2) - r_2\,(r_2 r_5 - r_3 r_4) + r_3\,(r_2 r_4 - r_3^2)\right] \tag{A.14}$$

Thus, from Cramer's Rule, the solutions for the unknown parameters are found to be

$$aD = s_0\begin{vmatrix} r_2 & r_3 & r_4 \\ r_3 & r_4 & r_5 \\ r_4 & r_5 & r_6 \end{vmatrix} - r_1\begin{vmatrix} s_1 & r_3 & r_4 \\ s_2 & r_4 & r_5 \\ s_3 & r_5 & r_6 \end{vmatrix} + r_2\begin{vmatrix} s_1 & r_2 & r_4 \\ s_2 & r_3 & r_5 \\ s_3 & r_4 & r_6 \end{vmatrix} - r_3\begin{vmatrix} s_1 & r_2 & r_3 \\ s_2 & r_3 & r_4 \\ s_3 & r_4 & r_5 \end{vmatrix} \quad \text{(A.15)}$$

$$\begin{aligned} a = \frac{1}{D}\Big\{ & s_0\left[r_2\ (r_4r_6 - r_5^2) - r_3\ (r_3r_6 - r_4r_5) + r_4\ (r_3r_5 - r_4^2)\right] \\ & -r_1\left[s_1\ (r_4r_6 - r_5^2) - r_3\ (s_2r_6 - s_3r_5) + r_4\ (s_2r_5 - s_3r_4)\right] \\ & +r_2\left[s_1\ (r_3r_6 - r_4r_5) - r_2\ (s_2r_6 - s_3r_5) + r_4\ (s_2r_4 - r_3s_3)\right] \\ & -r_3\left[s_1\ (r_3r_5 - r_4^2) - r_2\ (s_2r_5 - s_3r_4) + r_3\ (s_2r_4 - s_3r_3)\right]\Big\} \end{aligned}$$

(A.16)

$$bD = n\begin{vmatrix} s_1 & r_3 & r_4 \\ s_2 & r_4 & r_5 \\ s_3 & r_5 & r_6 \end{vmatrix} - s_0\begin{vmatrix} r_1 & r_3 & r_4 \\ r_2 & r_4 & r_5 \\ r_3 & r_5 & r_6 \end{vmatrix} + r_2\begin{vmatrix} r_1 & s_1 & r_4 \\ r_2 & s_2 & r_5 \\ r_3 & s_3 & r_6 \end{vmatrix} - r_3\begin{vmatrix} r_1 & s_1 & r_3 \\ r_2 & s_2 & r_4 \\ r_3 & s_3 & r_5 \end{vmatrix} \quad \text{(A.17)}$$

$$\begin{aligned} b = \frac{1}{D}\Big\{ & n\left[s_1\ (r_4r_6 - r_5^2) - r_3\ (s_2r_6 - s_3r_5) + r_4\ (s_2r_5 - s_3r_4)\right] \\ & -s_0\left[r_1\ (r_4r_6 - r_5^2) - r_3\ (r_2r_6 - r_3r_5) + r_4\ (r_2r_5 - r_3r_4)\right] \\ & +r_2\left[r_1\ (s_2r_6 - s_3r_5) - s_1\ (r_2r_6 - r_3r_5) + r_4\ (r_2s_3 - s_2r_3)\right] \\ & -r_3\left[r_1\ (s_2r_5 - s_3r_4) - s_1\ (r_2r_5 - r_3r_4) + r_3\ (r_2s_3 - s_2r_3)\right]\Big\} \end{aligned}$$

(A.18)

$$cD = n\begin{vmatrix} r_2 & s_1 & r_4 \\ r_3 & s_2 & r_5 \\ r_4 & s_3 & r_6 \end{vmatrix} - r_1\begin{vmatrix} r_1 & s_1 & r_4 \\ r_2 & s_2 & r_5 \\ r_3 & s_3 & r_6 \end{vmatrix} + s_0\begin{vmatrix} r_1 & r_2 & r_4 \\ r_2 & r_3 & r_5 \\ r_3 & r_4 & r_6 \end{vmatrix} - r_3\begin{vmatrix} r_1 & r_2 & s_1 \\ r_2 & r_3 & s_2 \\ r_3 & r_4 & s_3 \end{vmatrix} \tag{A.19}$$

$$\begin{aligned} c = \frac{1}{D}\Big\{ & n\left[r_2\ (s_2r_6 - s_3r_5) - s_1\ (r_3r_6 - r_4r_5) + r_4\ (r_3s_3 - s_2r_4)\right] \\ & -r_1\left[r_1\ (s_2r_6 - s_3r_5) - s_1\ (r_2r_6 - r_3r_5) + r_4\ (r_2s_3 - r_3s_2)\right] \\ & +s_0\left[r_1\ (r_3r_6 - r_4r_5) - r_2\ (r_2r_6 - r_3r_5) + r_4\ (r_2r_4 - r_3^2)\right] \\ & -r_3\left[r_1\ (r_3s_3 - s_2r_4) - r_2\ (r_2s_3 - s_2r_3) + s_1\ (r_2r_4 - r_3^2)\right]\Big\} \end{aligned} \tag{A.20}$$

$$dD = n\begin{vmatrix} r_2 & r_3 & s_1 \\ r_3 & r_4 & s_2 \\ r_4 & r_5 & s_3 \end{vmatrix} - r_1\begin{vmatrix} r_1 & r_3 & s_1 \\ r_2 & r_4 & s_2 \\ r_3 & r_5 & s_3 \end{vmatrix} + r_2\begin{vmatrix} r_1 & r_2 & s_1 \\ r_2 & r_3 & s_2 \\ r_3 & r_4 & s_3 \end{vmatrix} - s_0\begin{vmatrix} r_1 & r_2 & r_3 \\ r_2 & r_3 & r_4 \\ r_3 & r_4 & r_5 \end{vmatrix} \tag{A.21}$$

$$\begin{aligned} d = \frac{1}{D}\Big\{ & n\left[r_2\ (r_4s_3 - s_2r_5) - r_3\ (r_3s_3 - s_2r_4) + s_1\ (r_3r_5 - r_4^2)\right] \\ & -r_1\left[r_1\ (r_4s_3 - s_2r_5) - r_3\ (r_2s_3 - s_2r_3) + s_1\ (r_2r_5 - r_3r_4)\right] \\ & +r_2\left[r_1\ (r_3s_3 - s_2r_4) - r_2\ (r_2s_3 - s_2r_3) + s_1\ (r_2r_4 - r_3^2)\right] \\ & -s_0\left[r_1\ (r_3r_5 - r_4^2) - r_2\ (r_2r_5 - r_3r_4) + r_3\ (r_2r_4 - r_3^2)\right]\Big\} \end{aligned} \tag{A.22}$$

Given an antenna power pattern expressed in decibels, equations (A.2), (A.8), (A.9), (A.14), (A.16), (A.18), (A.20), and (A.22) are sufficient to determine the polynomial approximation (A.1) to the voltage pattern.

APPENDIX B

DERIVATION OF MAGNITUDE AND PHASE OF THE COMPLEX REFLECTION COEFFICIENT

In this appendix expressions for the magnitude C_r and the phase δ of the complex reflection coefficient $C_R e^{j\delta}$ are derived. Beginning with equations (5.11) and (5.12),

$$C_R e^{j\delta} = \frac{n^2 \sin\psi - [n^2 - \cos^2\psi]^{1/2}}{n^2 \sin\psi + [n^2 - \cos^2\psi]^{1/2}} \qquad \text{(B.1)}$$

and

$$n^2 = \varepsilon_r - jK \qquad \text{(B.2)}$$

one may insert the latter into the former to obtain

$$C_R e^{j\delta} = \frac{\varepsilon_r \sin\psi - jK\sin\psi - \left[\varepsilon_r - \cos^2\psi - jK\right]^{1/2}}{\varepsilon_r \sin\psi - jK\sin\psi + \left[\varepsilon_r - \cos^2\psi - jK\right]^{1/2}} \qquad \text{(B.3)}$$

Next, the following substitution may be made:

$$\left[\varepsilon_r - \cos^2\psi - jK\right]^{1/2} = [S + jT]^{1/2} \qquad \text{(B.4)}$$

where

$$S = \varepsilon_r - \cos^2\psi \qquad \text{(B.5)}$$

and

$$T = -K \qquad \text{(B.6)}$$

But it is also known that

$$[S + jT]^{1/2} = \left[Ve^{j\alpha}\right]^{1/2} = [V]^{1/2}\cos(\alpha/2) + j[V]^{1/2}\sin(\alpha/2) \qquad \text{(B.7)}$$

where

$$V = \left[S^2 + T^2\right]^{1/2} \tag{B.8}$$

and

$$\alpha = \tan^{-1}(T/S) \tag{B.9}$$

Thus, from (B.4), (B.7), (B.8), and (B.9),

$$\left[\varepsilon_r - \cos^2 \ - jK\right]^{1/2} = \left[S^2 + T^2\right]^{1/4} \cos\left(\frac{1}{2}\tan^{-1}\left(\frac{T}{S}\right)\right)$$

$$+\ j\left[S^2 + T^2\right]^{1/4} \sin\left(\frac{1}{2}\tan^{-1}\left(\frac{T}{S}\right)\right) \tag{B.10}$$

Substituting (B.10) into (B.3) one obtains

$$C_R e^{j\delta} = \frac{\left\{\varepsilon_r \sin\psi - \left[S^2+T^2\right]^{1/4}\cos\left(\frac{1}{2}\tan^{-1}\left(\frac{T}{S}\right)\right)\right\} + j\left\{-K\sin\psi - \left[S^2+T^2\right]^{1/4}\sin\left(\frac{1}{2}\tan^{-1}\left(\frac{T}{S}\right)\right)\right\}}{\left\{\varepsilon_r \sin\psi + \left[S^2+T^2\right]^{1/4}\cos\left(\frac{1}{2}\tan^{-1}\left(\frac{T}{S}\right)\right)\right\} + j\left\{-K\sin\psi + \left[S^2+T^2\right]^{1/4}\sin\left(\frac{1}{2}\tan^{-1}\left(\frac{T}{S}\right)\right)\right\}} \tag{E.11}$$

But equation (B.11) is of the form

$$C_R e^{j\delta} = \frac{W + jX}{Y + jZ} = \frac{\left[W^2 + X^2\right]^{1/2} e^{j\tan^{-1}(X/W)}}{\left[Y^2 + Z^2\right]^{1/2} e^{j\tan^{-1}(Z/Y)}}$$

$$= \left[\frac{W^2 + X^2}{Y^2 + Z^2}\right]^{1/2} e^{j\left[\tan^{-1}(X/W) - \tan^{-1}(Z/Y)\right]} \tag{B.12}$$

Finally, by inspection of (B.12), the following expressions may be written:

$$C_R = \left[\frac{W^2 + X^2}{Y^2 + Z^2}\right]^{1/2} \tag{B.13}$$

$$\delta = \tan^{-1}(X/W) - \tan^{-1}(Z/Y) \tag{B.14}$$

The expressions for W, X, Y, and Z can be determined from inspection of equation (B.11) and are included in the body of the thesis as equations (5.16) through (5.19), respectively.

APPENDIX C

RADIATION PATTERNS USED IN APPLICATIONS OF THE MODELS

The data used to prepare radiations patterns for use by the CDC 6600 computer were obtained from factory test patterns prepared by the individual manufacturers of the antennas. Patterns for the standard antenna[23], the Hazeltine open array antenna[24], the ARSR-2 beacon feed modification of Texas Instruments[25,26], TI's separate rotator antenna[27,28], and the separate rotator of Westinghouse[29], were tabulated at regular intervals, typically every one or two degrees. The horizontal patterns used were those measured at the elevation of the maximum directivity of the antenna, while vertical patterns were extracted from the ones measured at an azimuth of 0^{o}.

The radiation patterns used as inputs to the complex simulation model were, for the most part, obtained by regular tabulation of the points in the measured data, and by linear interpolation between the tabulated points. Near the boresight of the horizontal patterns, however, and in the vicinity of the horizon for vertical patterns, a least-squares fit to the measured data was effected in order to preserve the smoothness of the curves in these critical areas. In those portions of the curves that follow where a least-squares fit was used, the individual points to which the curve was fit are denoted by squares. Generally, the curves pass through the points, indicating a close fit.

The plots of radiation patterns that follow as Figures C.1 through C.41 are grouped by antenna manufacturer, beginning with plots of the standard antenna and its associated omnidirectional antennas. The standard FA-8043 antenna has both a terminal omni, called the FA-8044, and an en route omni, the FA-8045, with a special bracket used for mounting the omni in the top of the en route ARSR radome. Two plots of each directional antenna in the azimuthal plane are included. The first is a complete azimuth plot from -180° to $+180^{\circ}$. The second plot is restricted to cover the region from -12° to $+12^{\circ}$ in order to show detail in the vicinity of antenna boresight. Two plots in azimuth for the uplink (1030 MHz) are followed by the corresponding downlink patterns (1090 MHz). Next, the uplink and downlink patterns for the directional antenna are shown.

Except for the two omnidirectional antennas associated with the standard FA-8043 antenna, the directional antenna patterns are followed by their respective omni patterns, first the uplink azimuth pattern, then the uplink elevation pattern. The FA-8044 and FA-8045 omnidirectional antennas have such uniform patterns in azimuth that their plots have been omitted. Rather, it is assumed that the FA-8044 and FA-8045 each have no attenuation at any azimuth. Downlink radiation patterns for the omni antennas are assumed to be equal to the uplink patterns. The downlink patterns are used, of course, in the RSLS investigations. The last plot is an ideal elevation pattern with no attenuation above

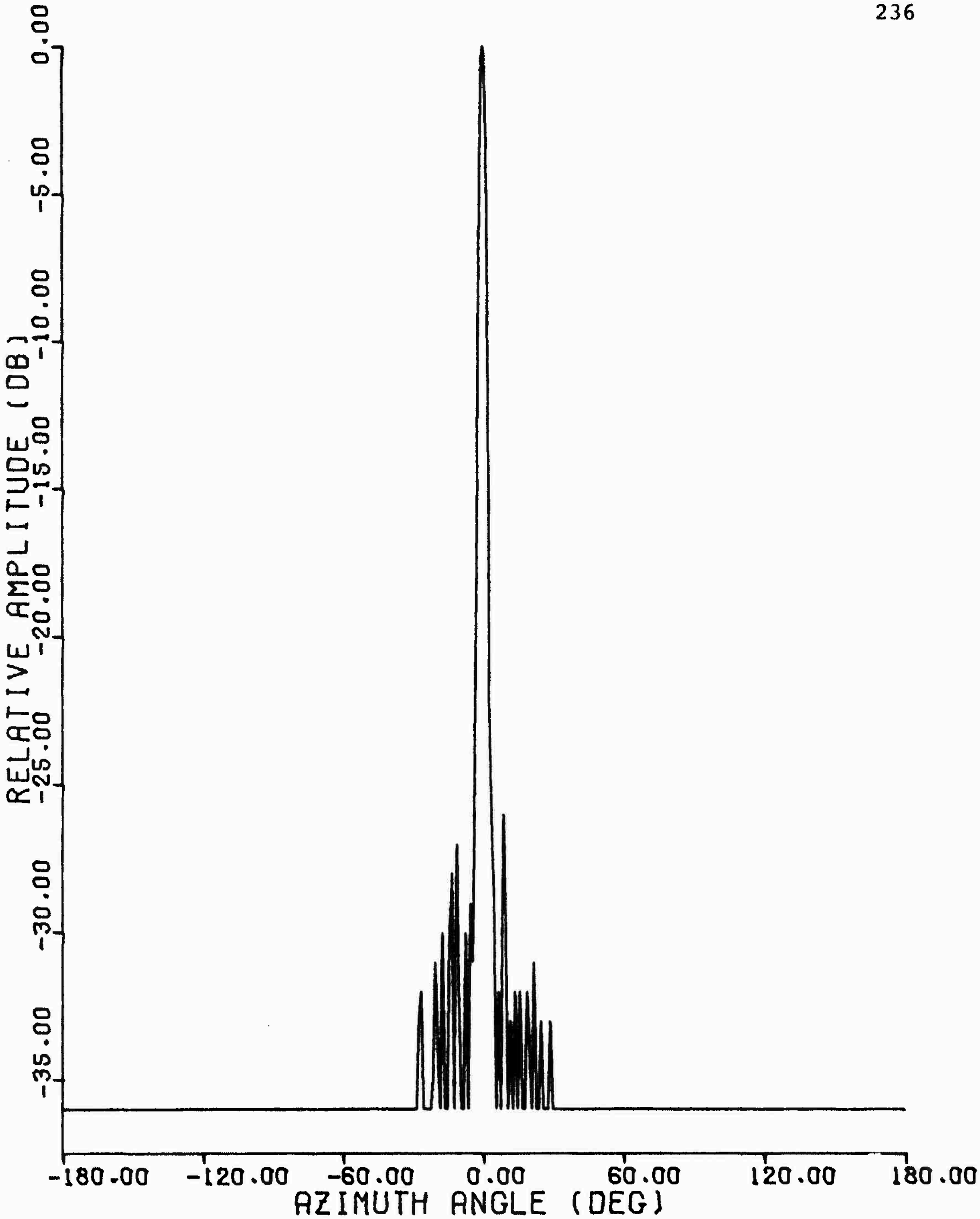

Figure C.1 1030 MHz Azimuth Pattern, FA-8043 Antenna, -180° to $+180^{\circ}$

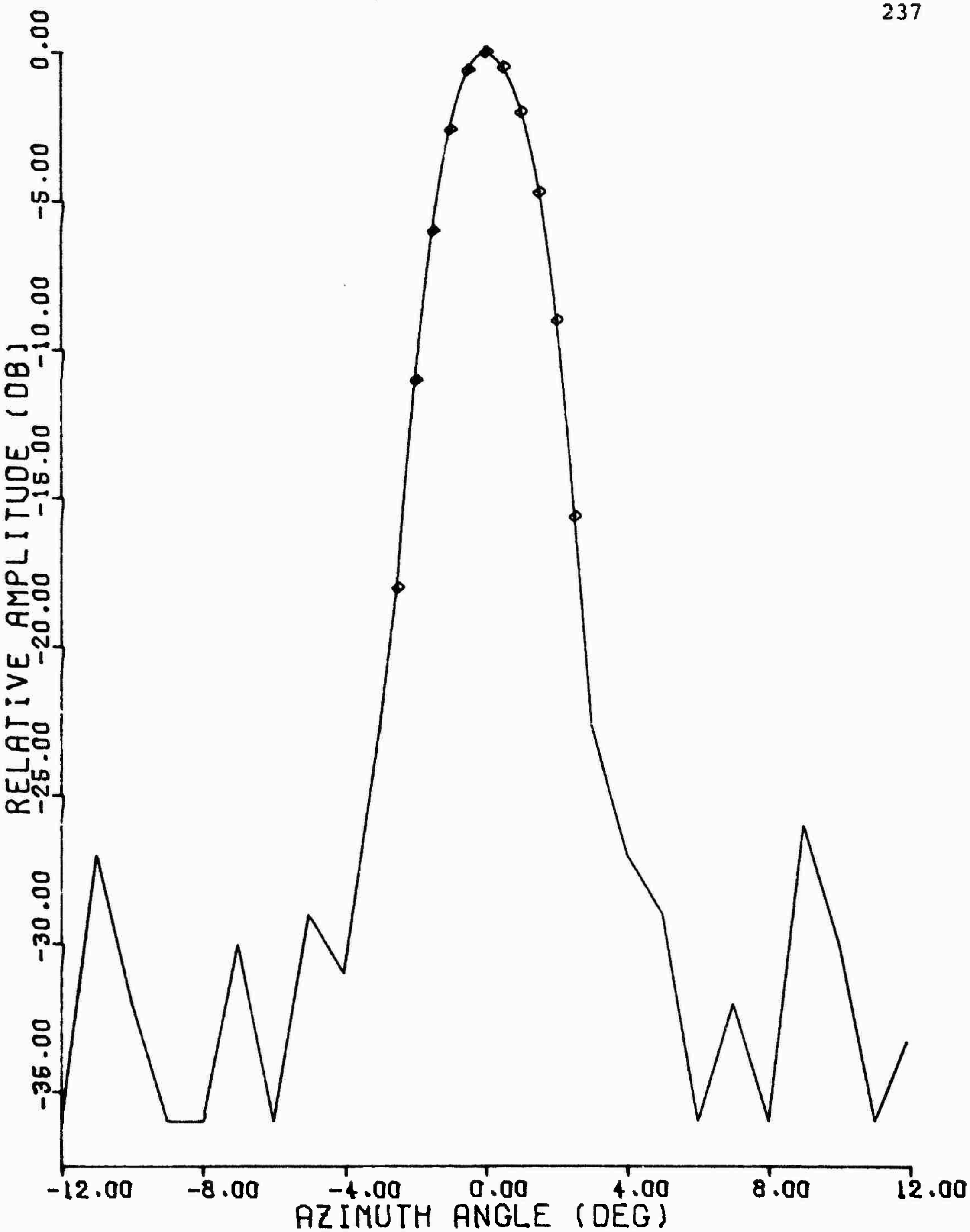

Figure C.2 1030 MHz Azimuth Pattern, FA-8043 Antenna, -12° to +12°

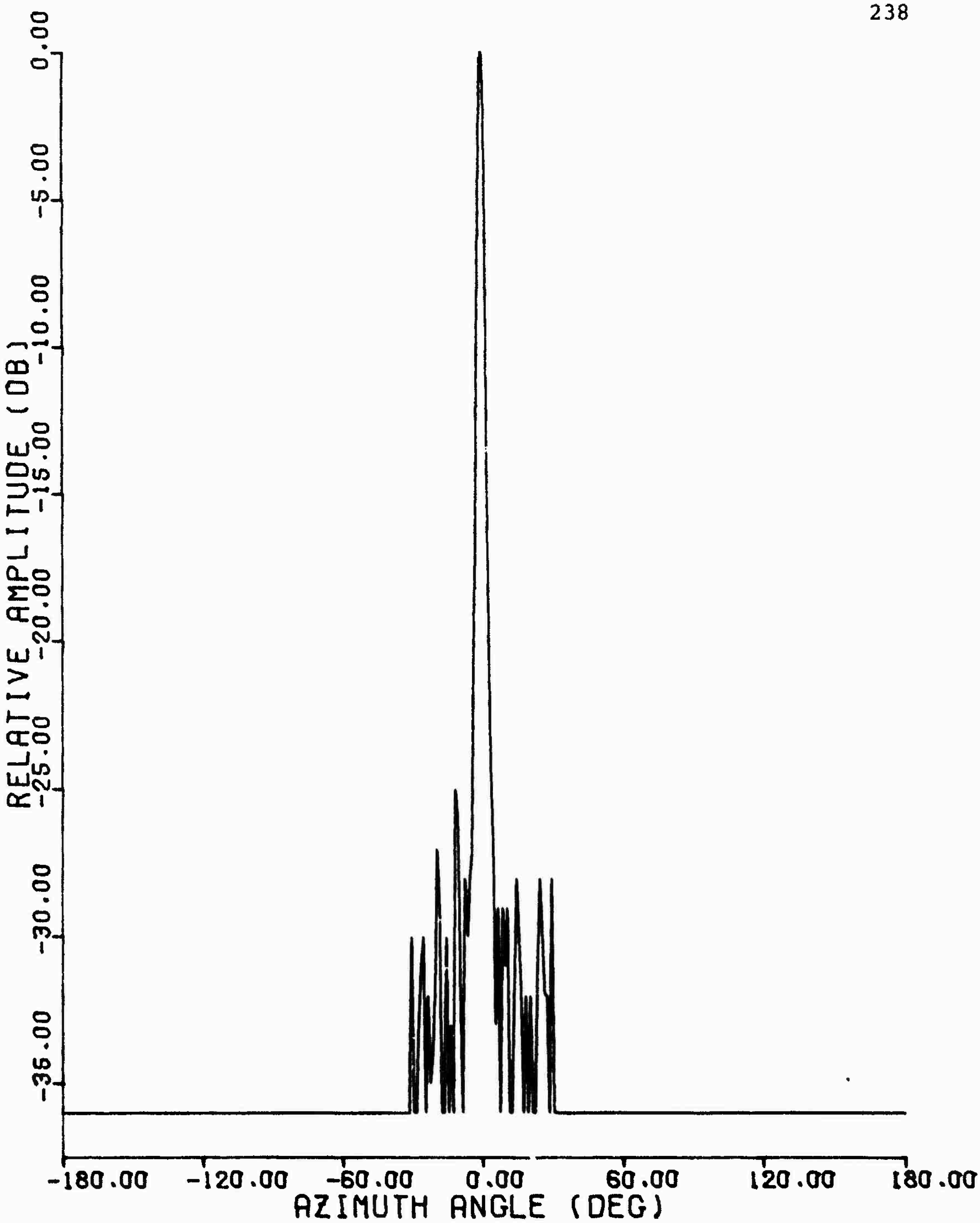

Figure C.3 1090 MHz Azimuth Pattern, FA-8043 Antenna, -180° to $+180^{\circ}$.

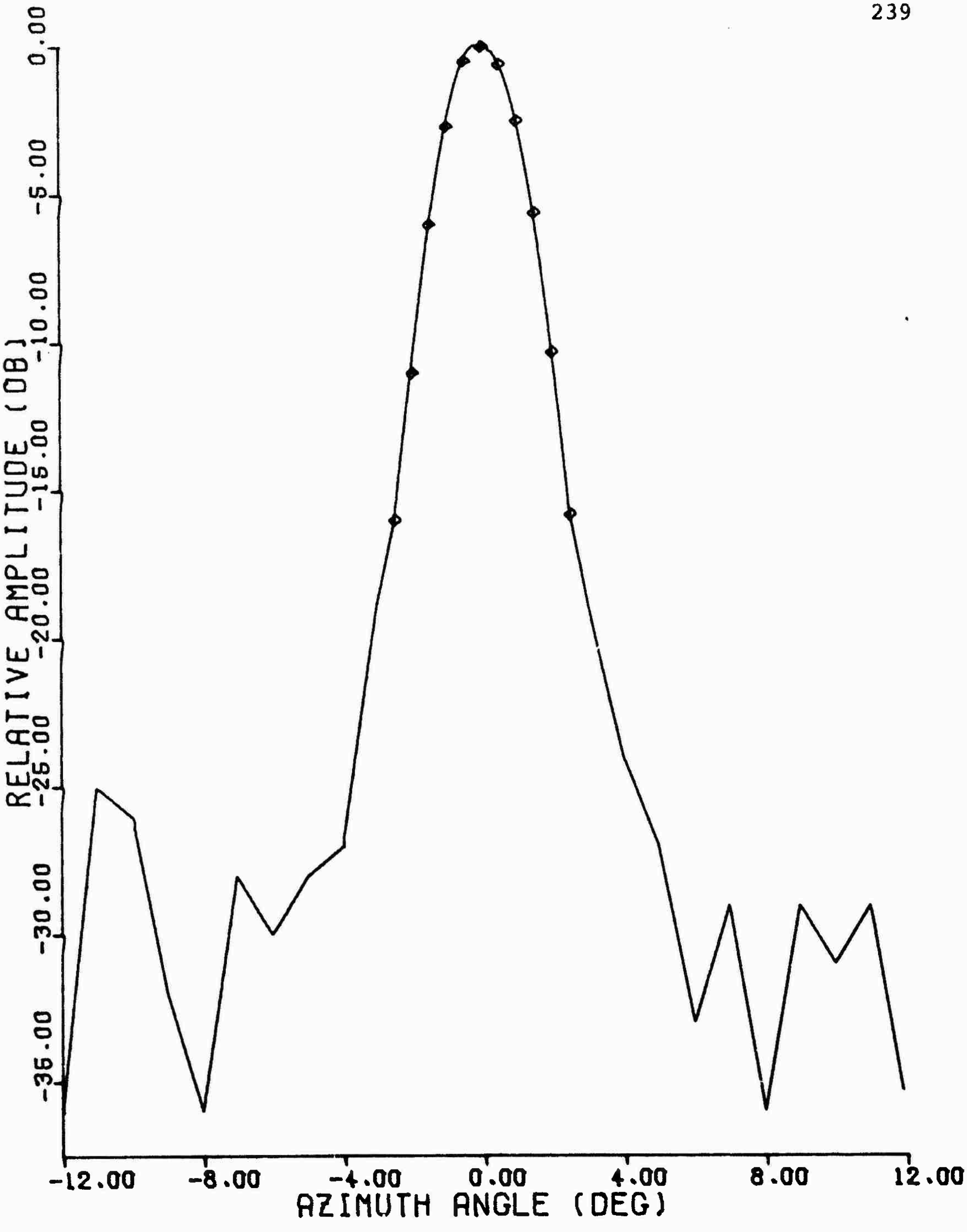

Figure C.4 1090 MHz Azimuth Pattern, FA-8043 Antenna, -12^{o} to $+12^{o}$

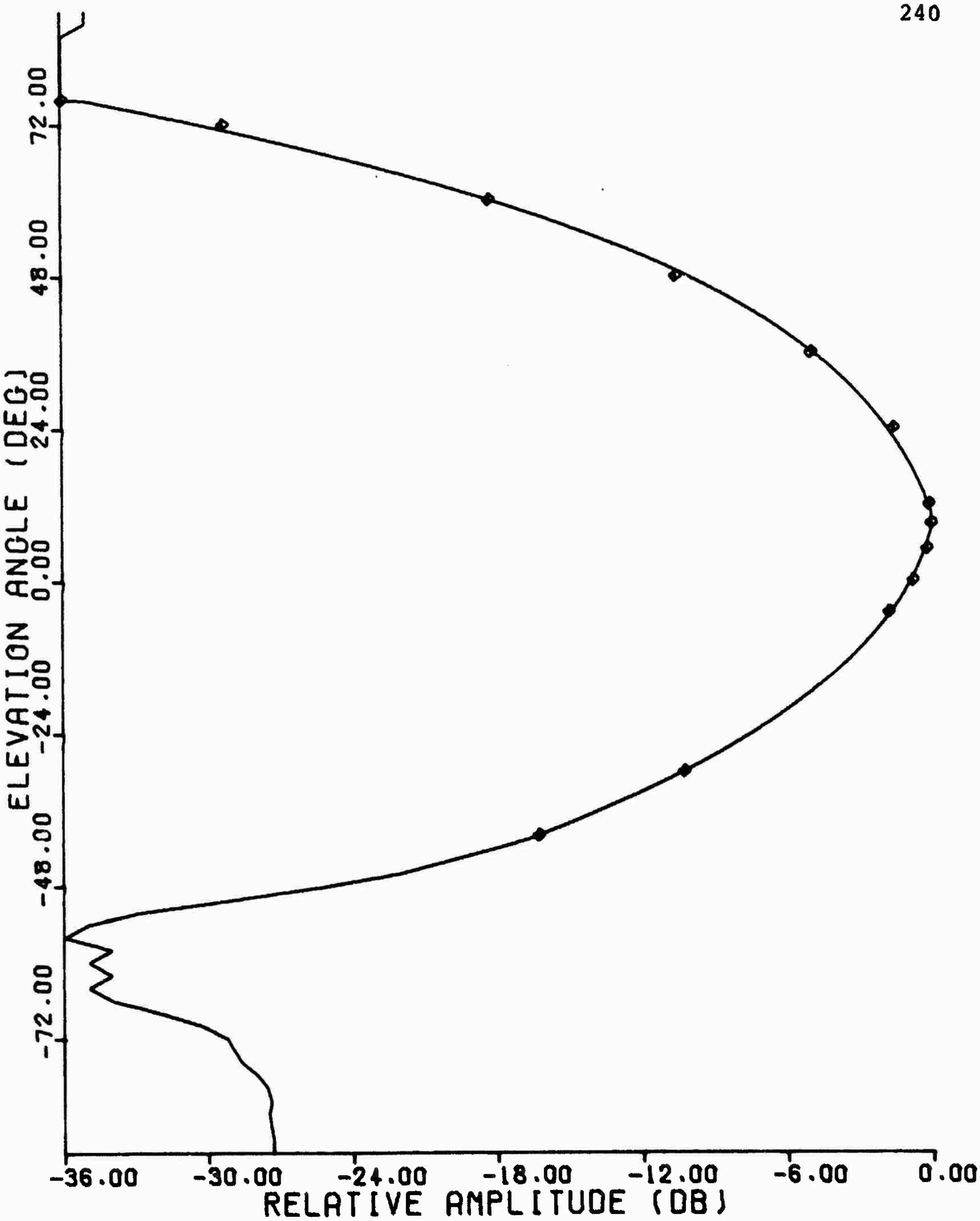

Figure C.5 1030 MHz Elevation Pattern, FA-8043 Antenna

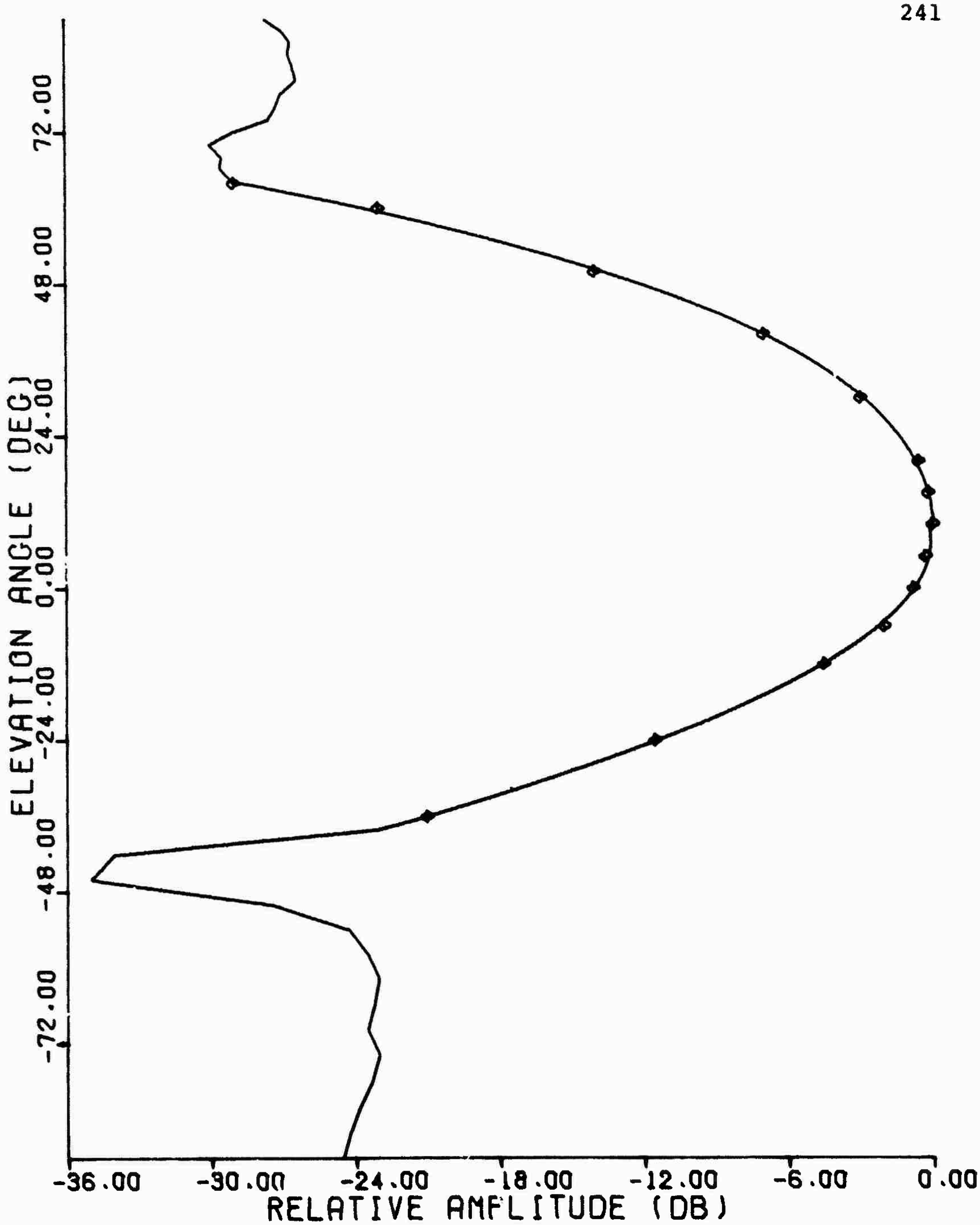

Figure C.6 1090 MHz Elevation Pattern, FA-8043 Antenna

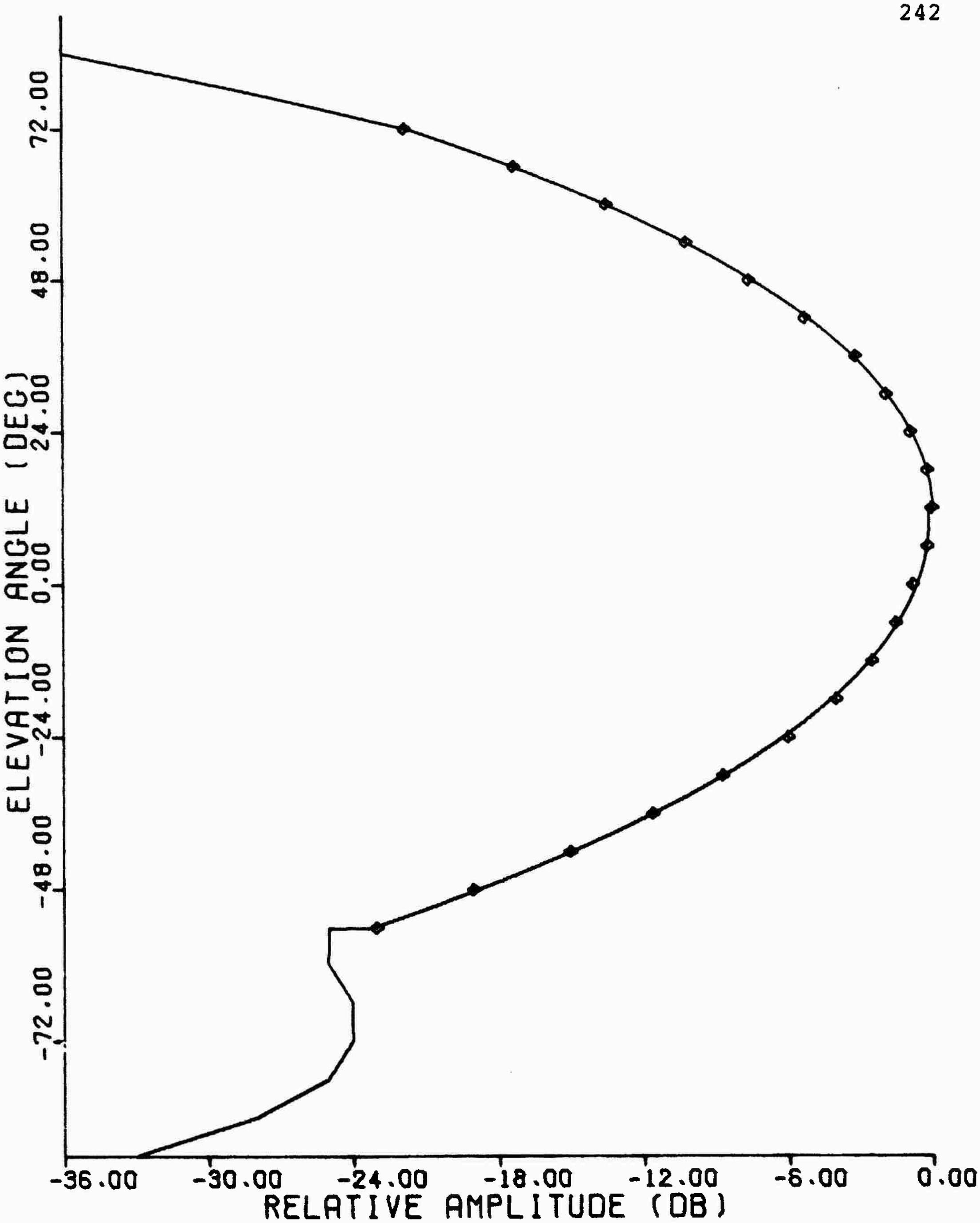

Figure C.7 1030 MHz Elevation Pattern, FA-8044 Antenna

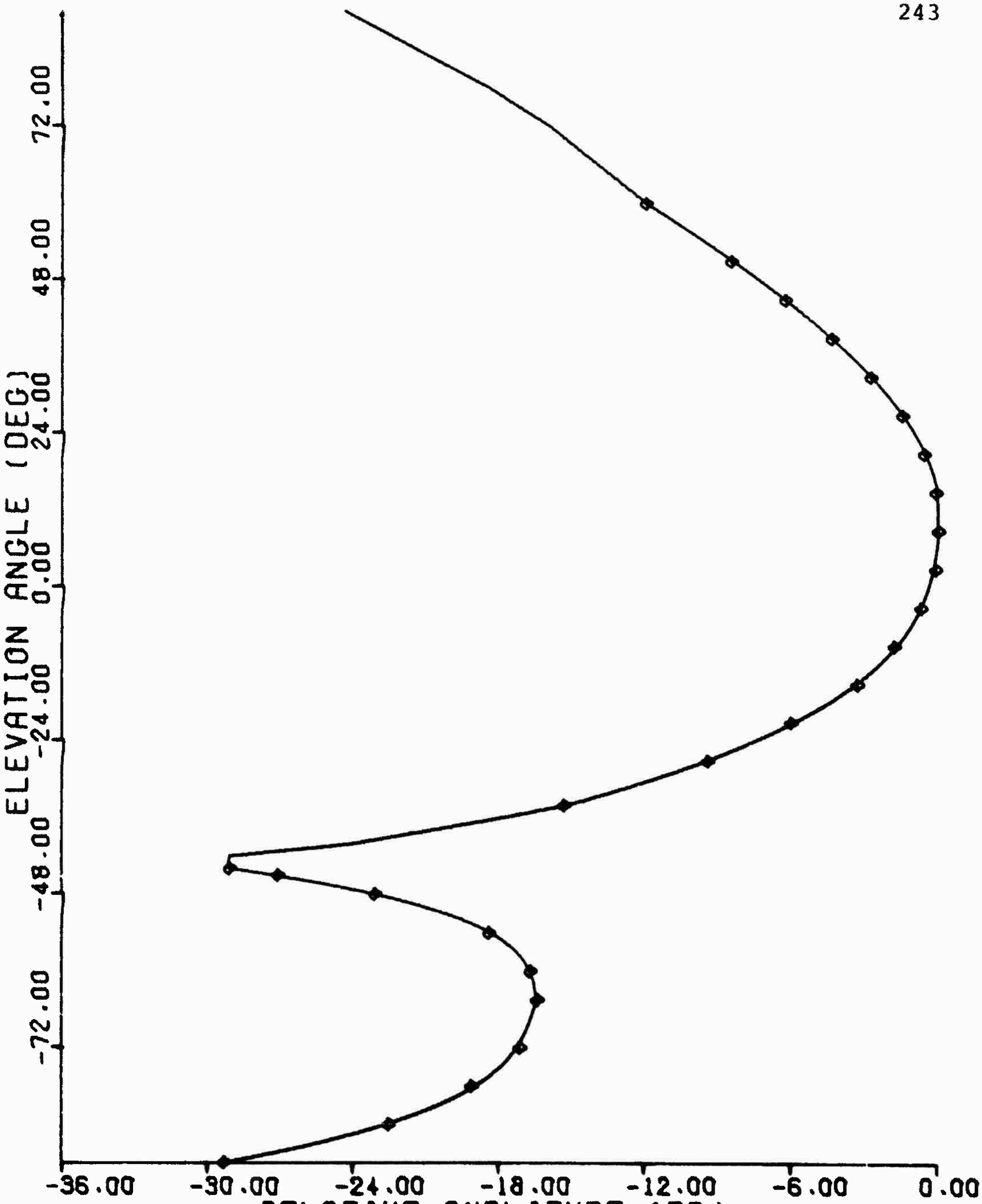

Figure C.8 1030 MHz Elevation Pattern, FA-8045 Antenna

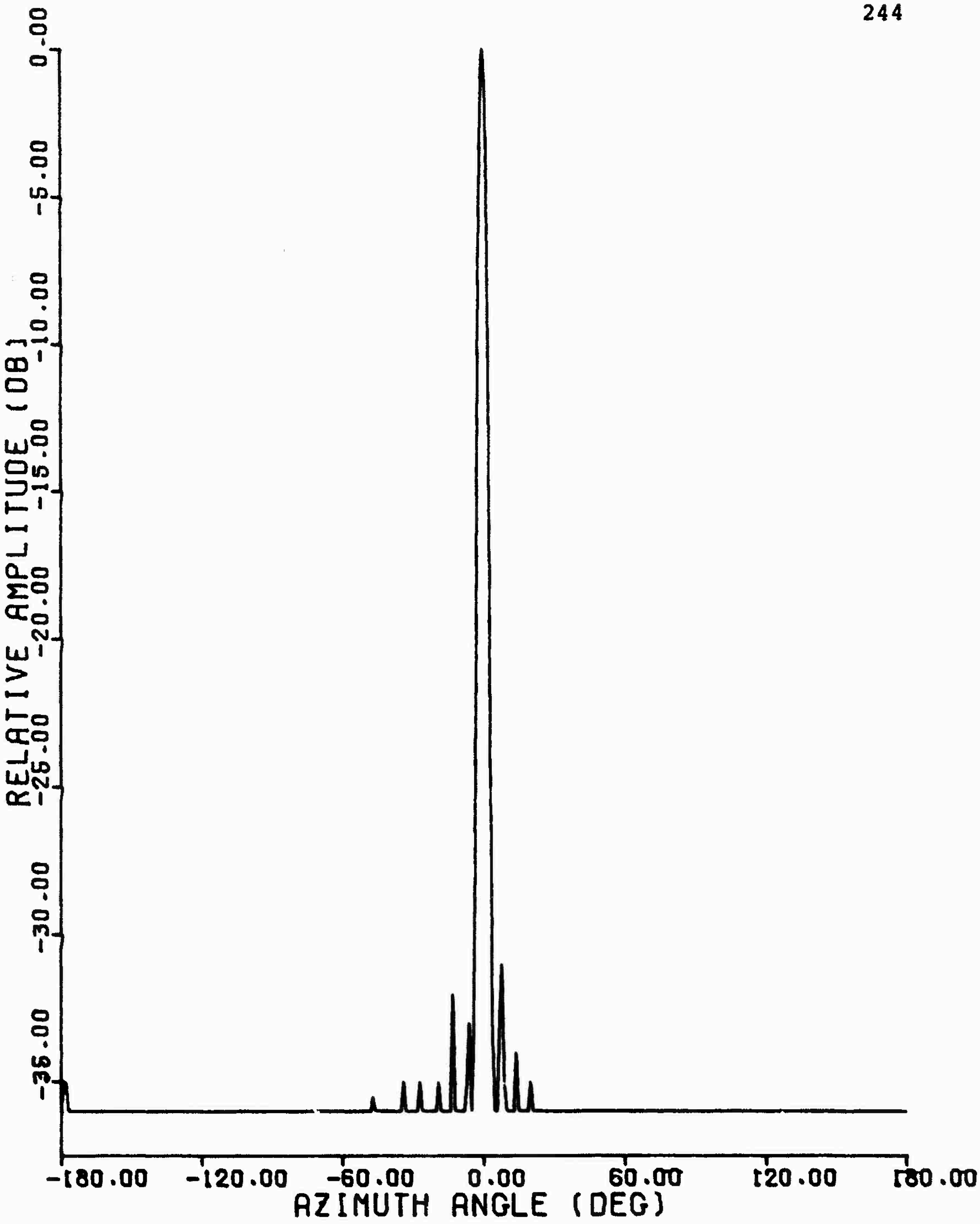

Figure C.9 1030 MHz Azimuth Pattern, Hazeltine Antenna, -180° to +180°

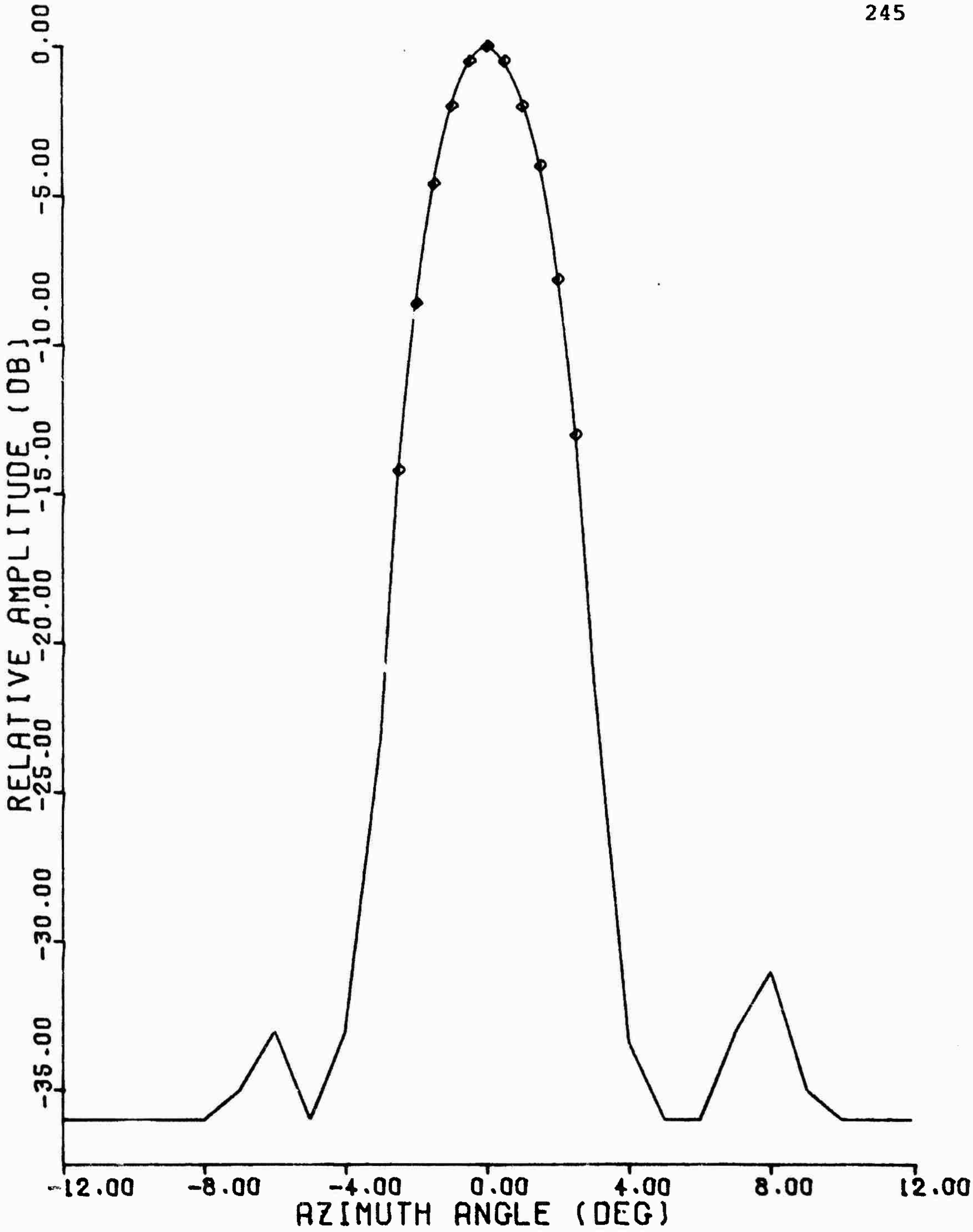

Figure C.10 1030 MHz Azimuth Pattern, Hazeltine Antenna, -12° to $+12^{\circ}$

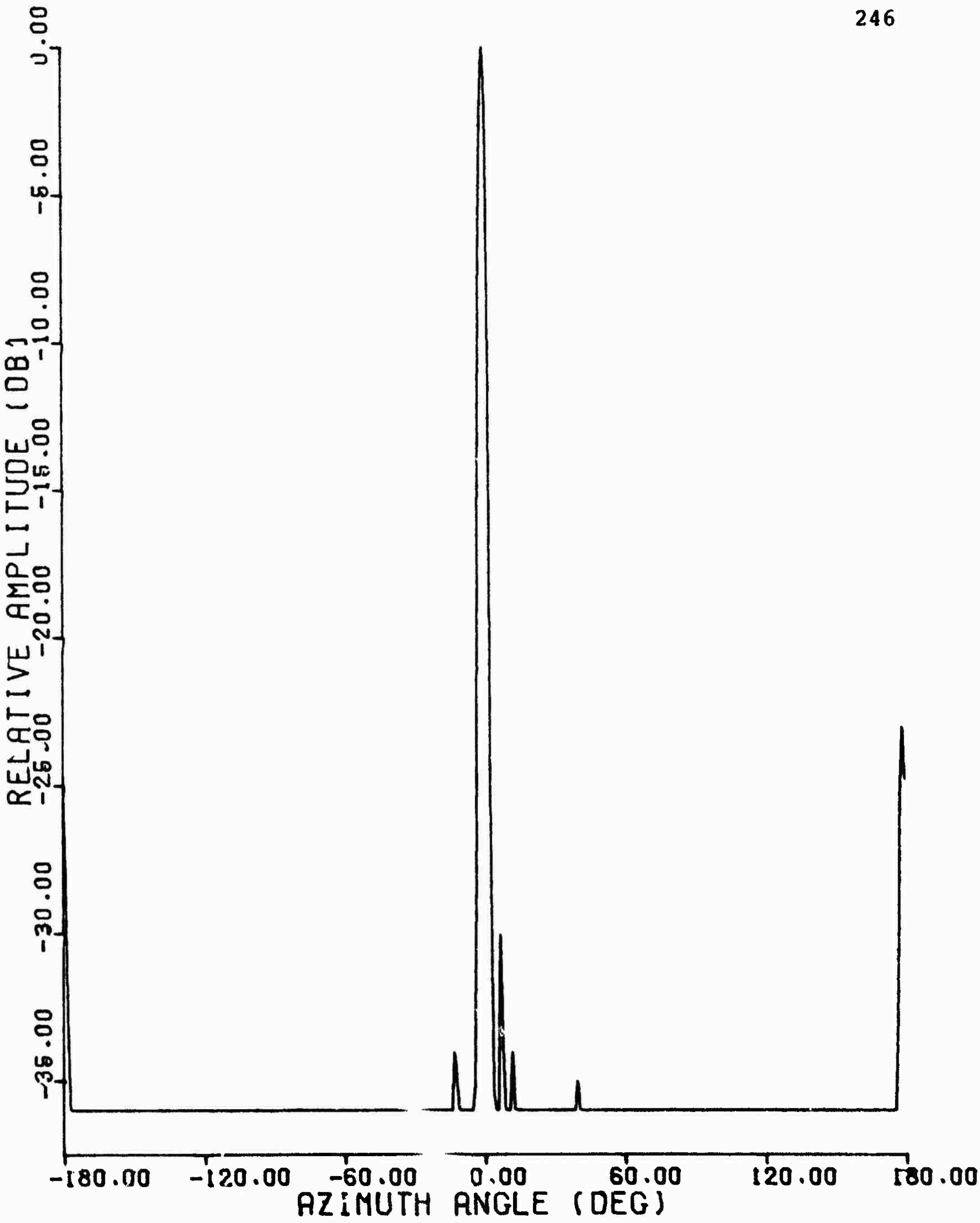

Figure C.11 1090 MHz Azimuth Pattern, Hazeltine Antenna, -180° to $+180^{\circ}$

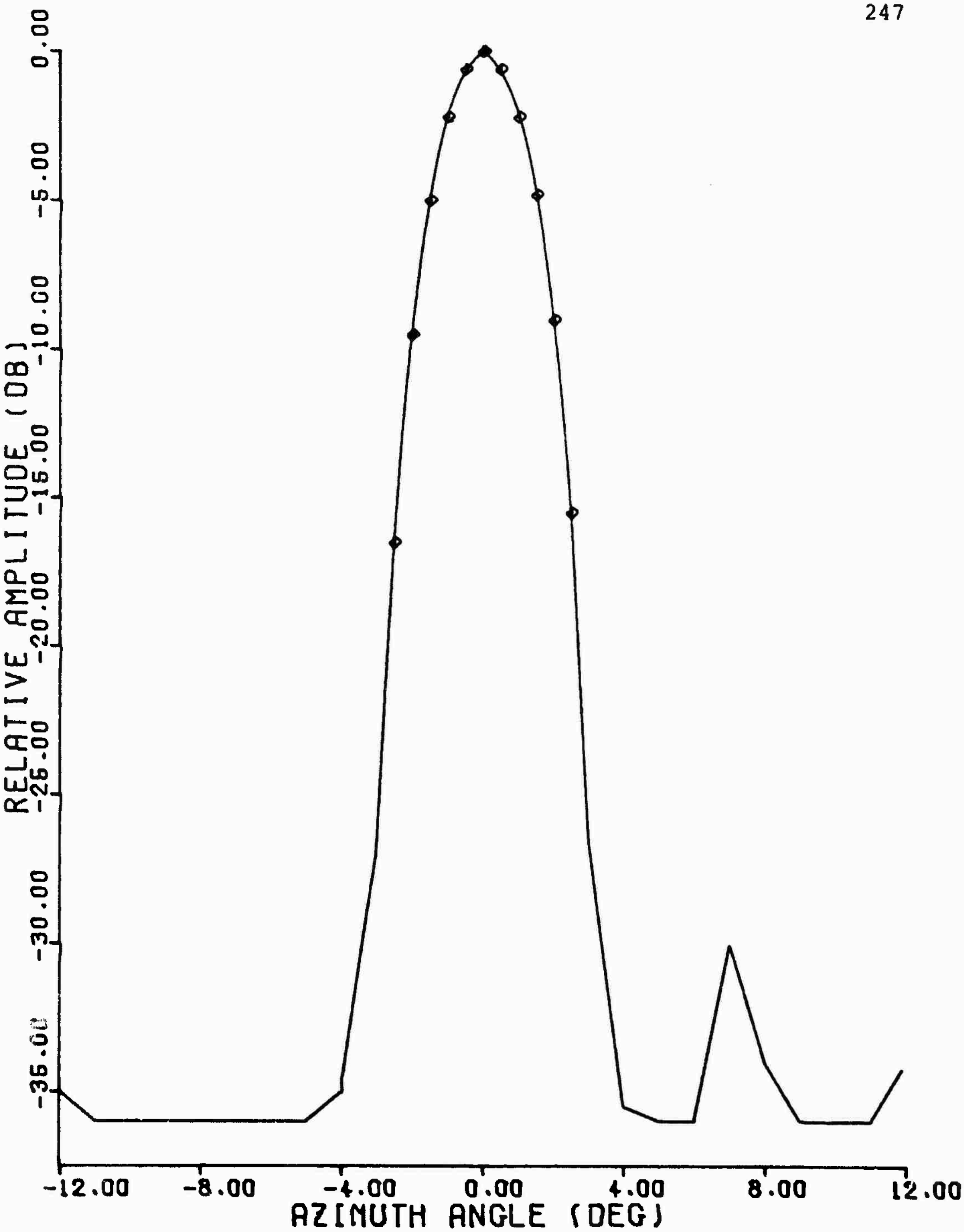

Figure C.12 1090 MHz Azimuth Pattern, Hazeltine Antenna, -12° to $+12^{\circ}$

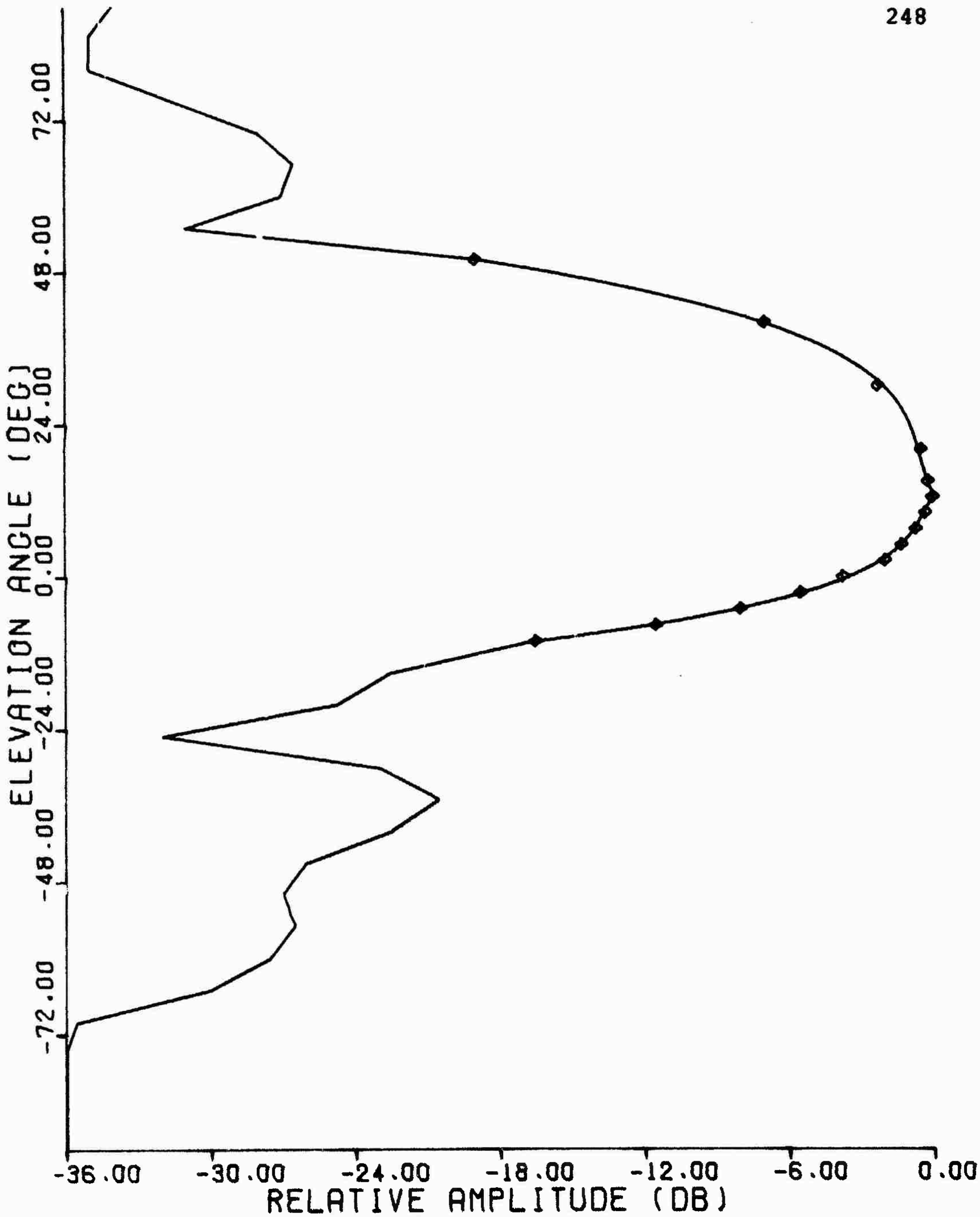

Figure C.13 1030 MHz Elevation Pattern, Hazeltine Antenna

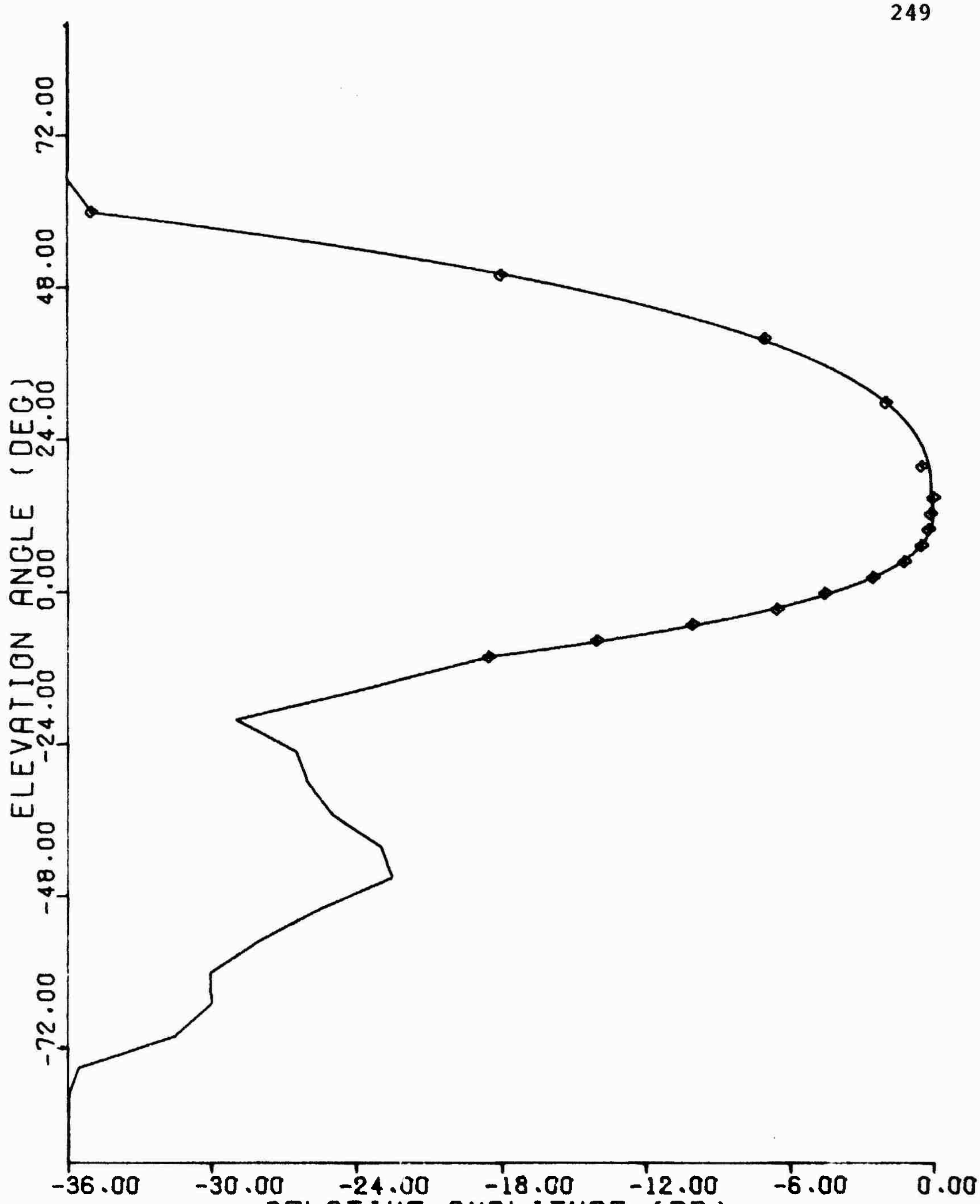

Figure C.14 1090 MHz Elevation Pattern, Hazeltine Antenna

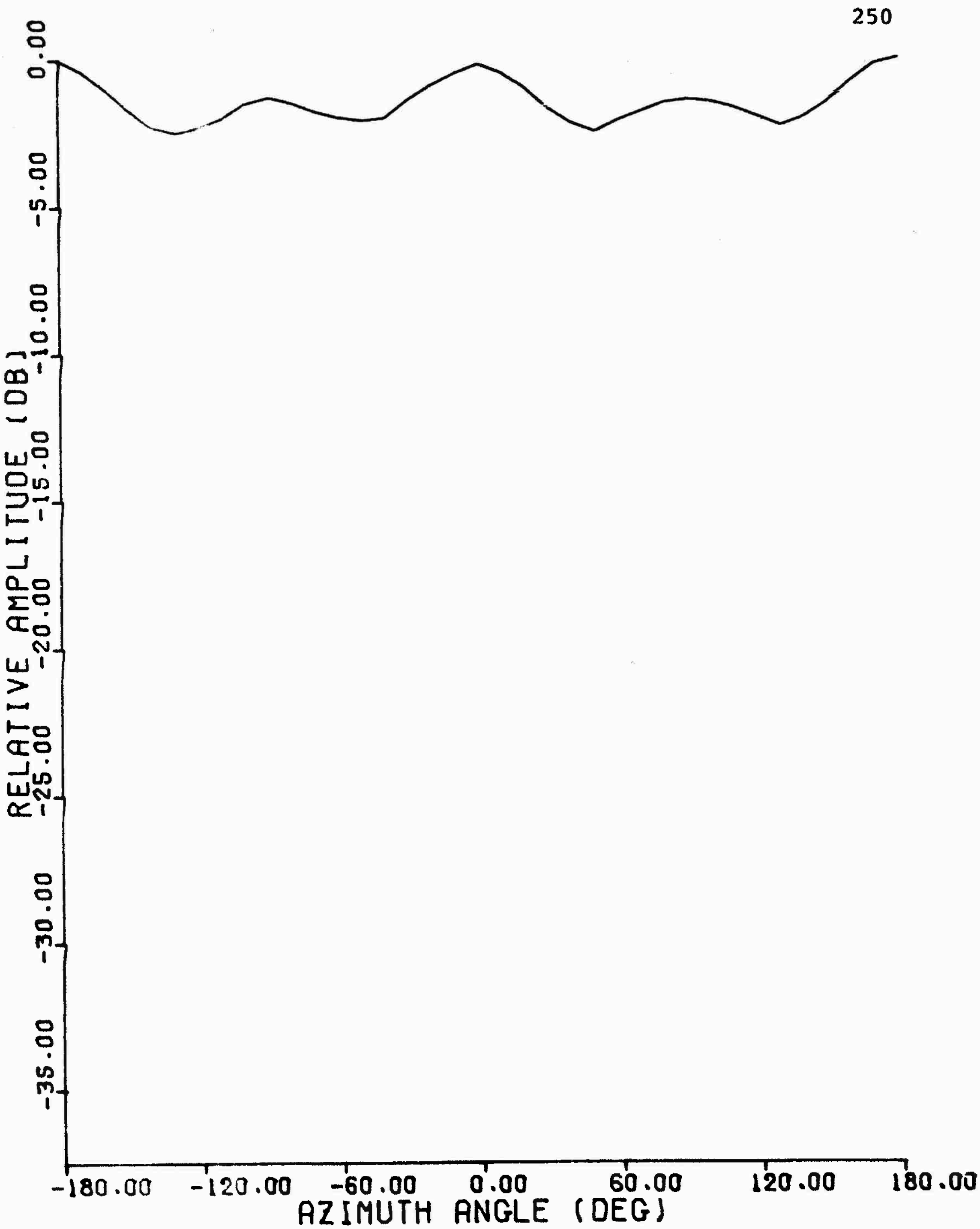

Figure C.15 1030 MHz Azimuth Pattern, Hazeltine Omni Antenna

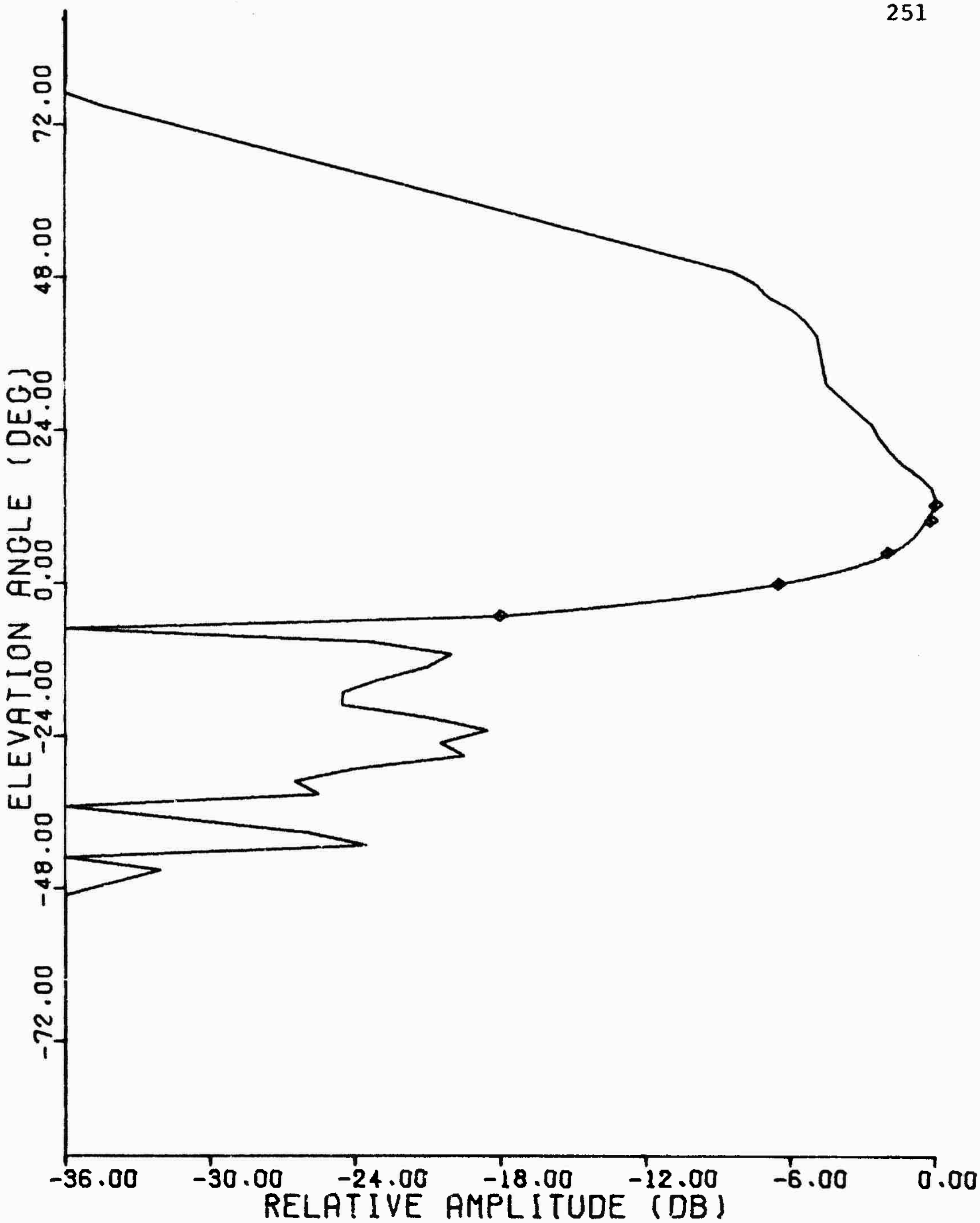

Figure C.16 1030 MHz Elevation Pattern, Hazeltine Omni Antenna

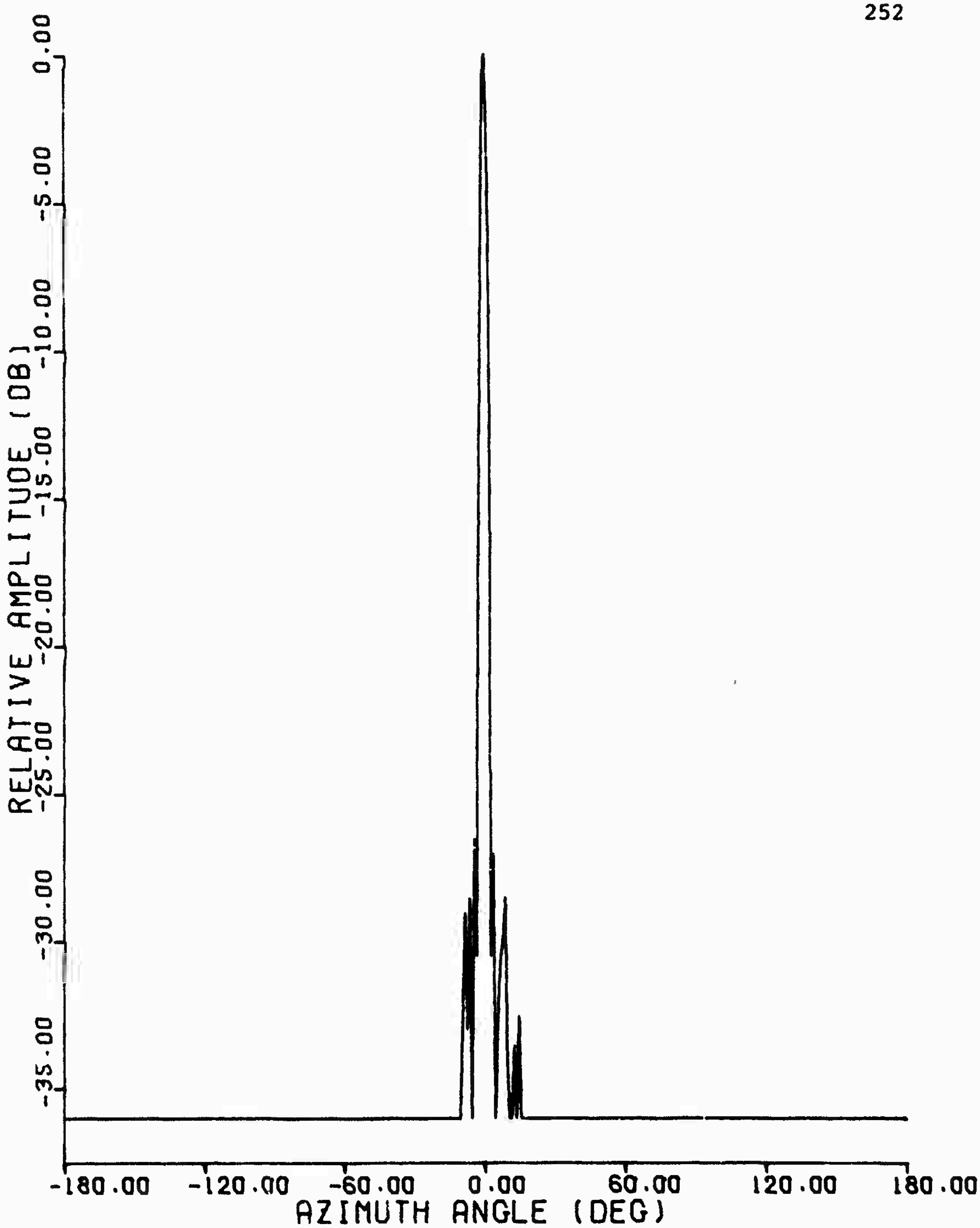

Figure C.17 1030 MHz Azimuth Pattern, ARSR Beacon Feed, -180° to $+180^{\circ}$

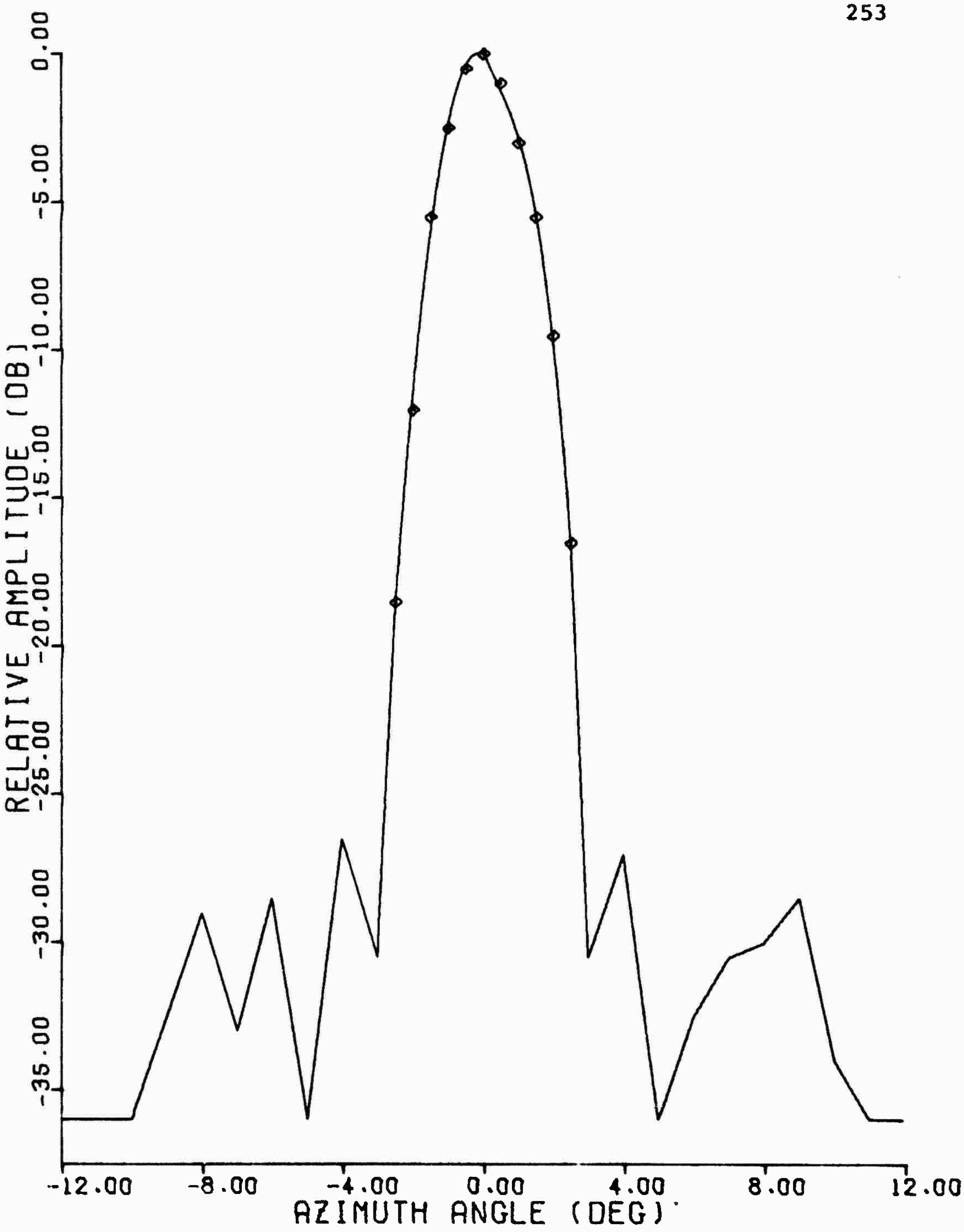

Figure C.18 1030 MHz Azimuth Pattern, ARSR Beacon Feed, -12° to $+12^{\circ}$

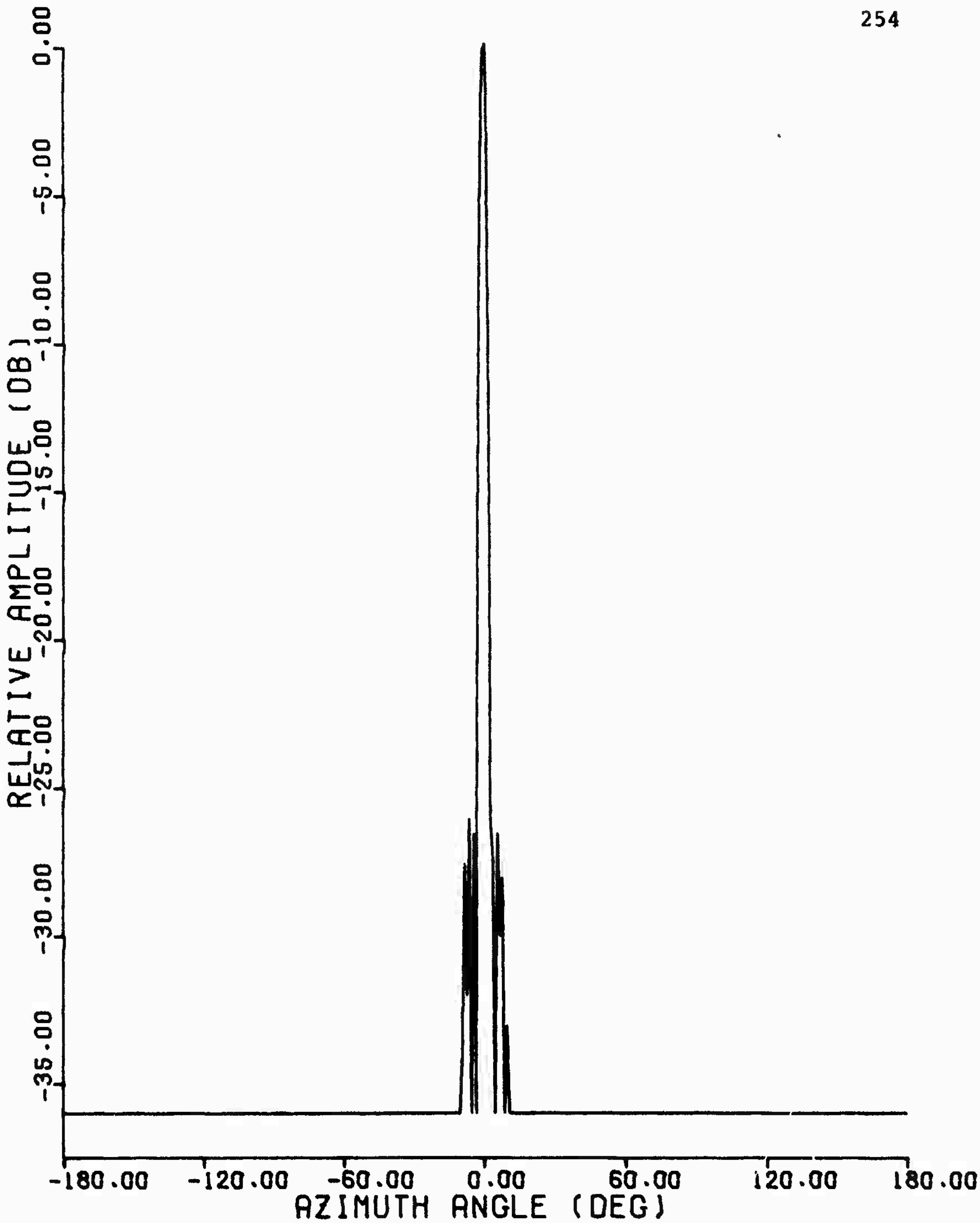

Figure C.19 1090 MHz Azimuth Pattern, ARSR Beacon Feed, -180° to $+180^{\circ}$

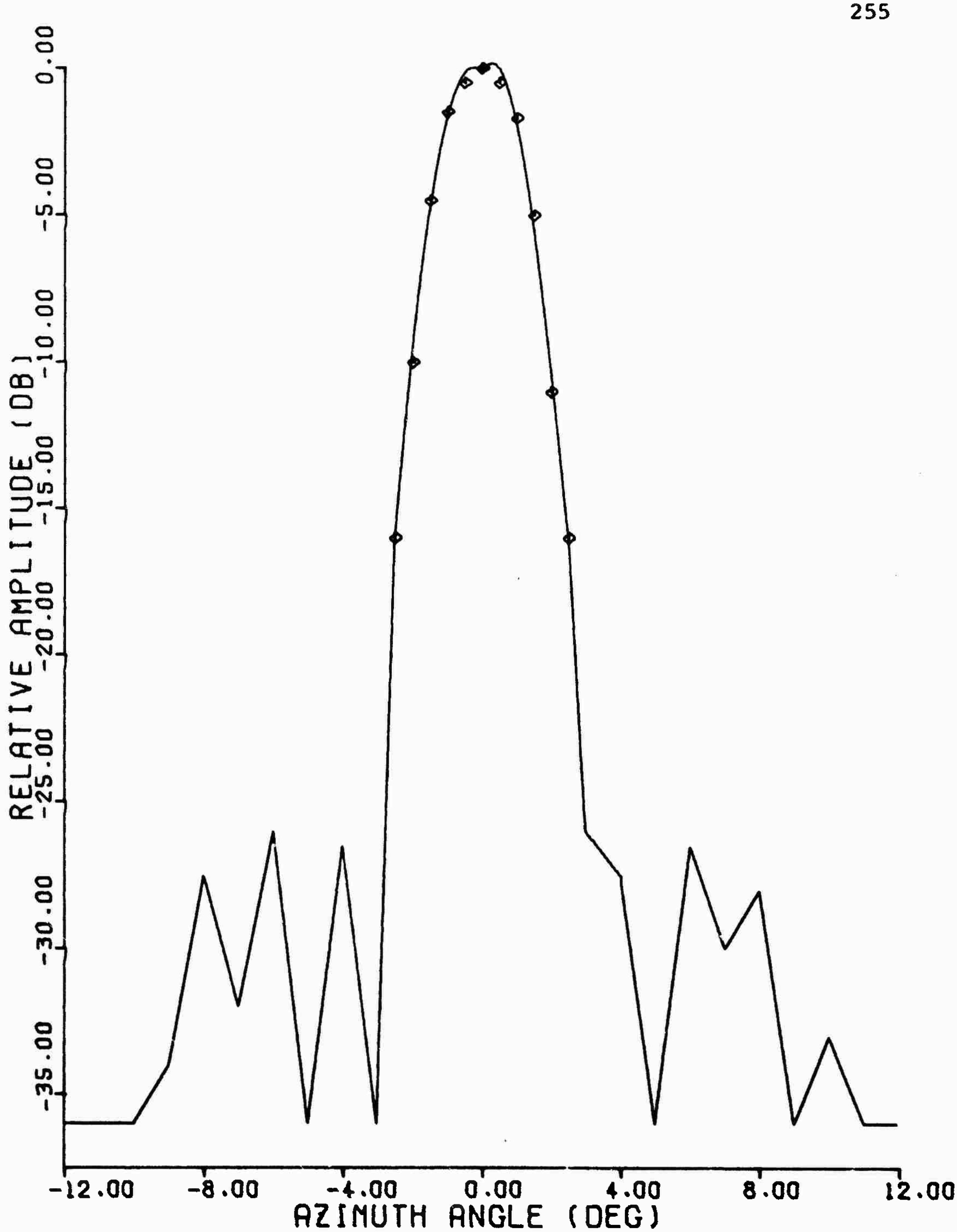

Figure C.20 1090 MHz Azimuth Pattern, ARSR Beacon Feed, -12° to $+12^{\circ}$

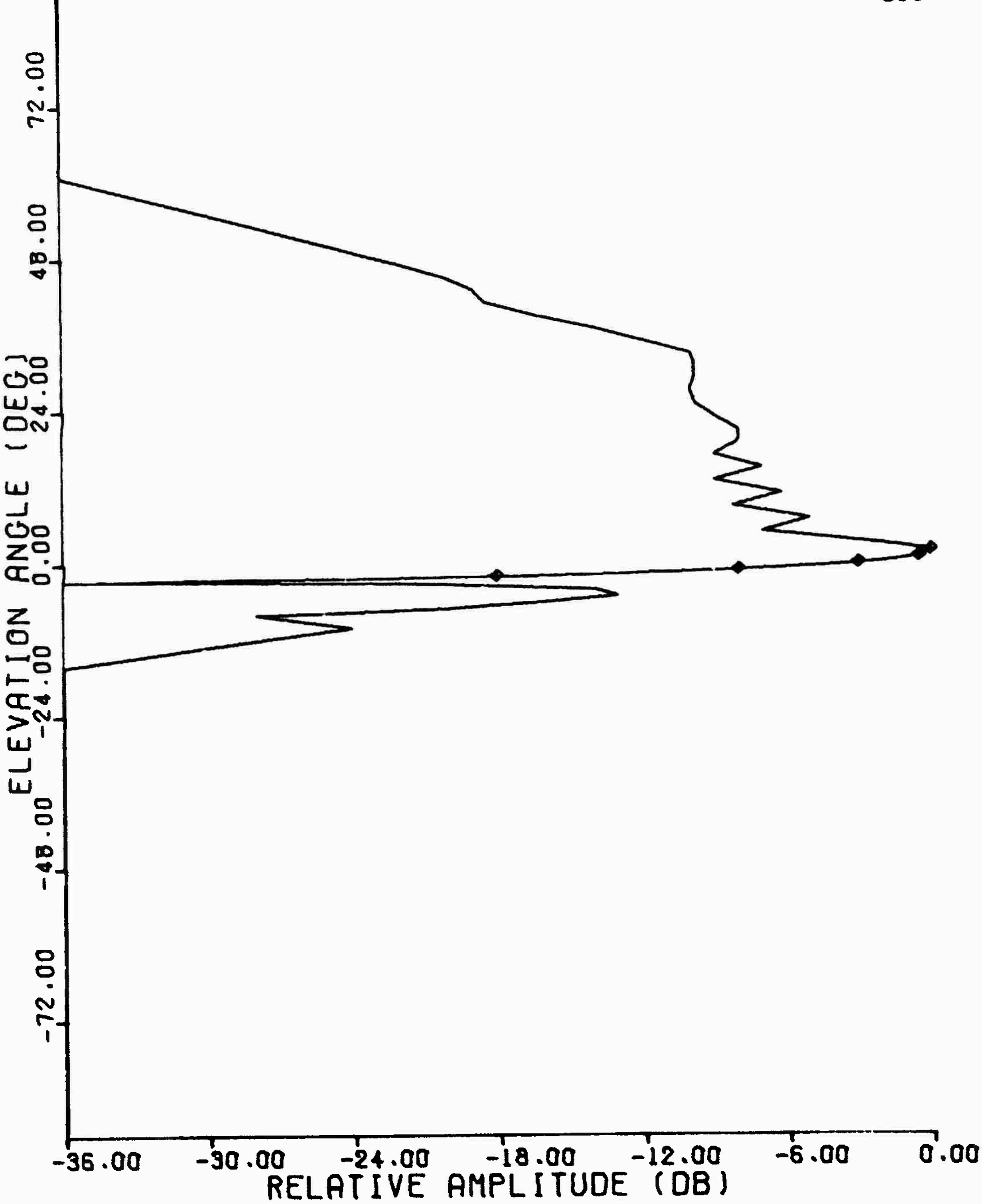

Figure C.21 1030 MHz Elevation Pattern, ARSR Beacon Feed

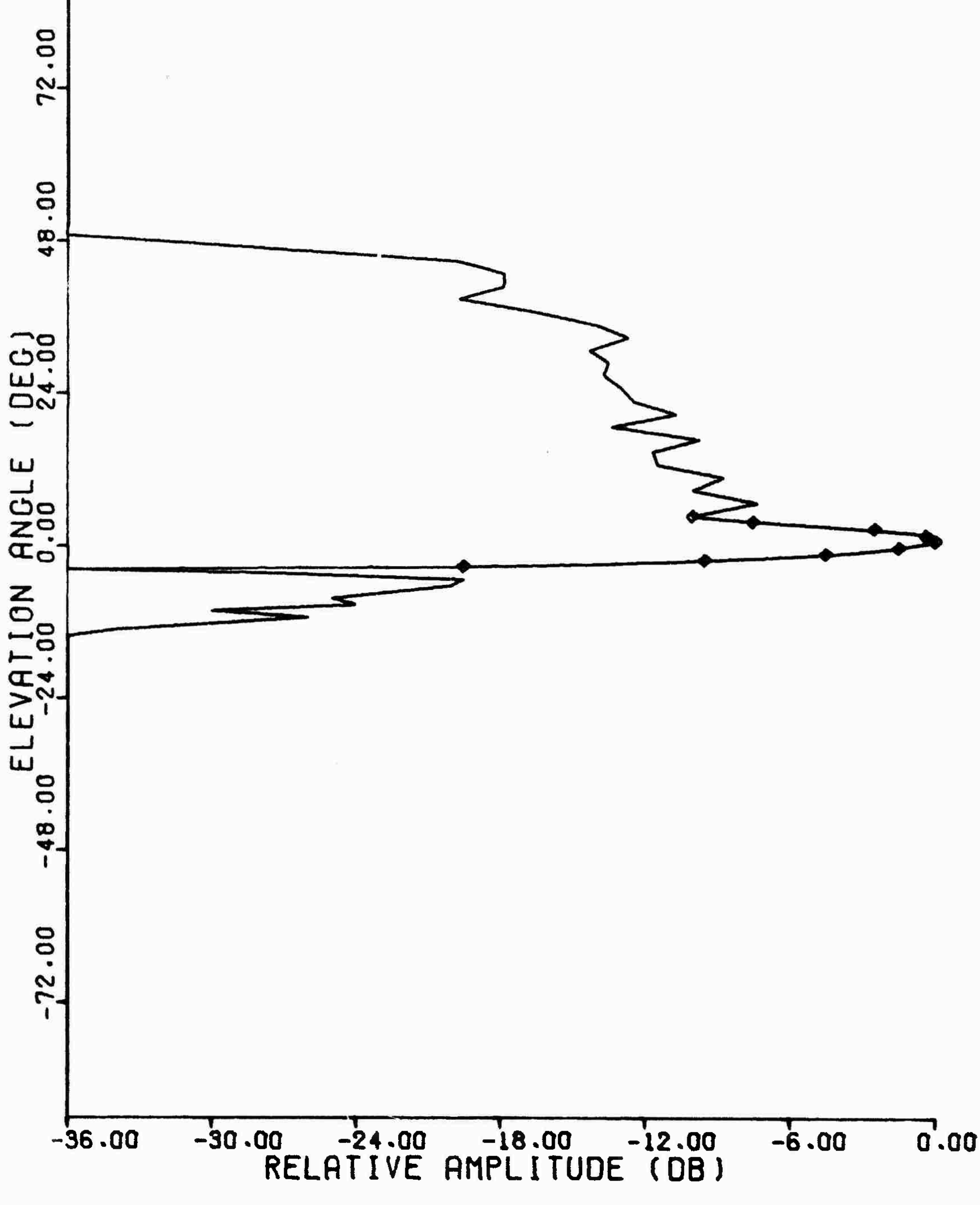

Figure C.22 1090 MHz Elevation Pattern, ARSR Beacon Feed

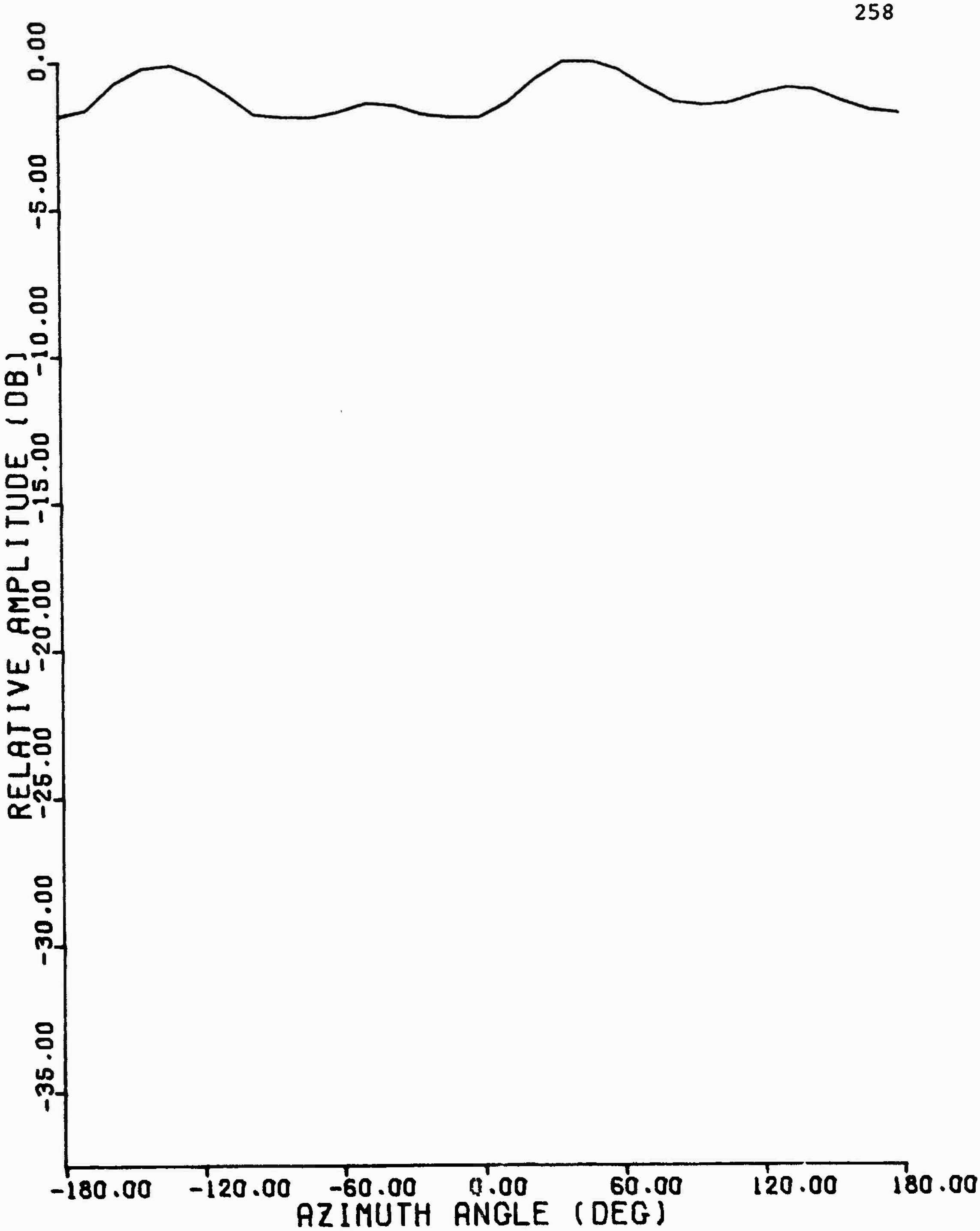

Figure C.23 1030 MHz Azimuth Pattern, ARSR Omni Antenna

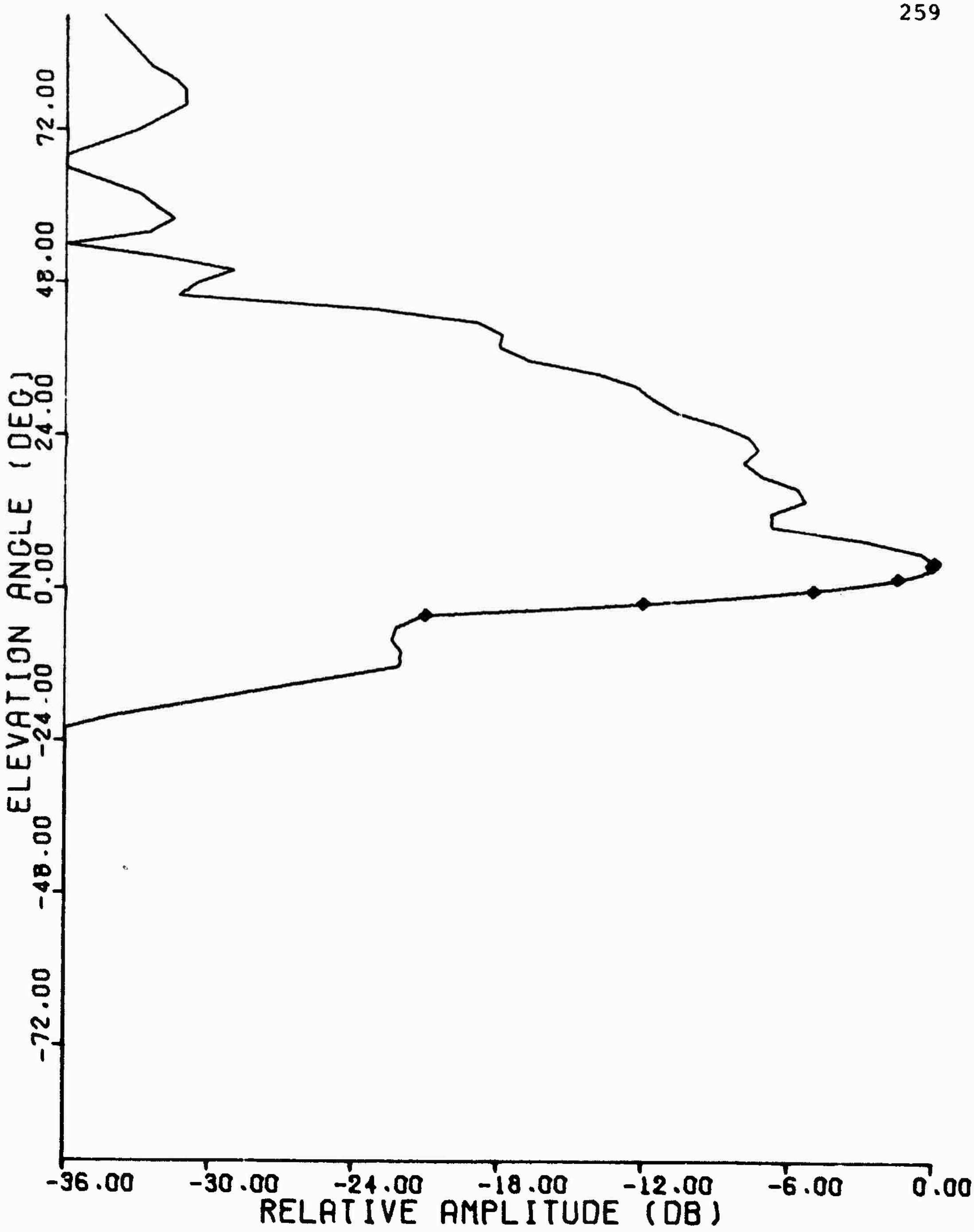

Figure C.24 1030 MHz Elevation Pattern, ARSR Omni Antenna

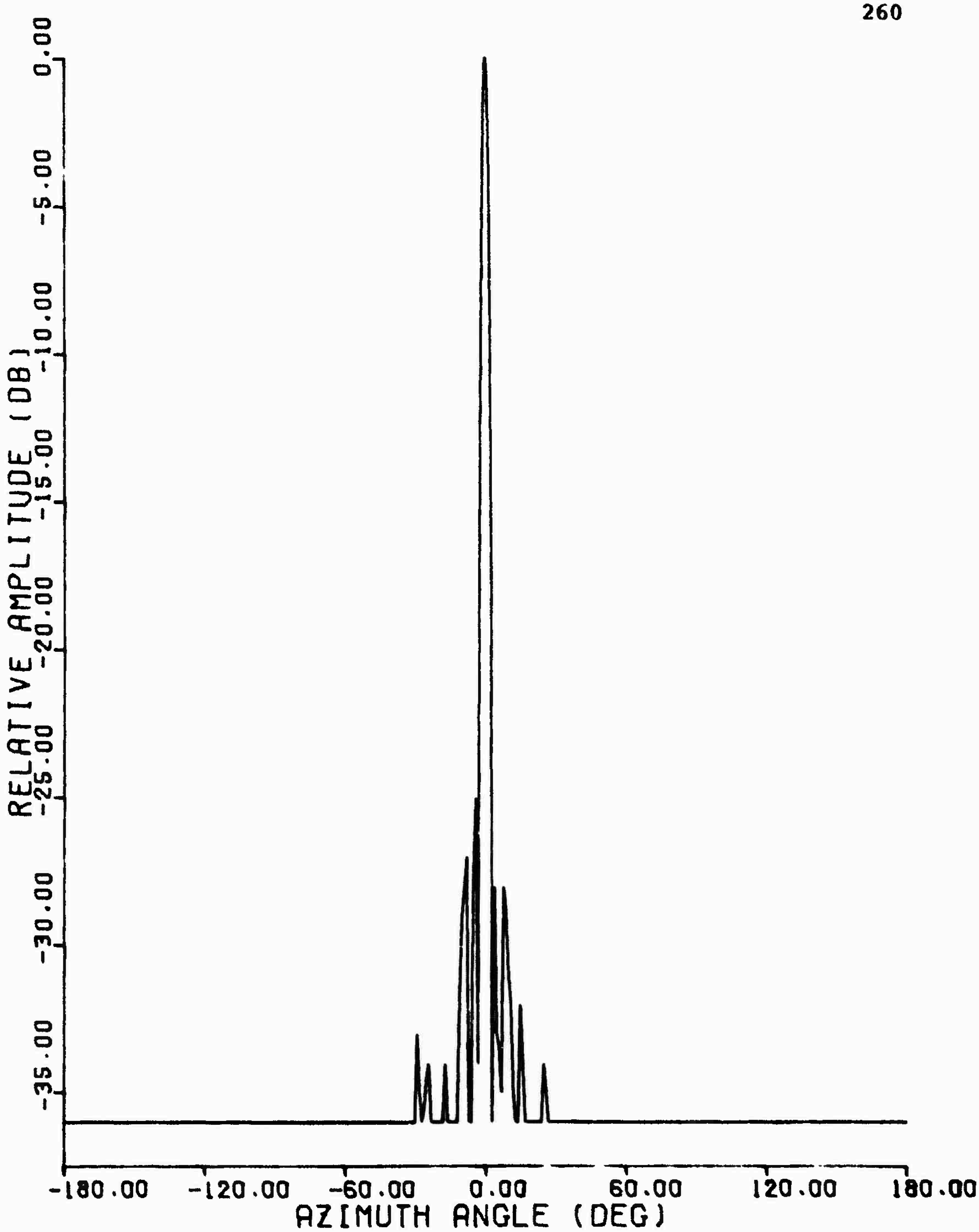

Figure C.25 1030 MHz Azimuth Pattern, TI Separate Rotator, -180° to +180°

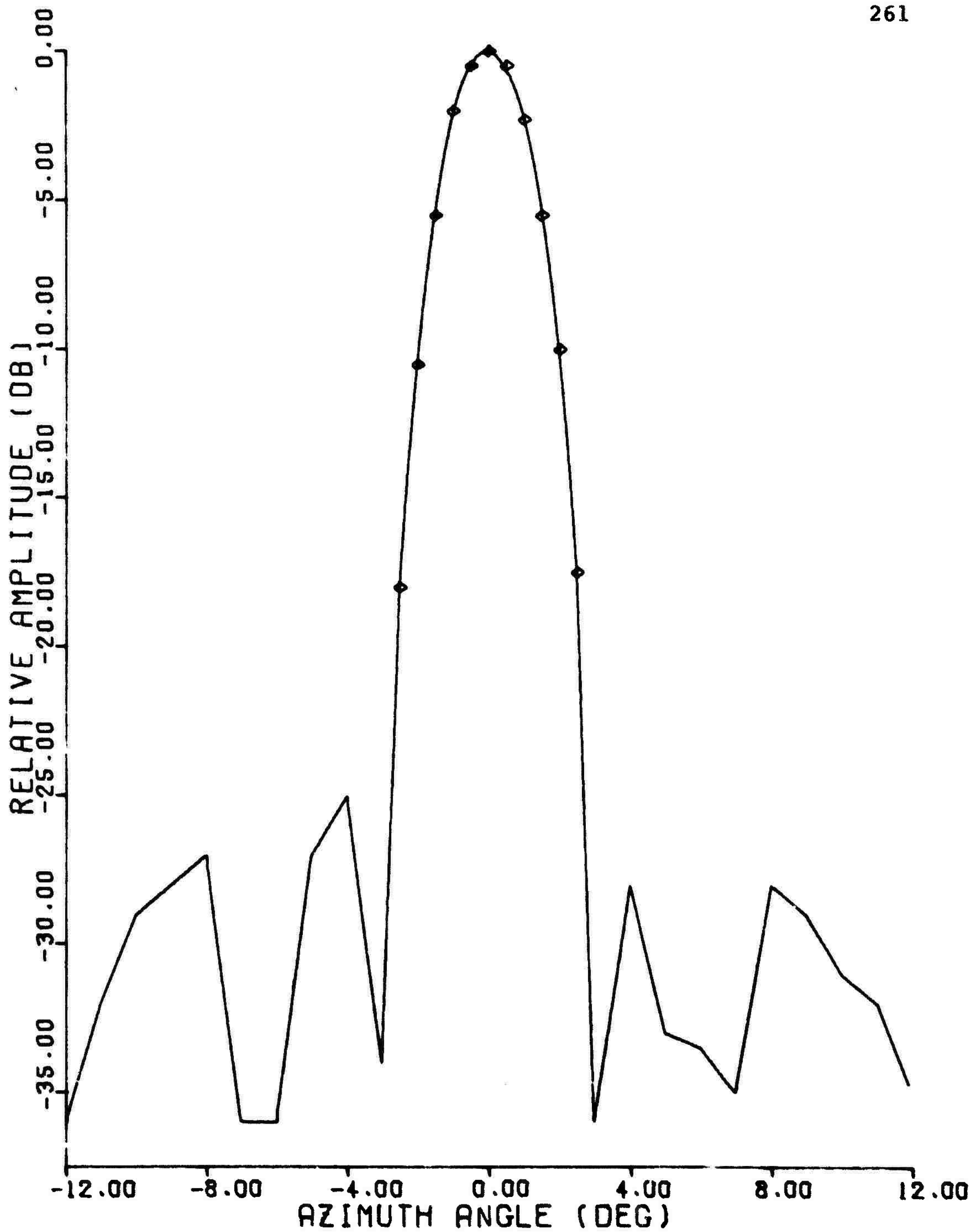

Figure C.26 1030 MHz Azimuth Pattern, TI Separate Rotator, -12° to $+12^{\circ}$

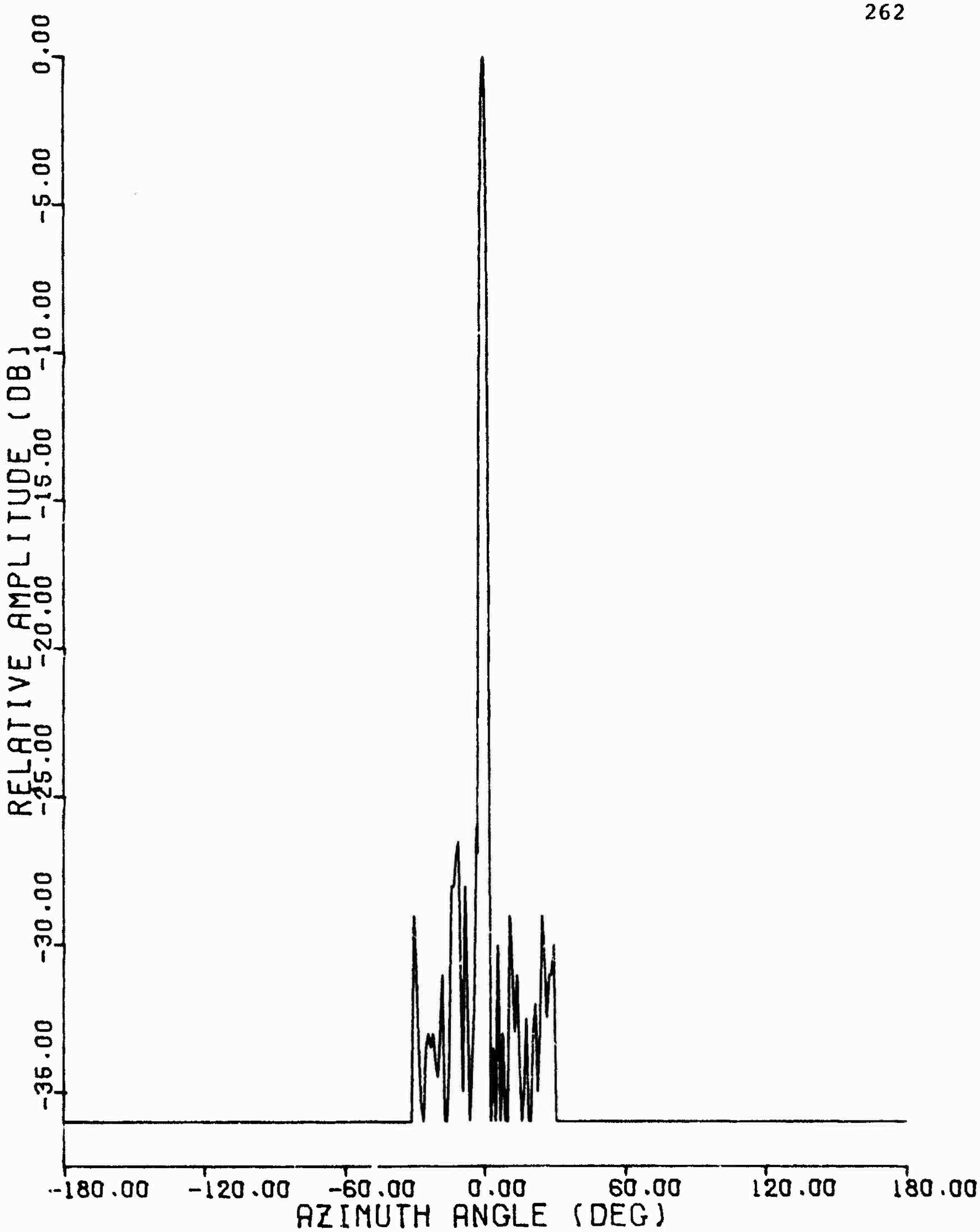

Figure C.27 1090 MHz Azimuth Pattern, TI Separate Rotator, -180^{o} to $+180^{o}$

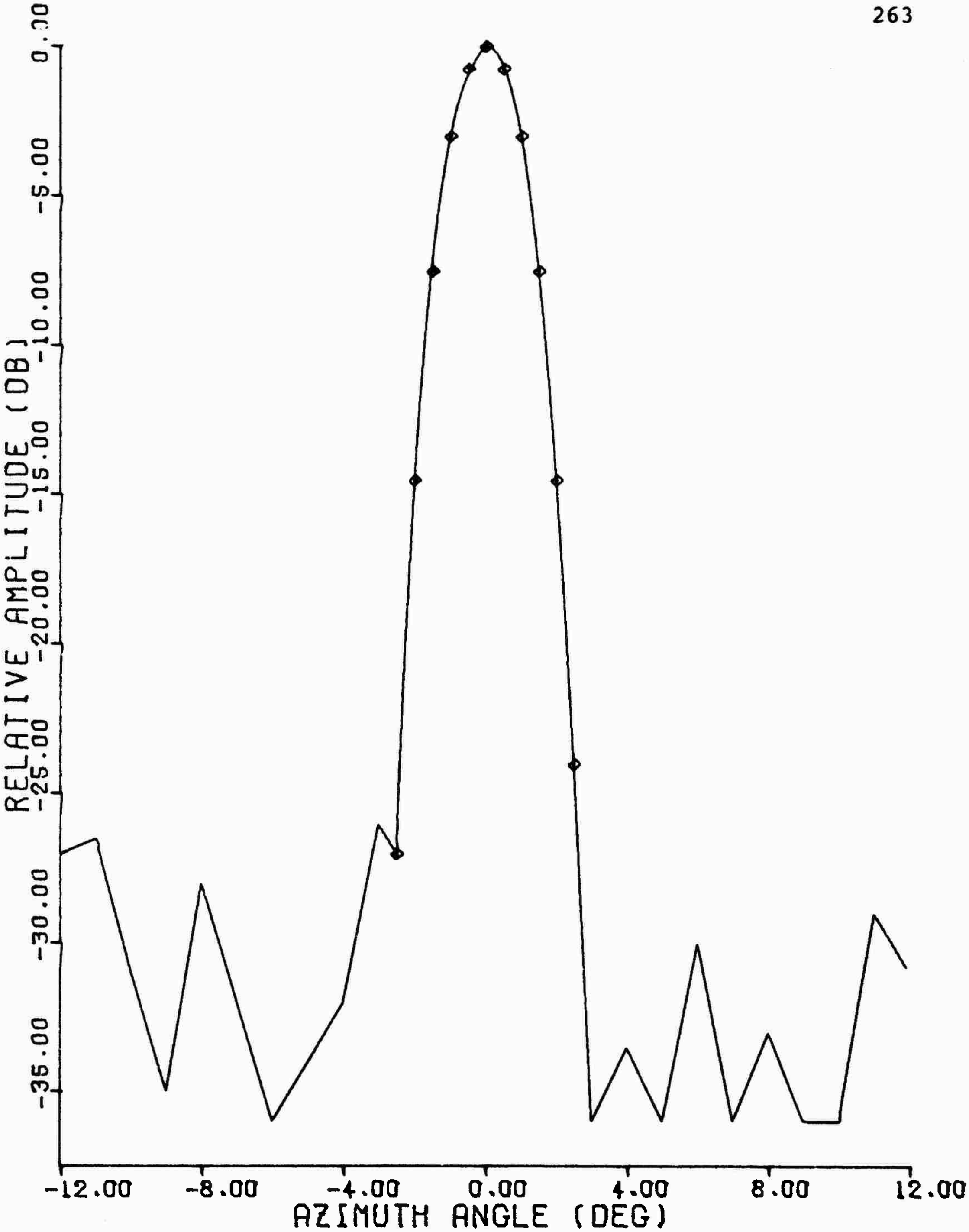

Figure C.28 1090 MHz Azimuth Pattern, TI Separate Rotator, -12° to $+12^{\circ}$

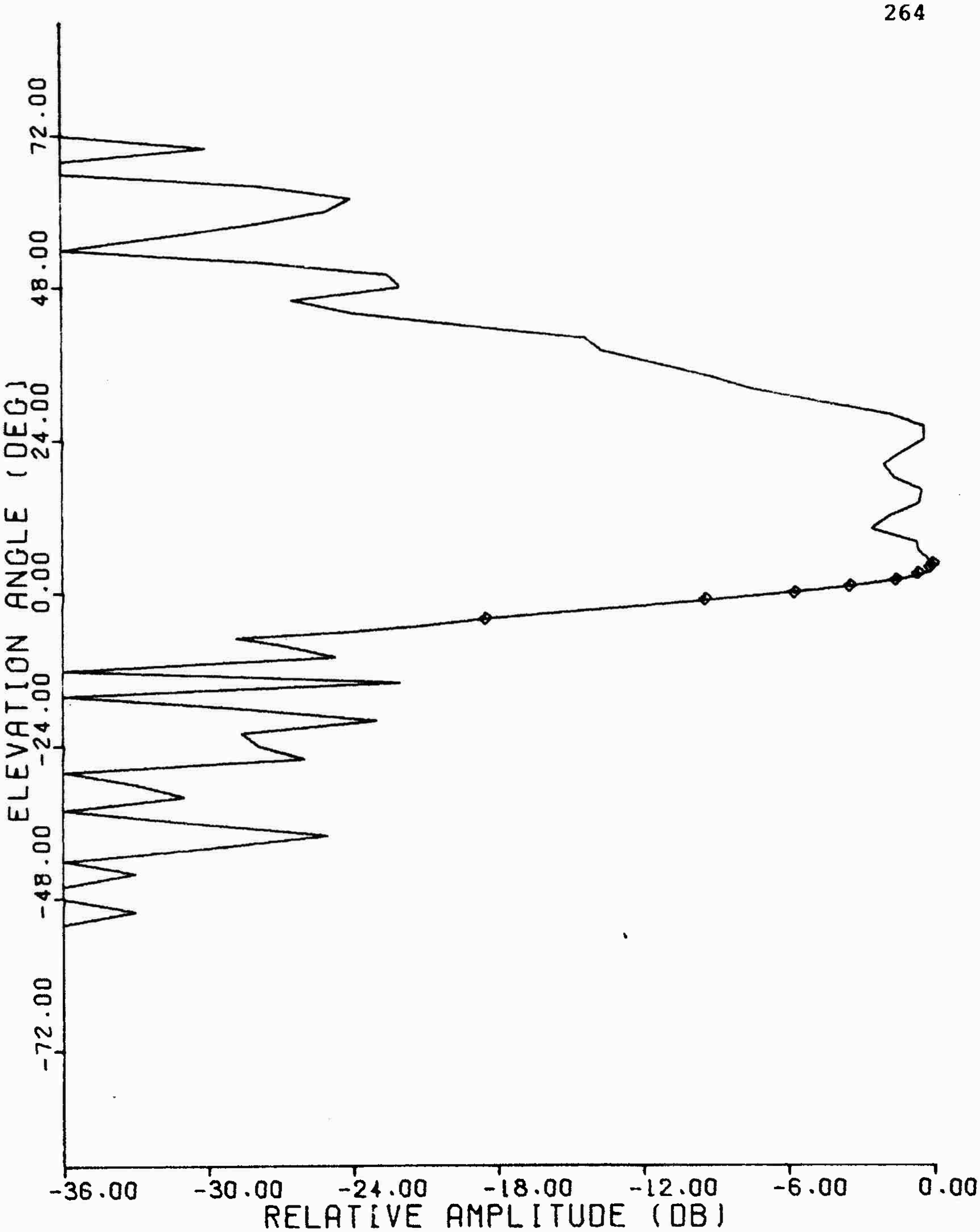

Figure C.29 1030 MHz Elevation Pattern, TI Separate Rotator

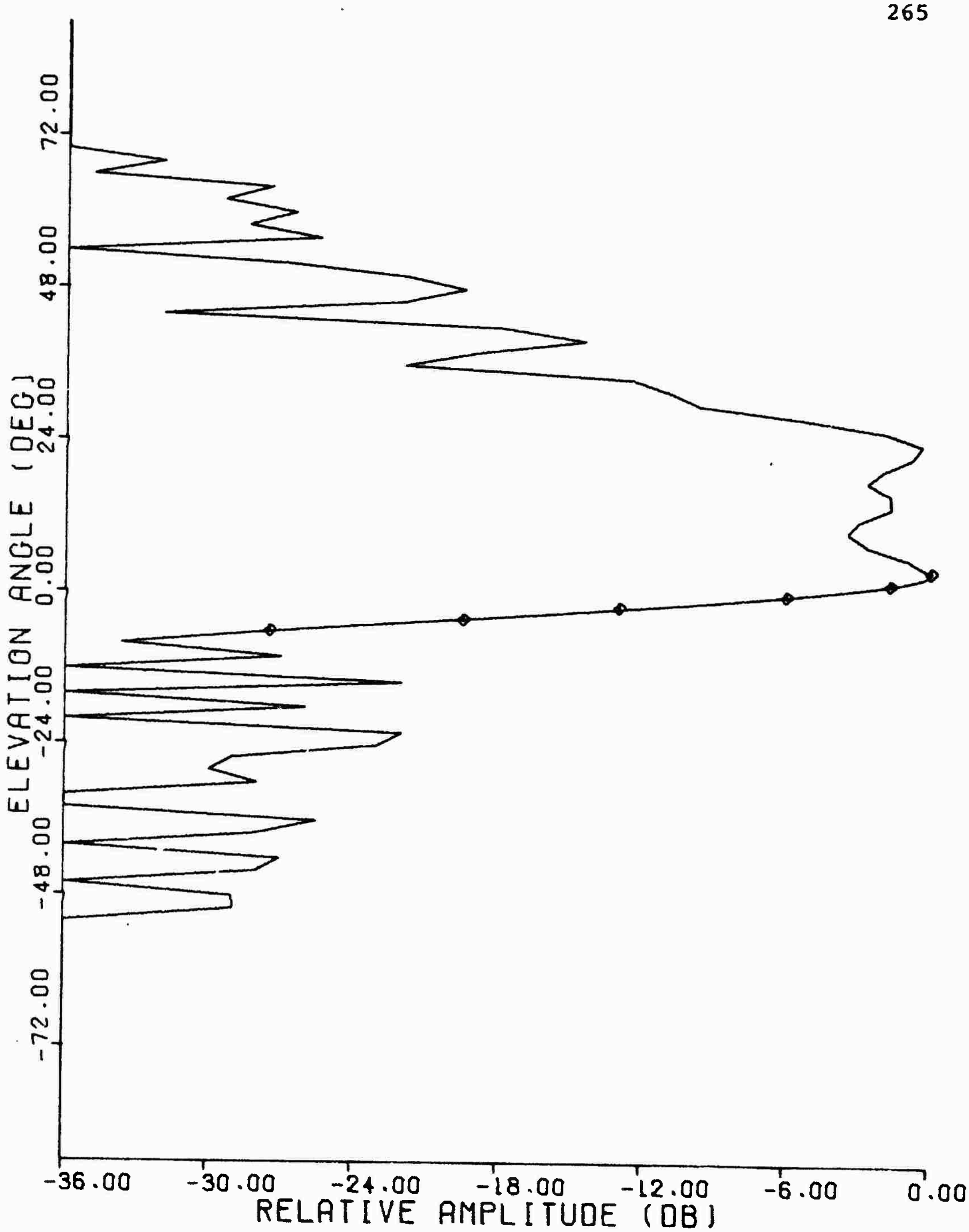

Figure C.30 1090 MHz Elevation Pattern, TI Separate Rotator

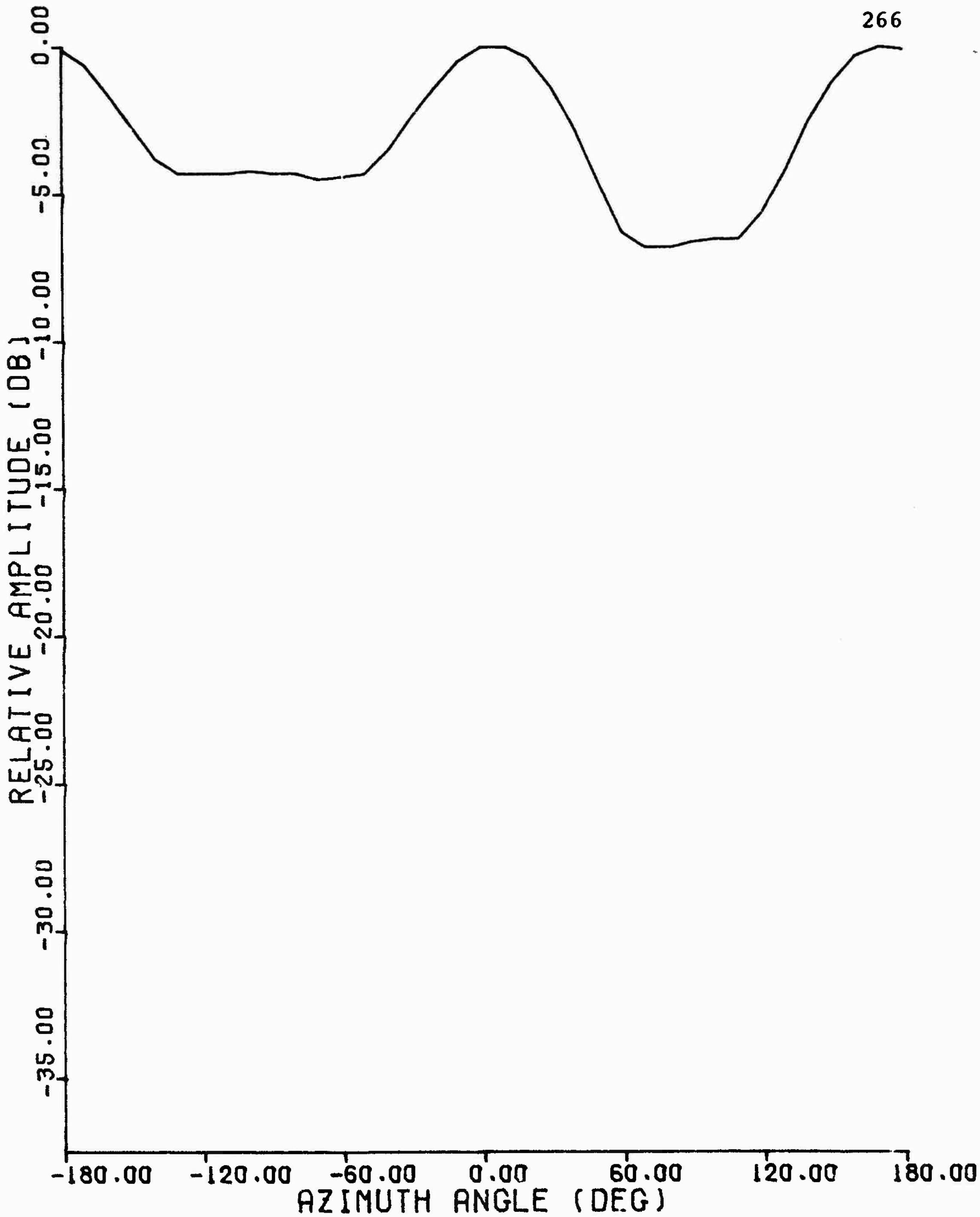

Figure C.31 1030 MHz Azimuth Pattern, TI Separate Rotator Omni

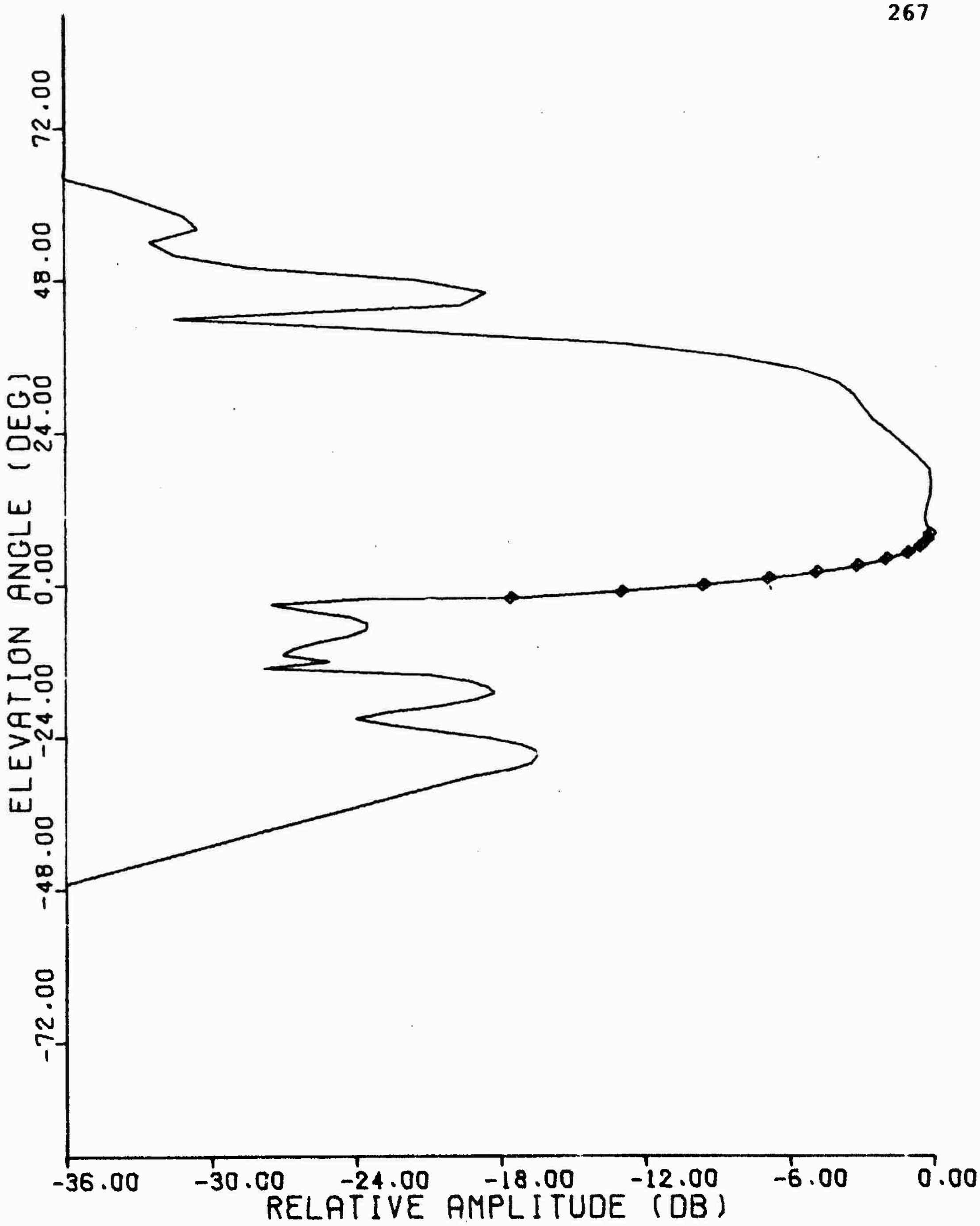

Figure C.32 1030 MHz Elevation Pattern, TI Separate Rotator Omni

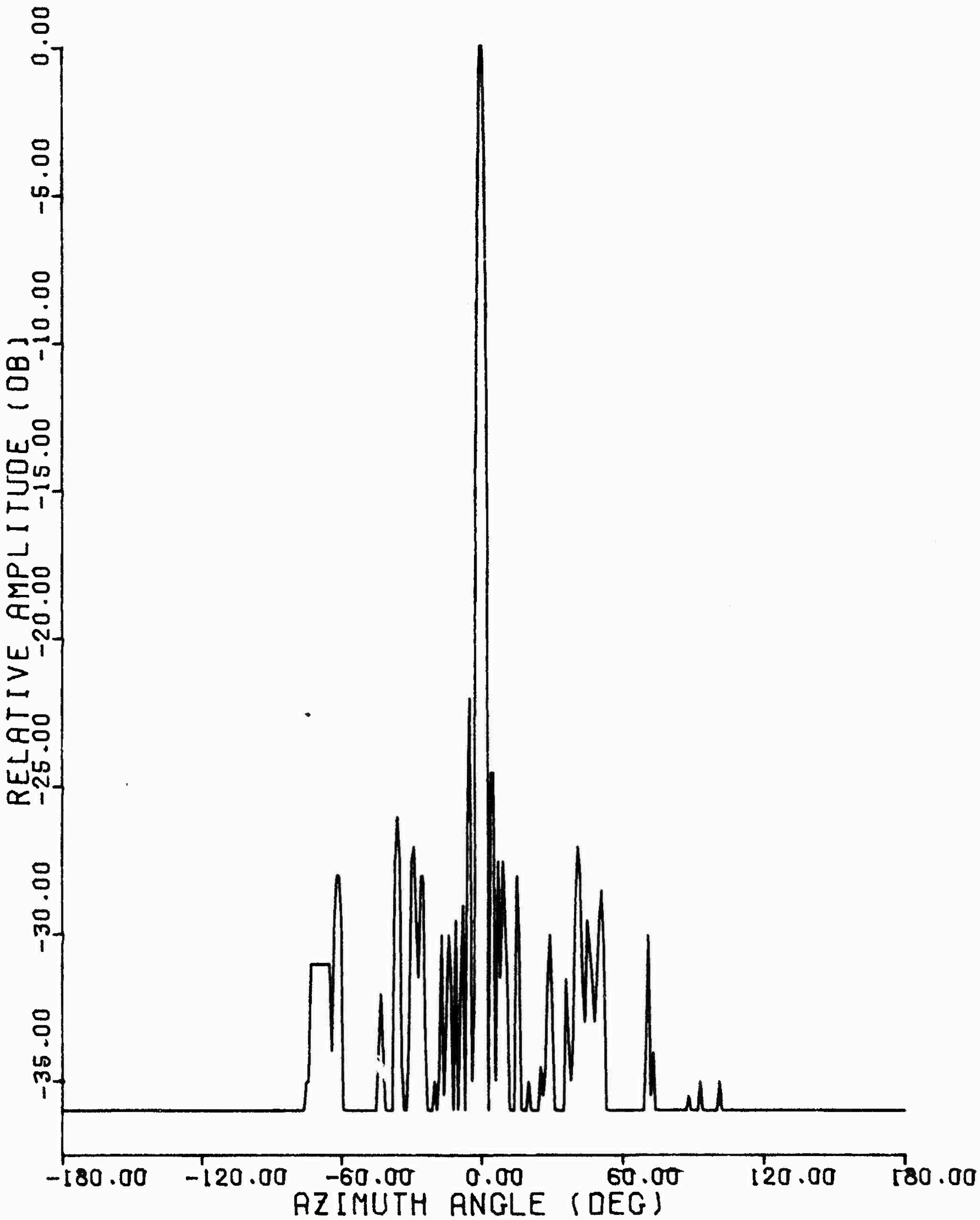

Figure C.33 1030 MHz Azimuth Pattern, Westinghouse Antenna, -180° to $+180^{\circ}$

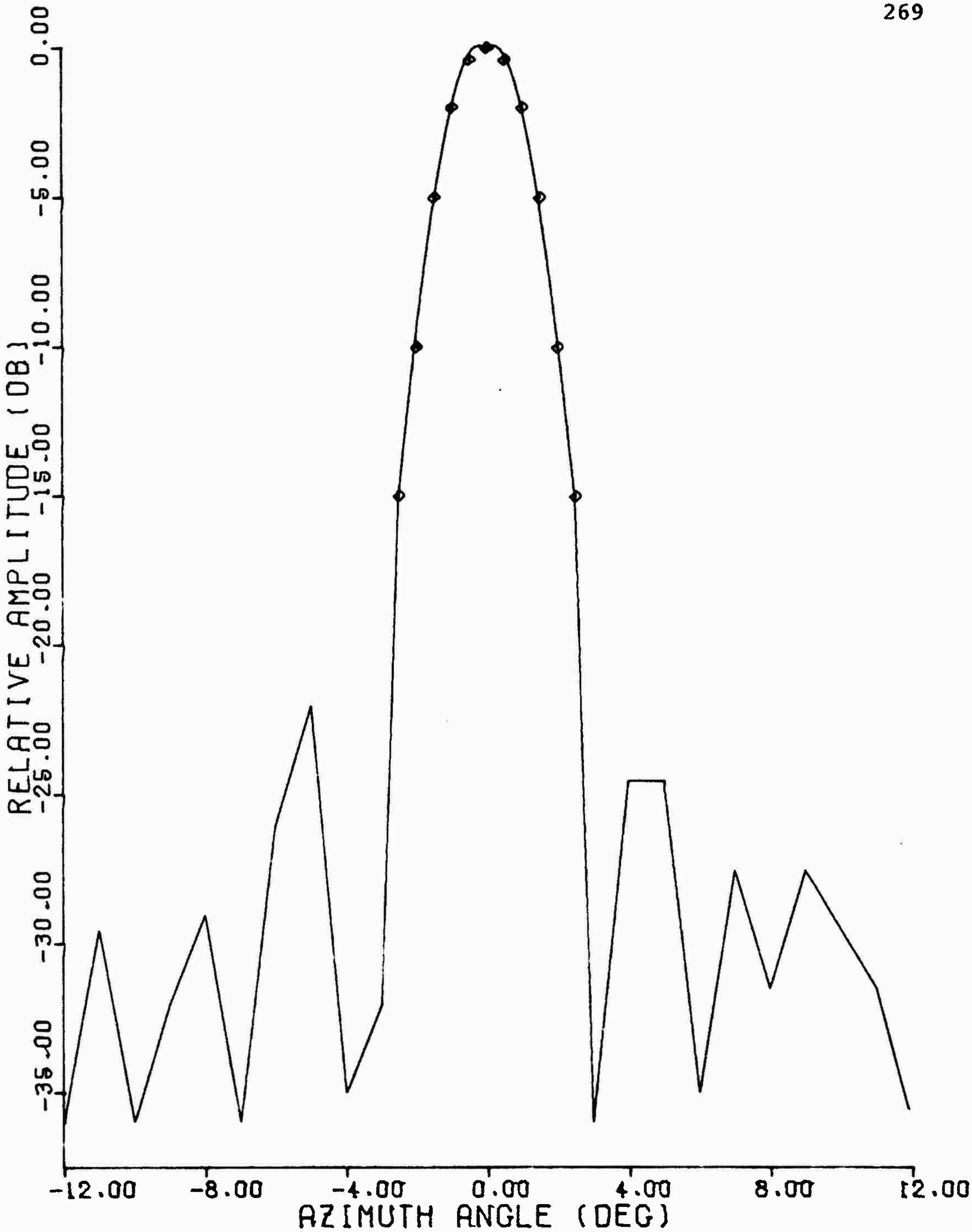

Figure C.34 1030 MHz Azimuth Pattern, Westinghouse Antenna, -12° to $+12^{\circ}$

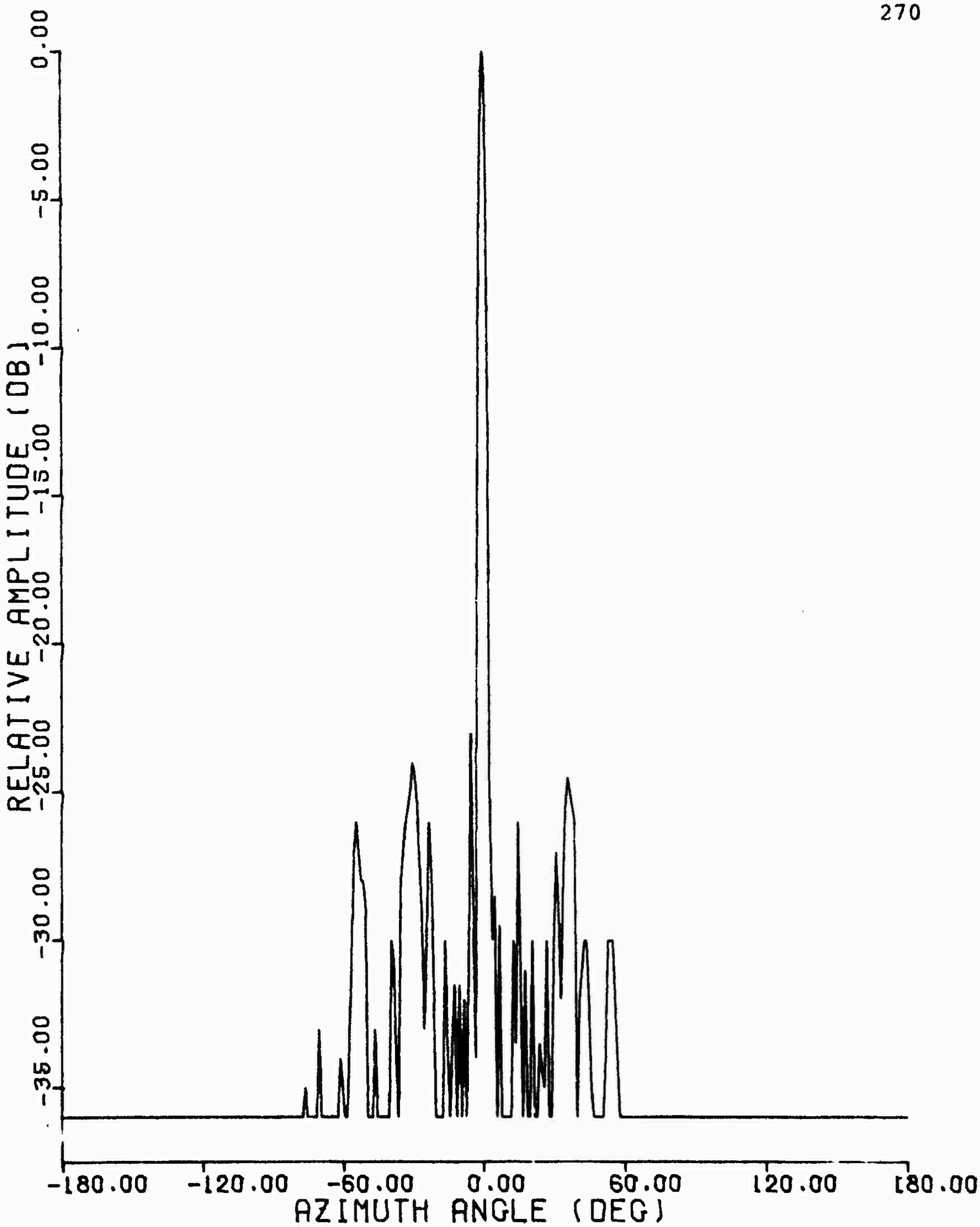

Figure C.35 1090 MHz Azimuth Pattern, Westinghouse Antenna, -180° to $+180^{\circ}$

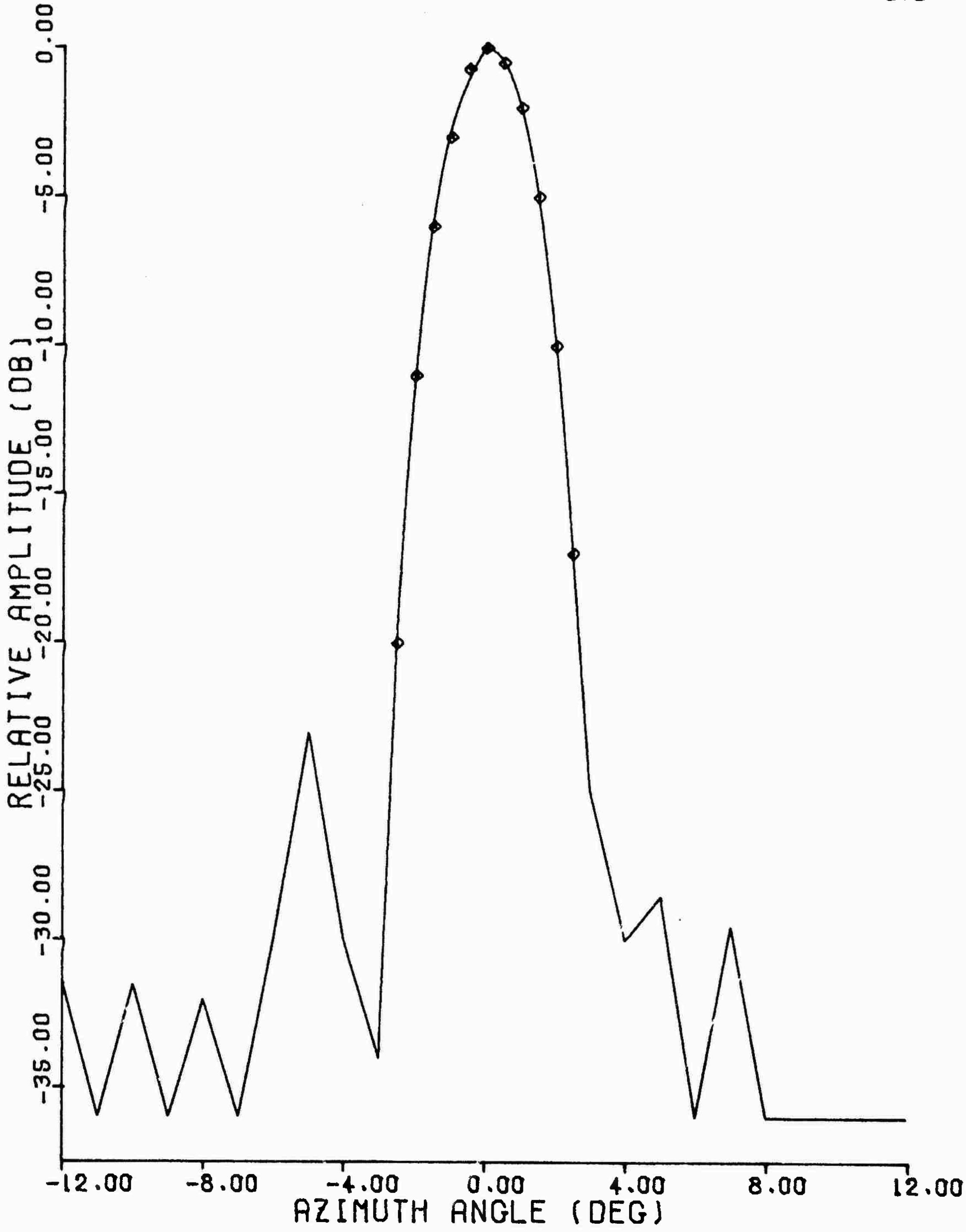

Figure C.36 1090 MHz Azimuth Pattern, Westinghouse Antenna, -12° to $+12^{\circ}$

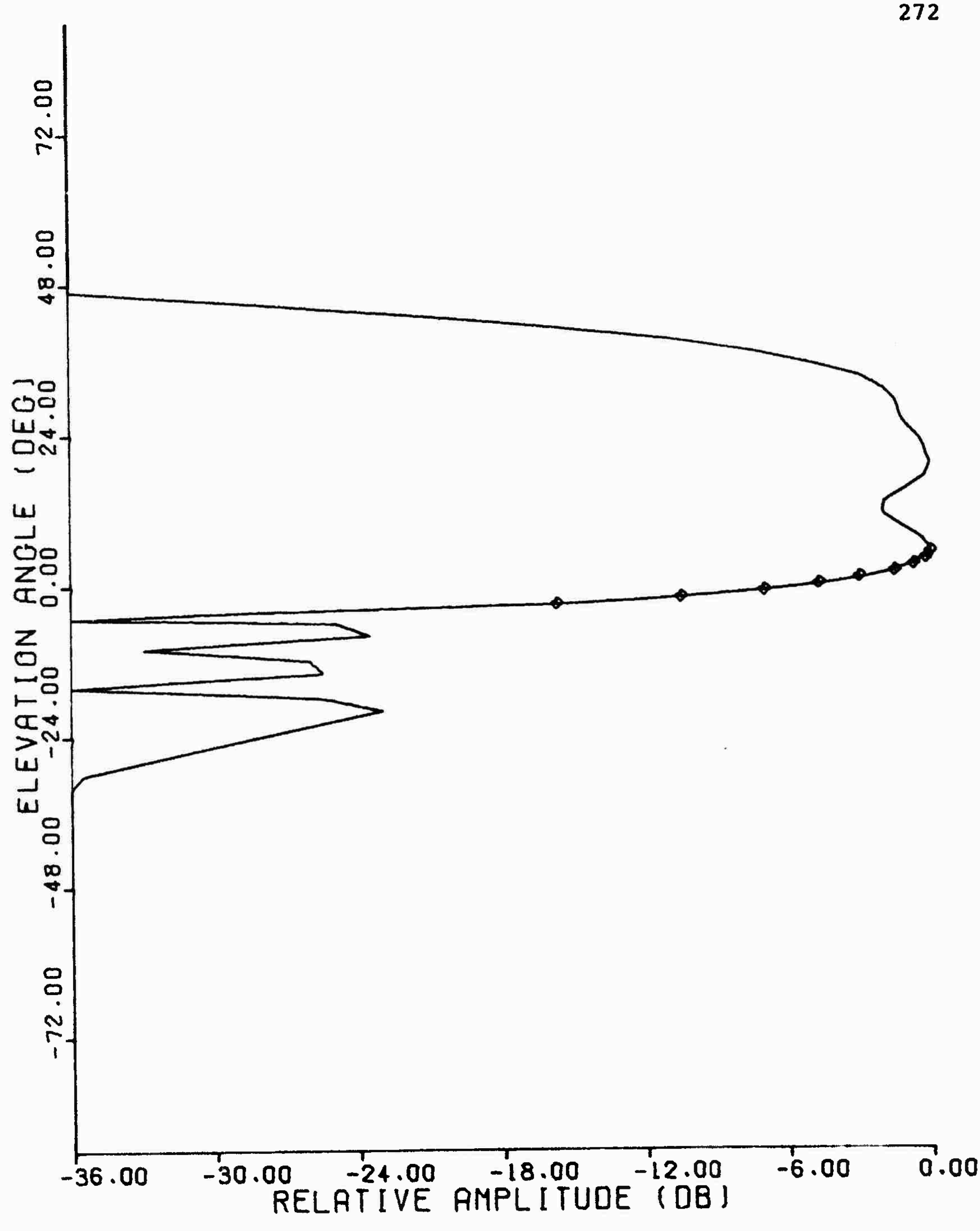

Figure C.37 1030 MHz Elevation Pattern, Westinghouse Antenna

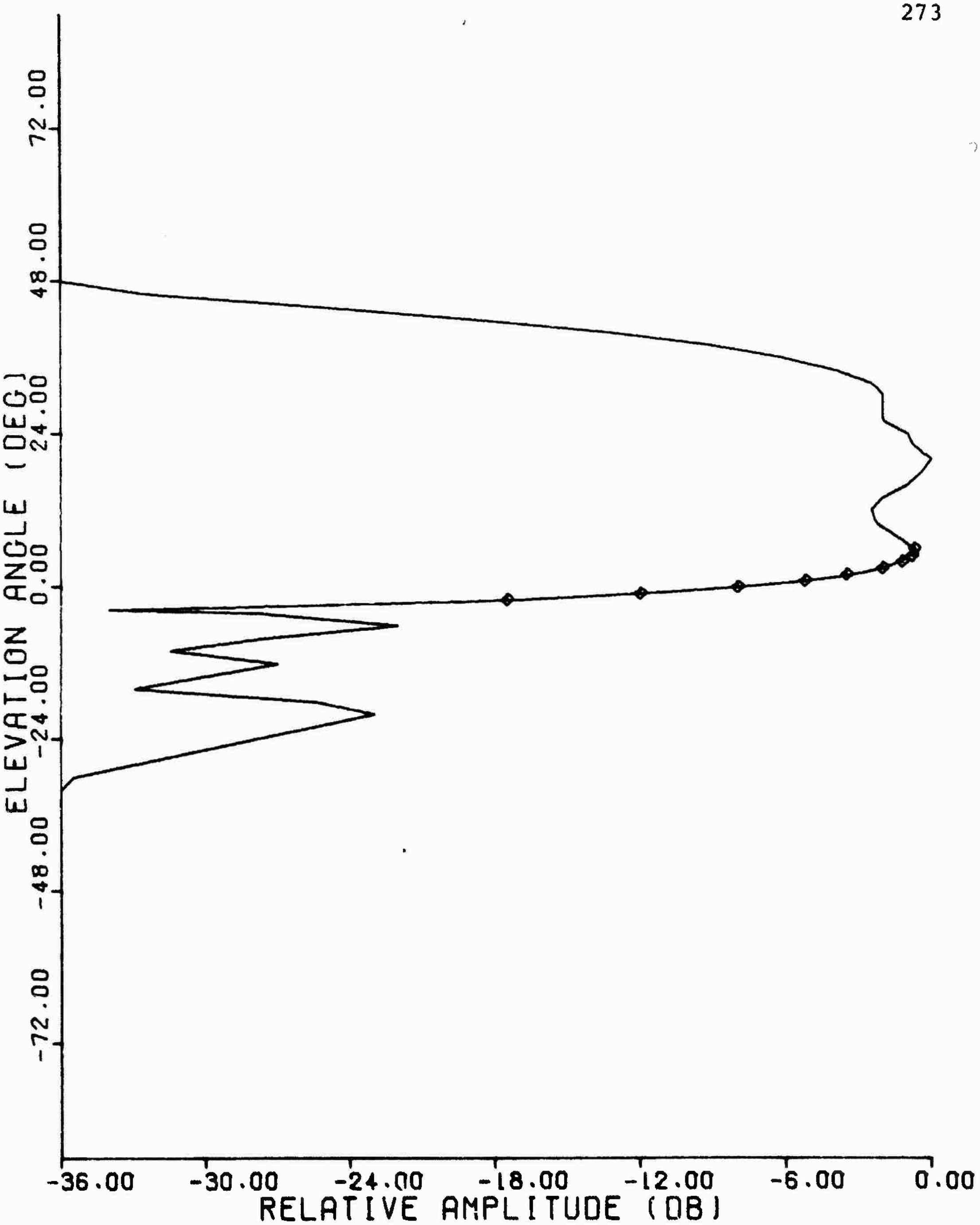

Figure C.38 1090 MHz Elevation Pattern, Westinghouse Antenna

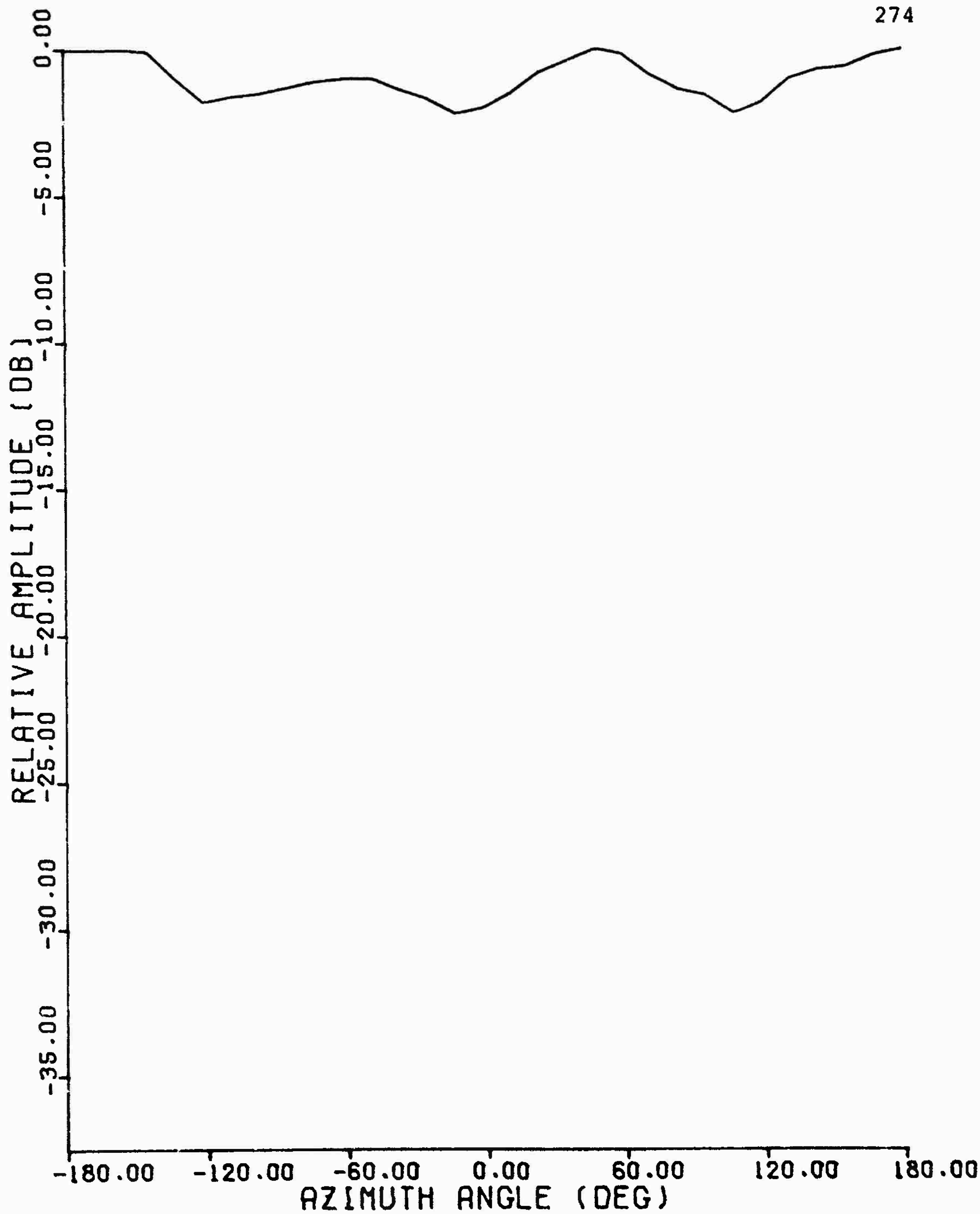

Figure C.39 1030 MHz Azimuth Pattern, Westinghouse Omni

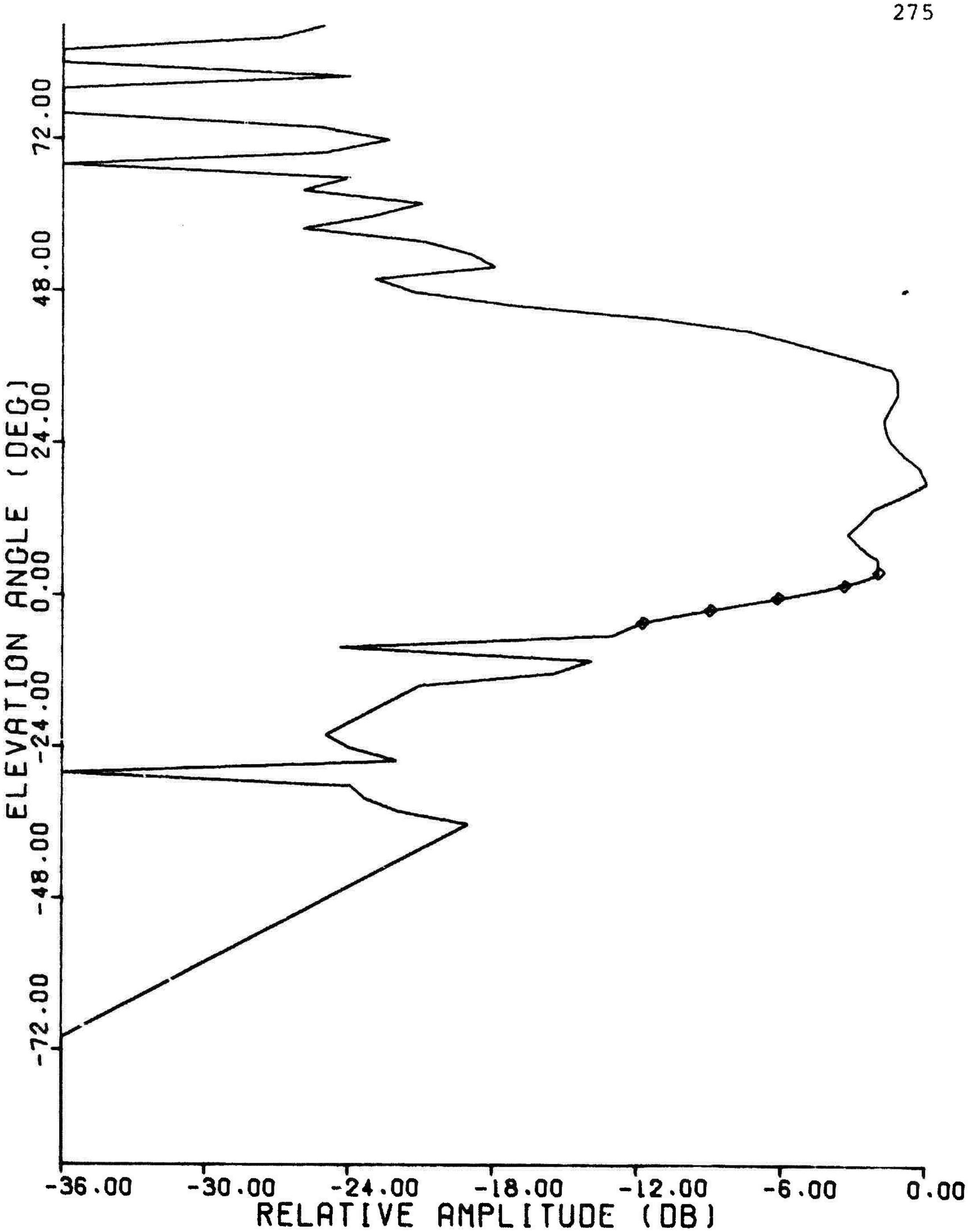

Figure C.40 1030 MHz Elevation Pattern, Westinghouse Omni

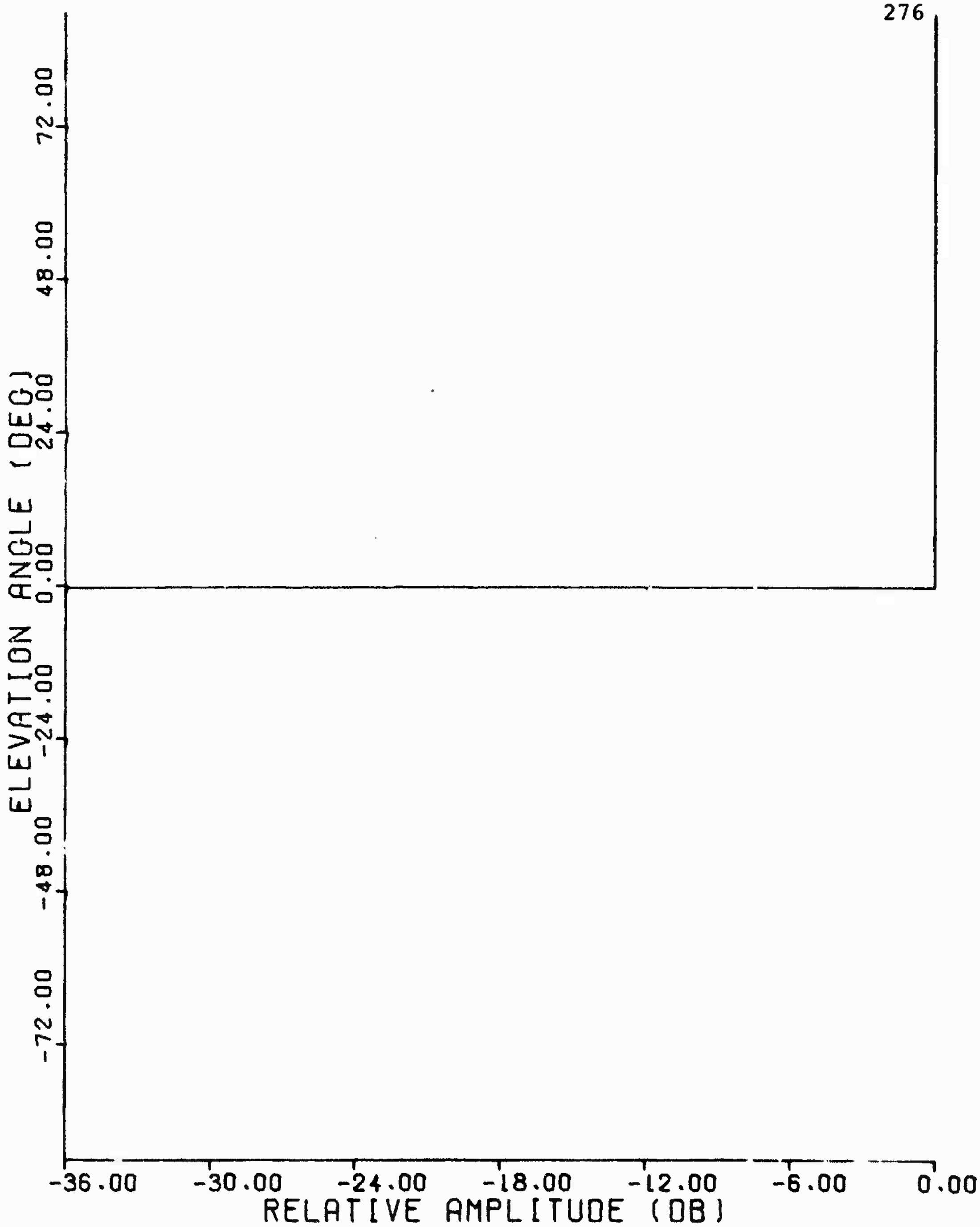

Figure C.41 1030/1090 MHz Elevation Pattern, Ideal Antenna

the horizon, but 36 dB attenuation below the horizon.

The next series of plots includes those used as inputs to the simple flat-earth model. The plots, therefore, are of the elevation patterns only. As previously, the patterns are grouped according to the manufacturer of the antenna, beginning with the standard FA-8043 and its omnis. There are thus four standard antenna plots, two for the directional patterns (uplink and downlink), and one for each of the two omnis (uplink only). Since RSLS is analyzed using the complex spherical-earth simulation model, the downlink patterns for the omnis are unnecessary as input to the simple model.

Figures C.42 through C.57 are obtained from the patterns used in the complex simulation model. The complex patterns are sampled at 0.1-degree intervals, and the resulting points used to initiate a least-squares fit according to the procedure of Appendix A as described in Chapter 4. The fit is performed over the interval from -5° to $+5^{\circ}$ to ensure an analytic expression that fits the empirical data closely, and also because most of the coverage gaps of interest lie in the region from the horizon to approximately 5° above it. The least-squares fit for these curves is made to satisfy the closed-form equation requirements of Chapter 4 rather than to provide an accurate means of interpolation. As for the curves plotted for the complex simulation model, the following curves involve the plotting of a square symbol for the point, and a line for the least-squares approximation.

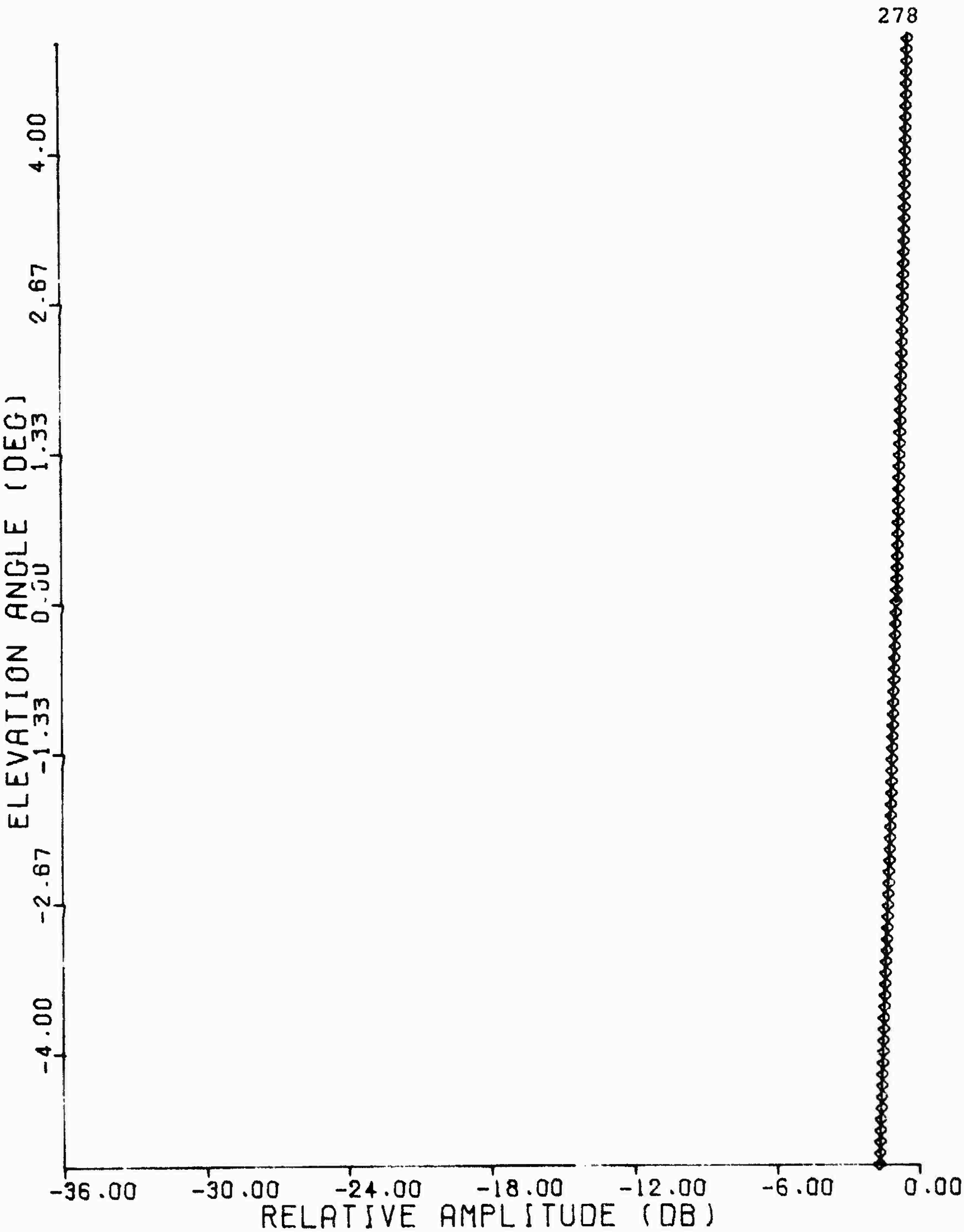

Figure C.42 Least-Squares Fit, 1030 MHz Elevation Pattern, FA-8043 Antenna

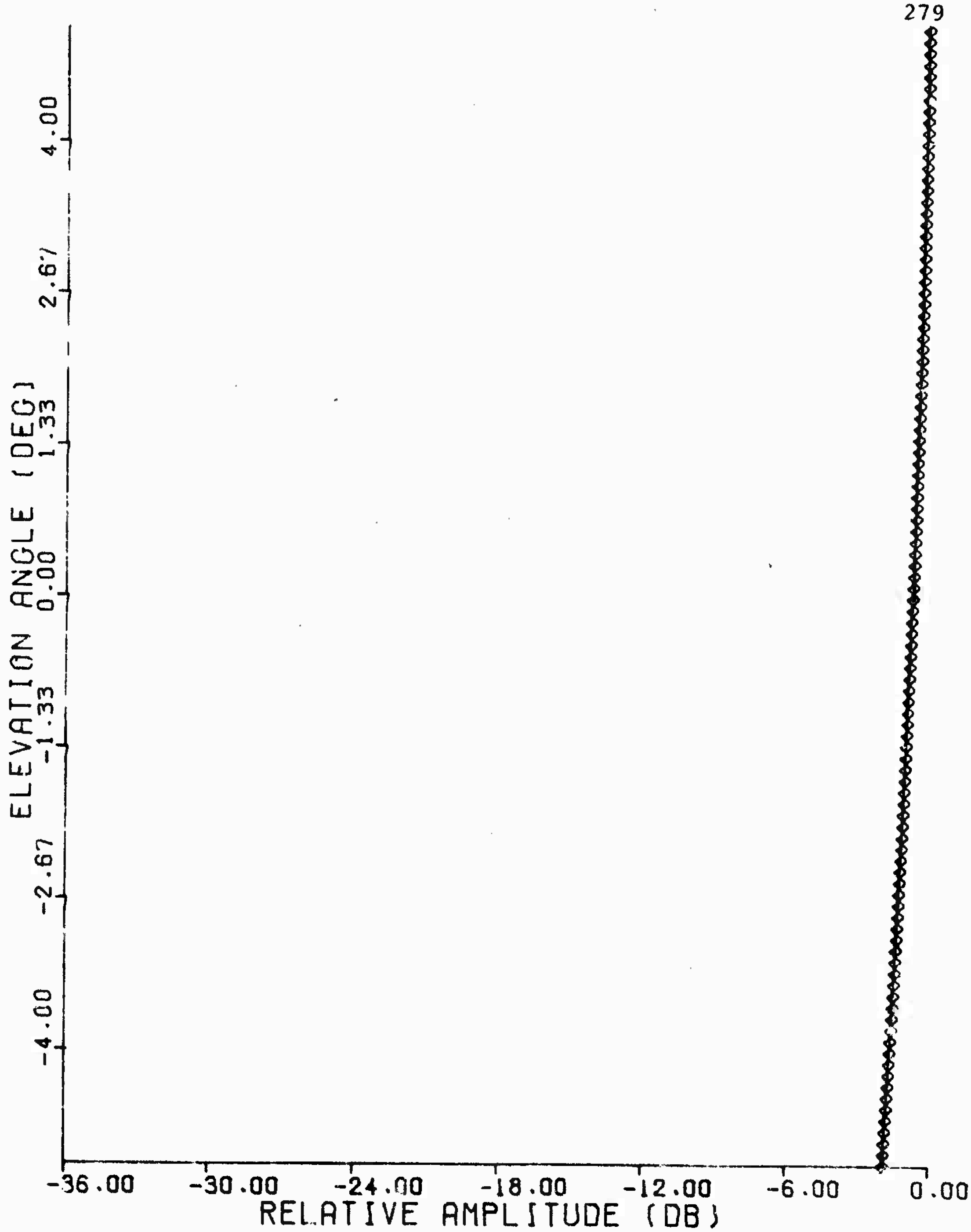

Figure C.43 Least-Squares Fit, 1090 MHz Elevation Pattern, FA-8043 Antenna

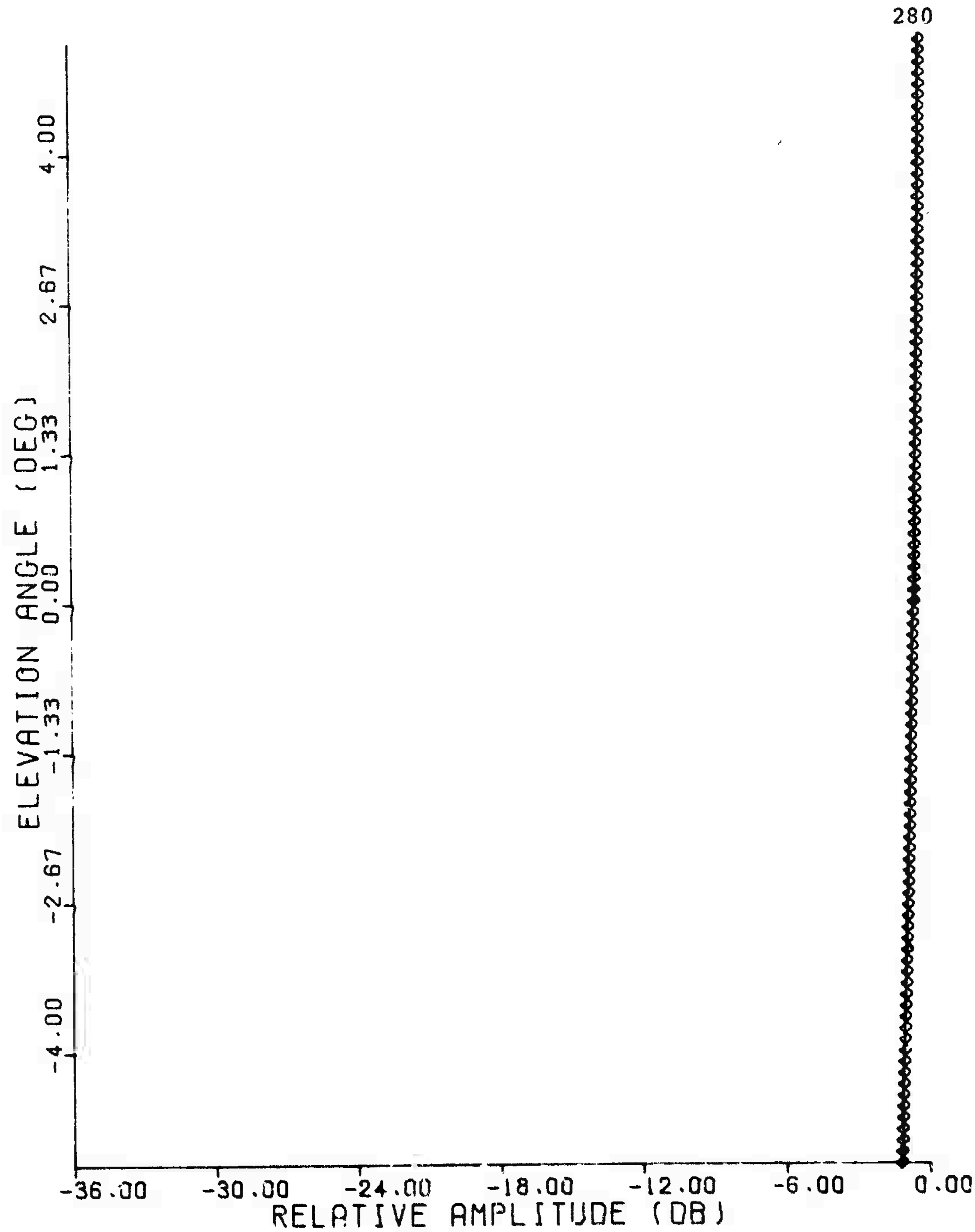

Figure C.44 Least-Squares Fit, 1030 MHz Elevation Pattern, FA-8044 Antenna

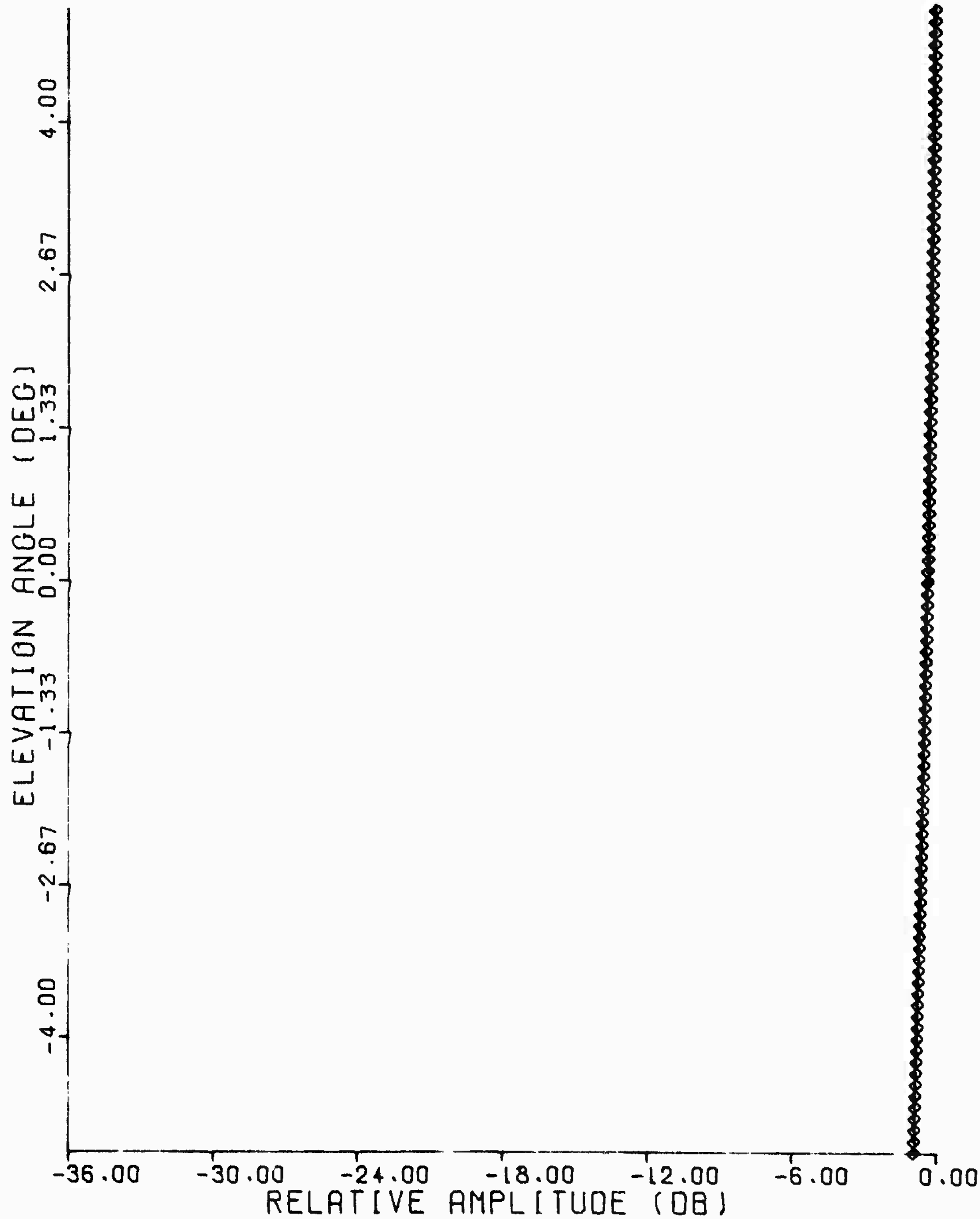

Figure C.45 Least-Squares Fit, 1030 MHz Elevation Pattern, FA-8045 Antenna

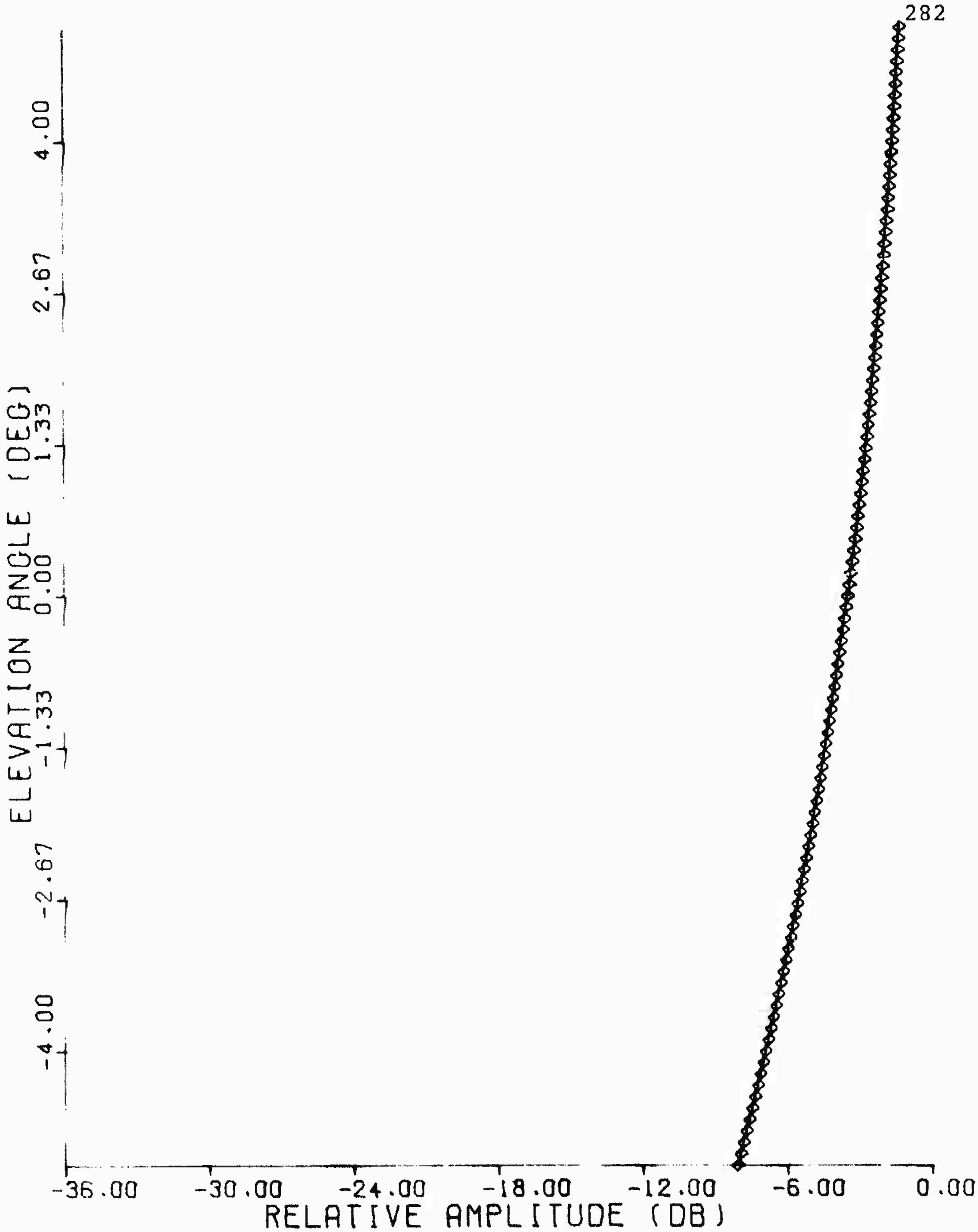

Figure C.46 Least-Squares Fit, 1030 MHz Elevation Pattern, Hazeltine Antenna

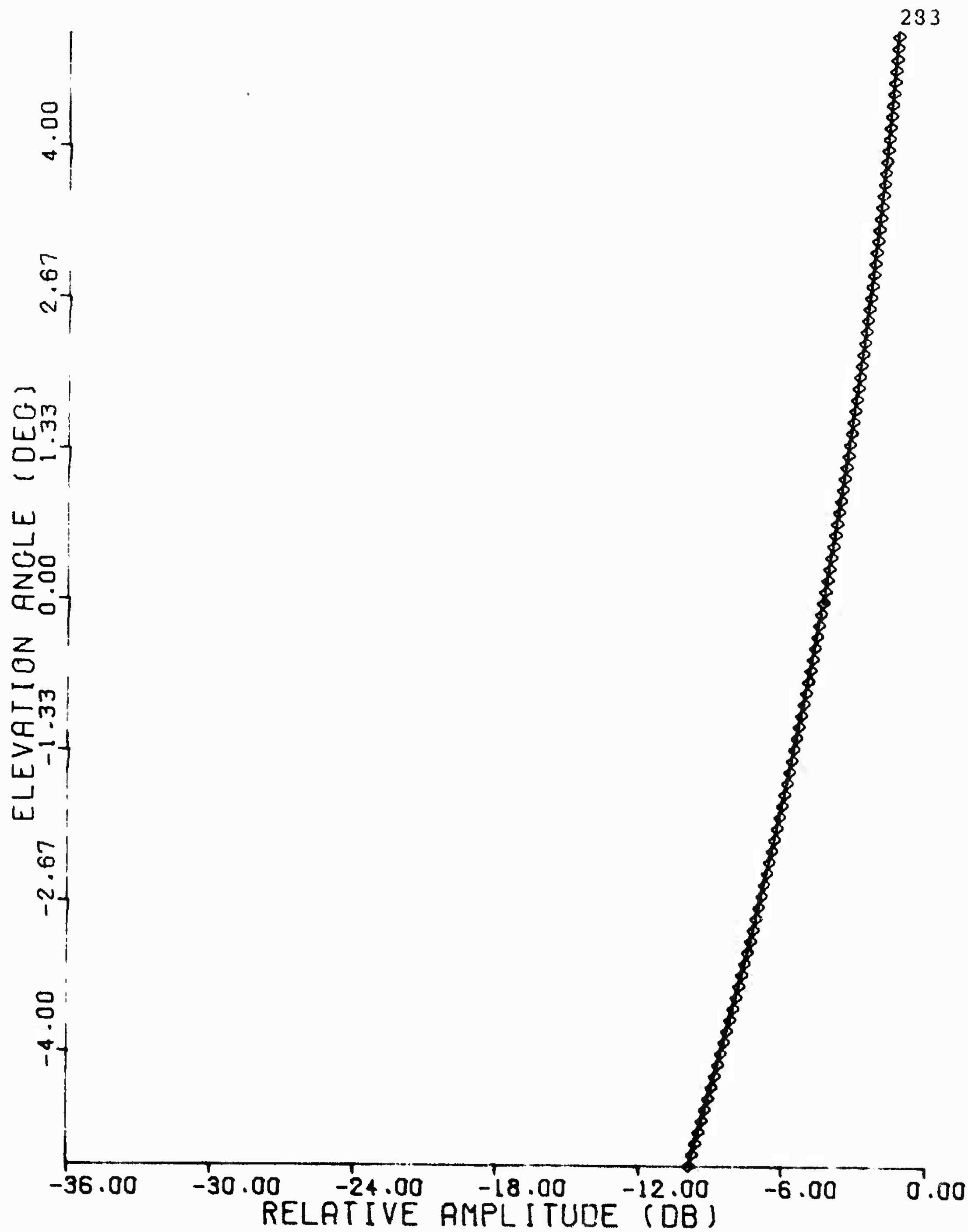

Figure C.47 Least-Squares Fit, 1090 MHz Elevation Pattern, Hazeltine Antenna

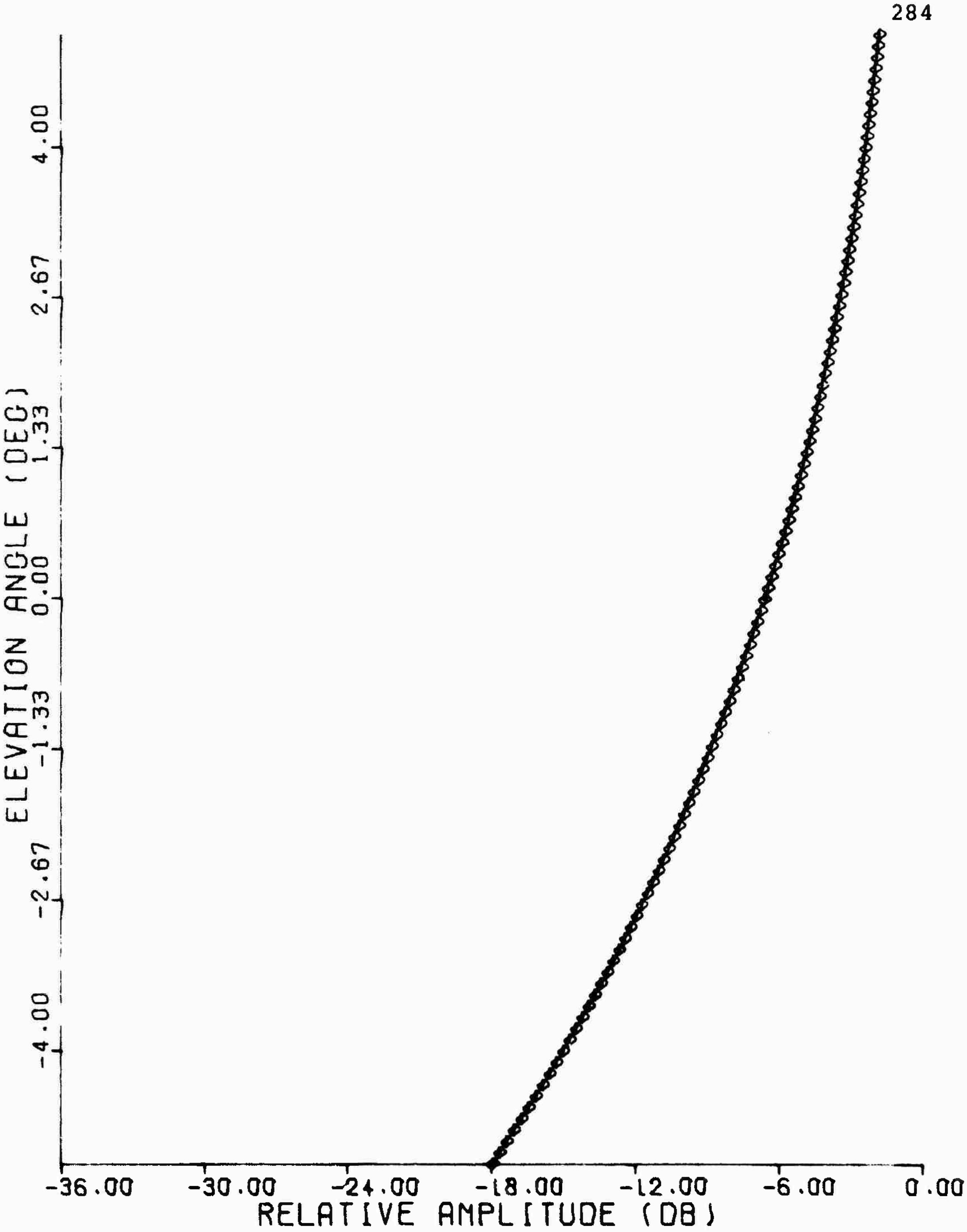

Figure C.48 Least-Squares Fit, 1030 MHz Elevation Pattern, Hazeltine Omni Antenna

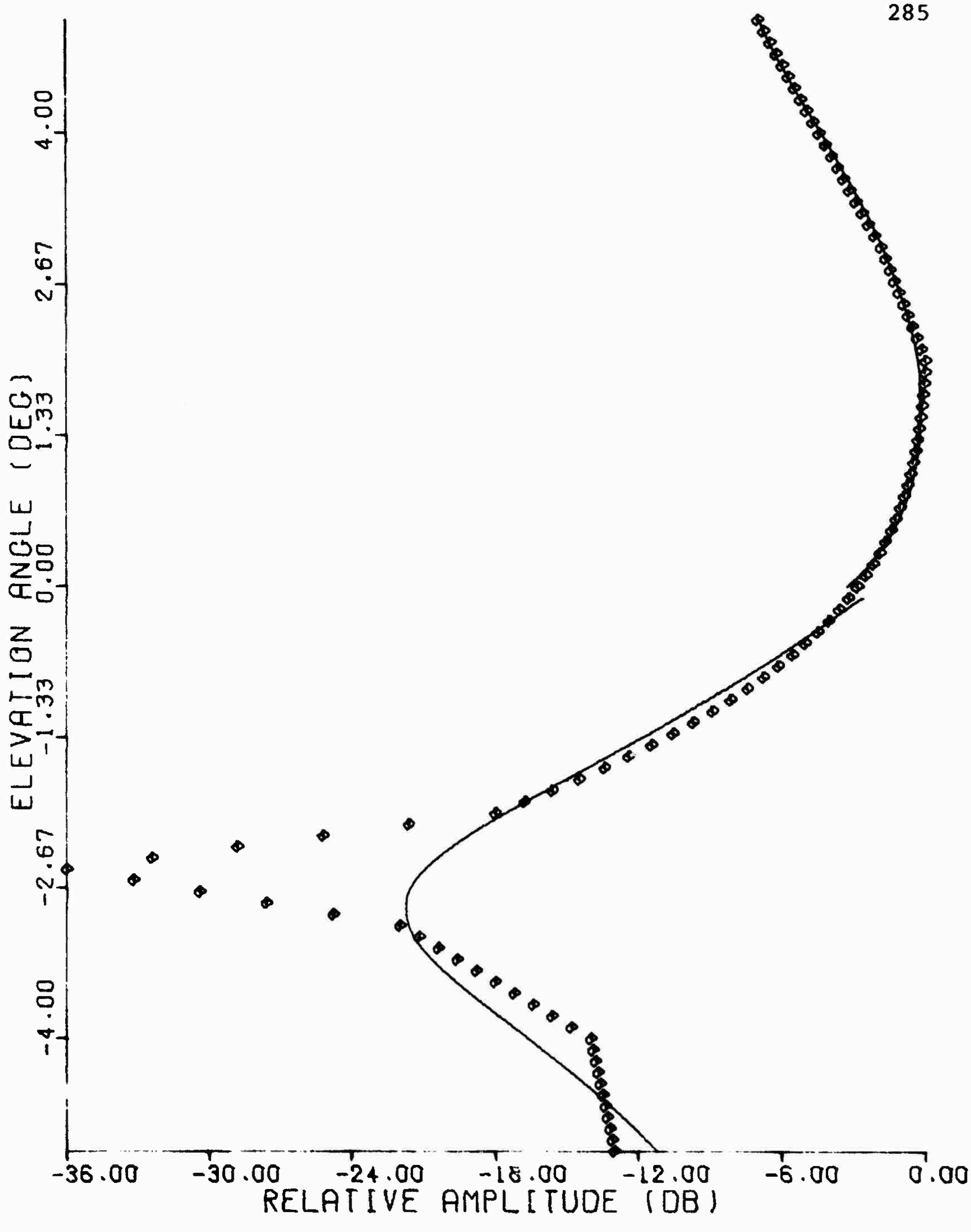

Figure C.49 Least-Squares Fit, 1030 MHz Elevation Pattern, ARSR Beacon Feed

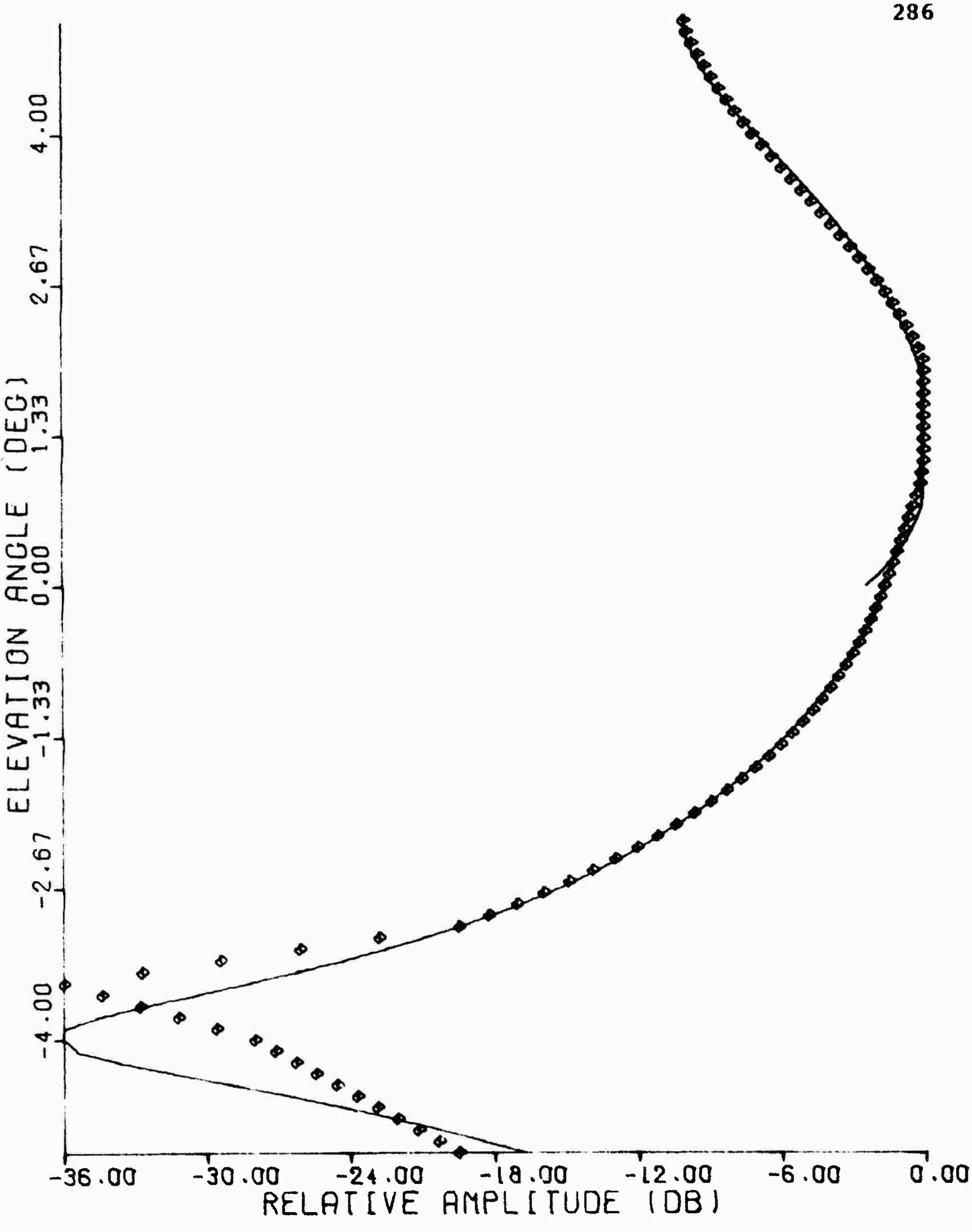

Figure C.50 Least-Squares Fit, 1090 MHz Elevation Pattern, ARSR Beacon Feed

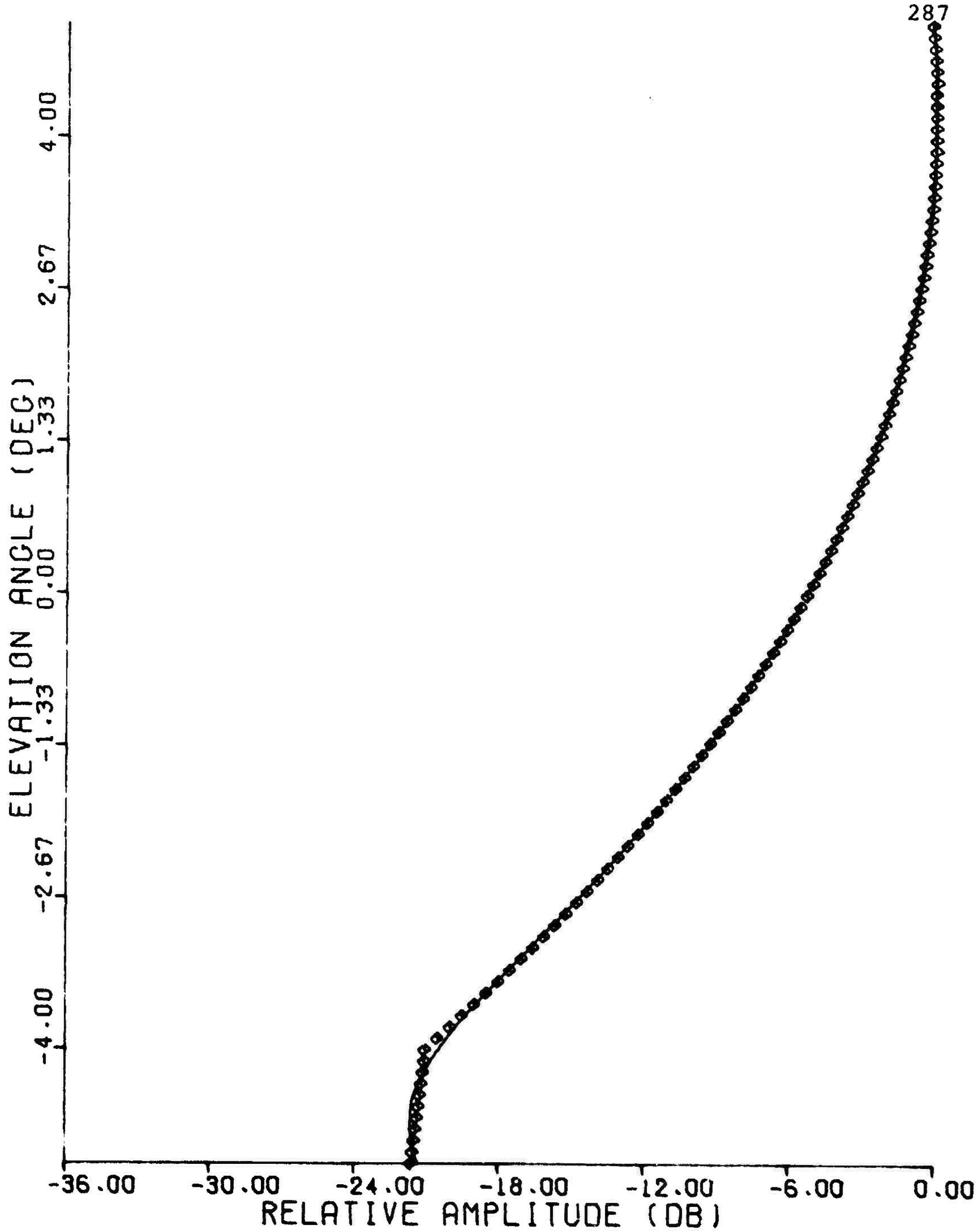

Figure C.51 Least-Squares Fit, 1030 MHz Elevation Pattern, ARSR Omni Antenna

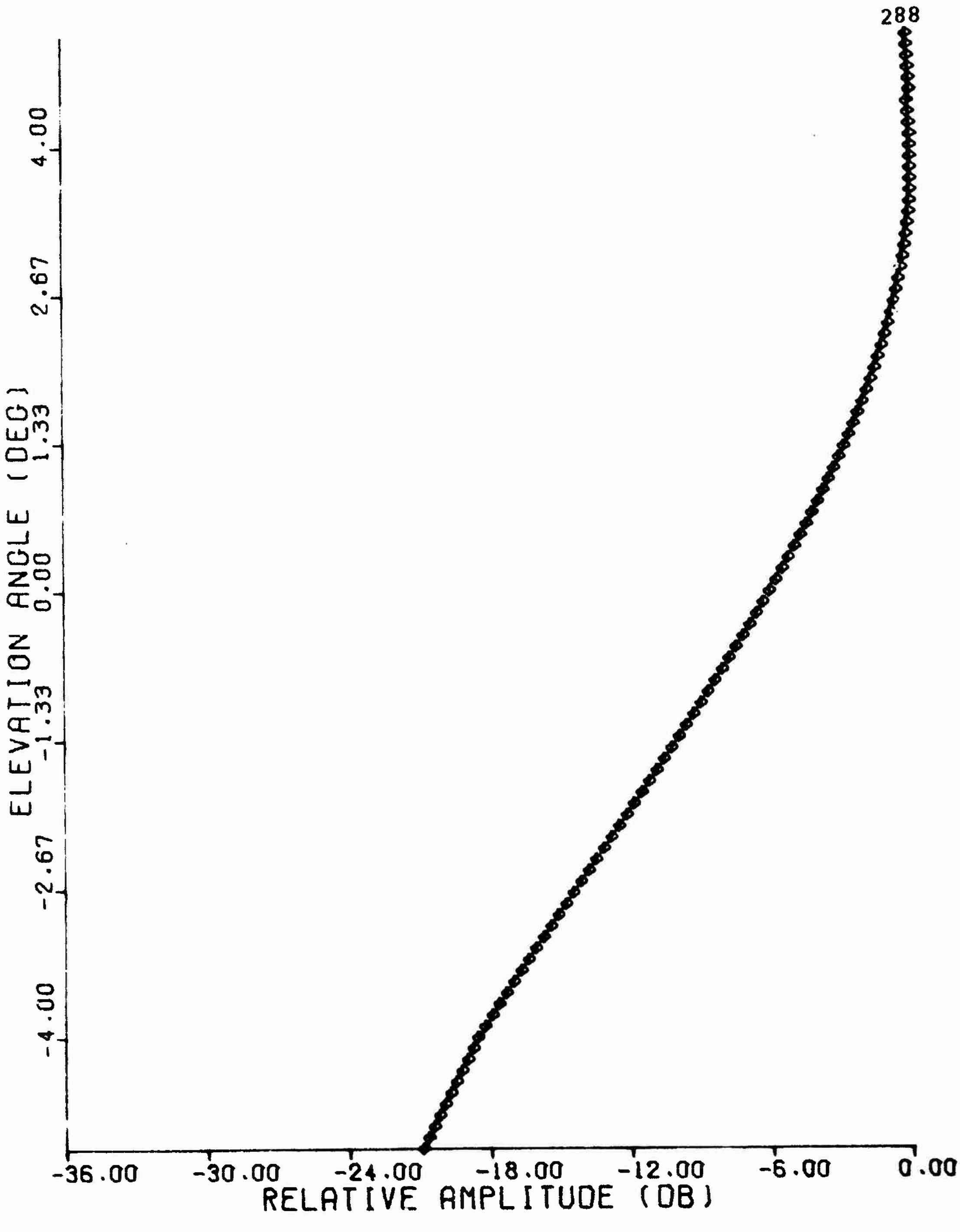

Figure C.52 Least-Squares Fit, 1030 MHz Elevation Pattern
TI Separate Rotator

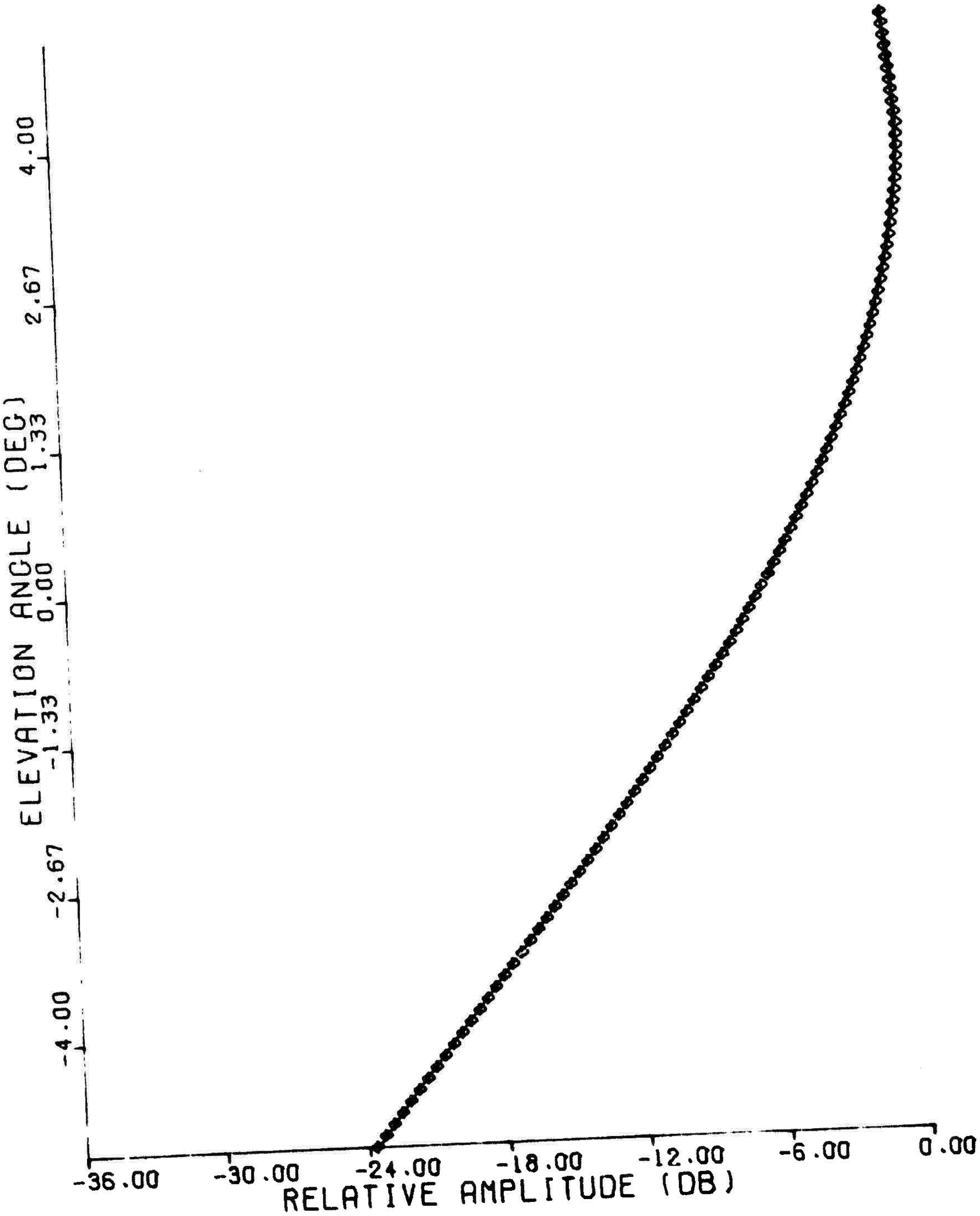

Figure C.53 Least-Squares Fit, 1090 MHz Elevation Pattern, TI Separate Rotator

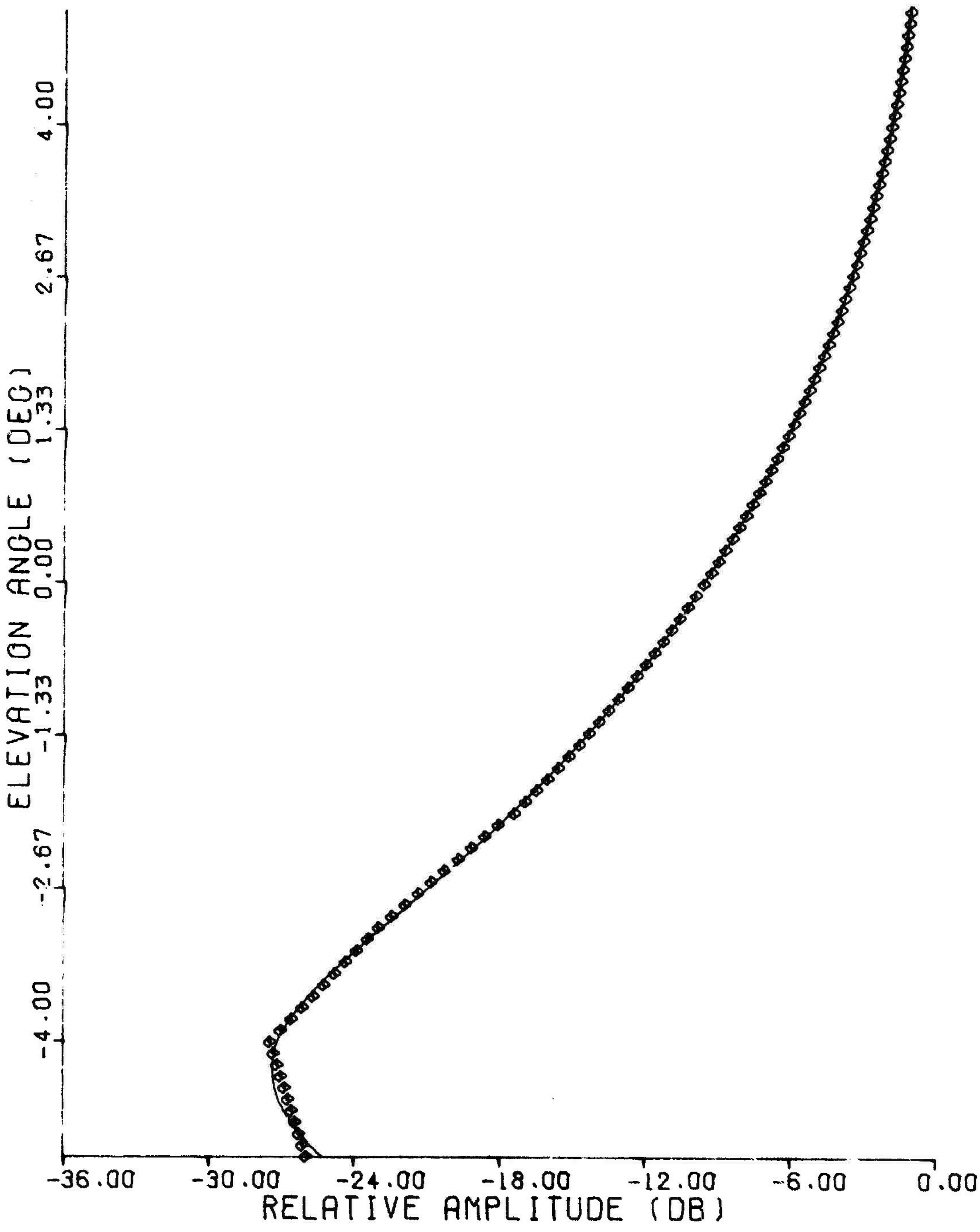

Figure C.54 Least-Squares Fit, 1030 MHz Elevation Pattern, TI Separate Rotator Omni

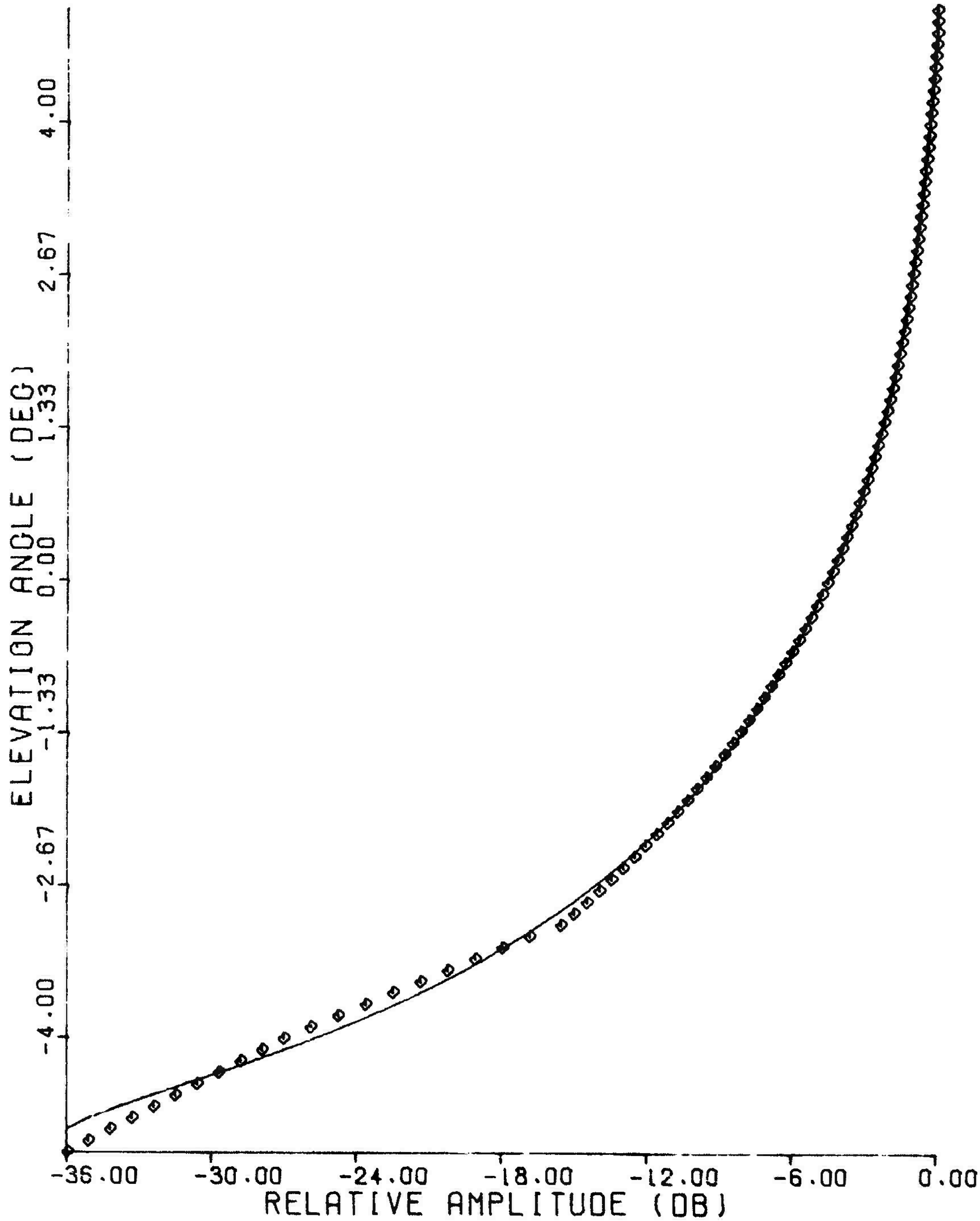

Figure C.55 Least-Squares Fit, 1030 MHz Elevation Pattern, Westinghouse Antenna

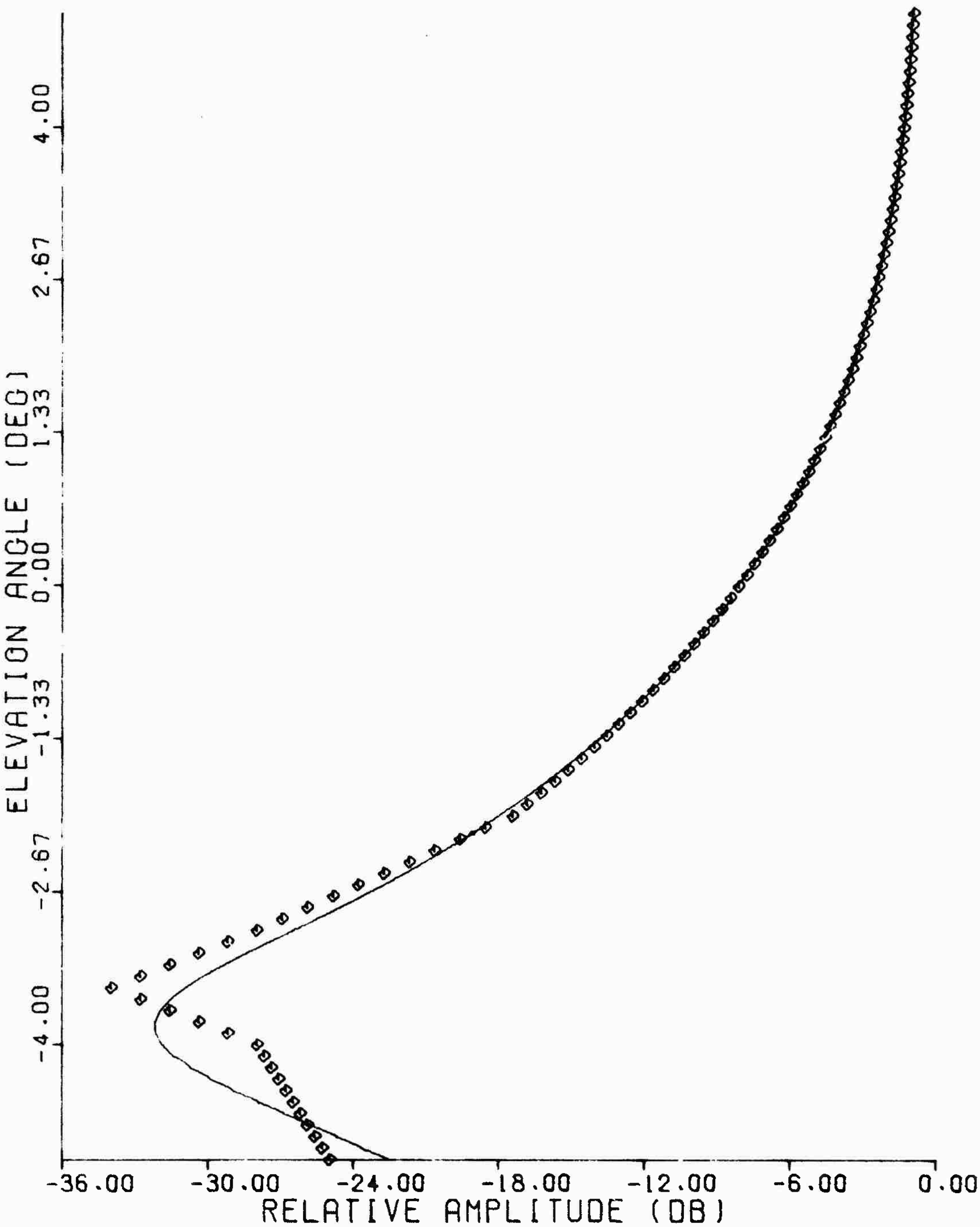

Figure C.56 Least-Squares Fit, 1090 MHz Elevation Pattern, Westinghouse Antenna

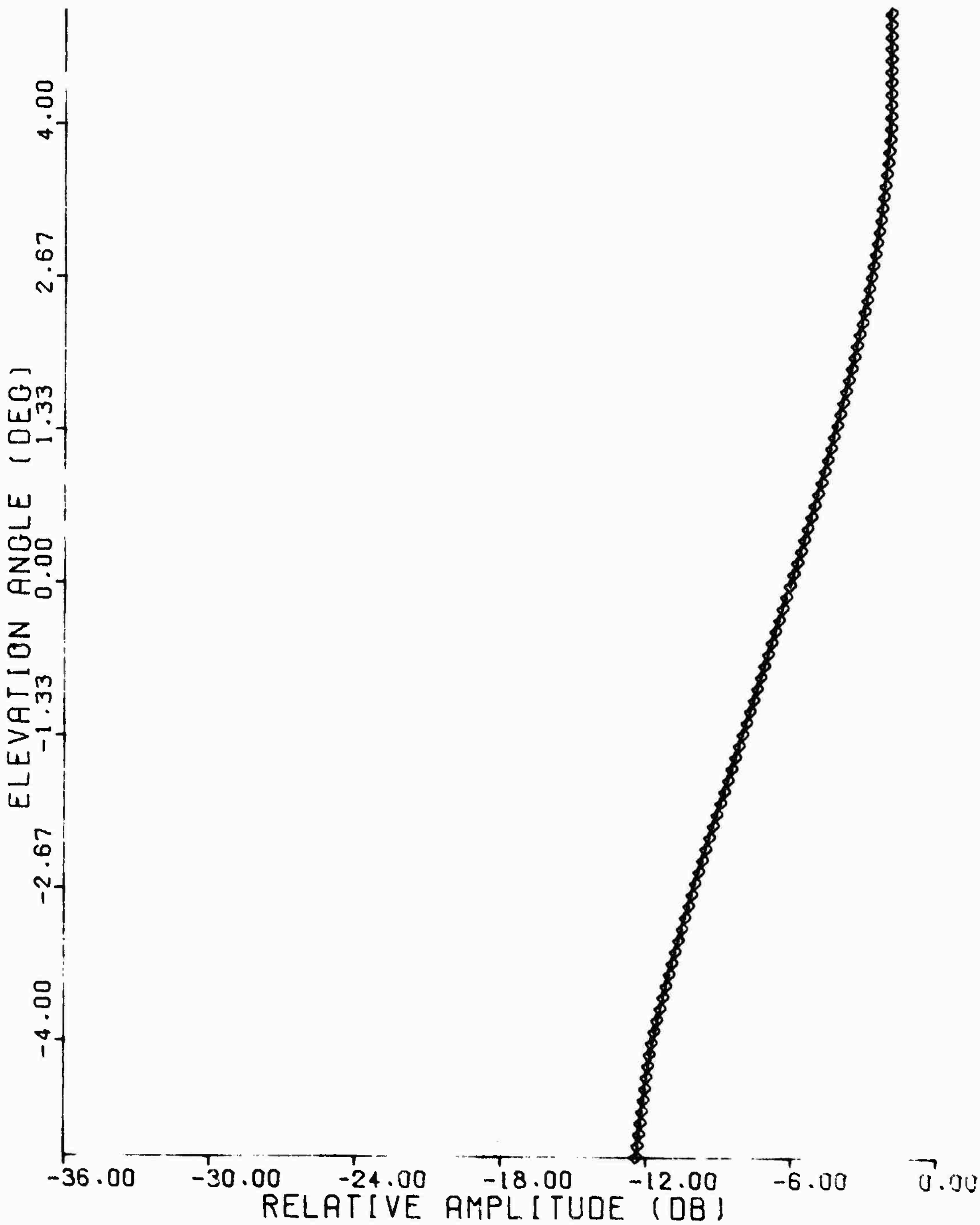

Figure C.57 Least-Squares Fit, 1030 MHz Elevation Pattern, Westinghouse Omni Antenna

REFERENCES

1. Report of Department of Transportation Air Traffic Control Advisory Committee, Vols. 1 and 2, U.S. Government Printing Office, Washington, December 1969.

2. "Discrete Address Beacon System, Phase II Engineering Requirements", Massachusetts Institute of Technology Lincoln Laboratory, Lincoln Manual 116, FAA-ER-240, November 1, 1974.

3. "National Improvement Program for ATCRBS", FAA Order 1000.30, Federal Aviation Administration, Washington, December 1973.

4. Shaw, K., "ATCRBS Performance Prediction for the John F. Kennedy Terminal", Report of the Department of Transportation Air Traffic Control Advisory Committee, Vol. 2, pp. 253-60, December 1969.

5. Kleiman, L.A. and M.J. Miner, "SOAR (Simulation of the Air Traffic Control Radar Beacon System): Functional Description and Application to Investigation of a Discrete Address Beacon System", Report No. DOT-TSC-FAA-74-23, U.S. Department of Transportation, August 1974.

6. Jones, S.R., "Evaluation of ATCRBS Performance in an Interference Environment", MITRE Technical Report MTR-6239, August 4, 1972.

7. Cameron, A.G. and D.H. Pruslin, "Empirical Assessment of ATCRBS", Project Report ATC-16, MIT Lincoln Laboratory, FAA-RD-73-139, October 31, 1973.

8. Cameron, A.G., "Further Studies of ATCRBS Based on ARTS-III Derived Data", Project Report ATC-38, MIT Lincoln Laboratory, FAA-RD-74-145, December 13, 1974.

9. "Quarterly Technical Summary, Development of a Discrete Address Beacon System", MIT Lincoln Laboratory, FAA-RD-75-4, January 1, 1975.

10. Schlieckert, G.J., "An Analysis of Aircraft L-Band Beacon Antenna Patterns", Project Report ATC-37, MIT Lincoln Laboratory, FAA-RD-74-144, January 15, 1975.

11. "Quarterly Technical Summary, ATC Surveillance/Communication Analysis and Planning", MIT Lincoln Laboratory, FAA-RD-74-105, June 1, 1974.

12. Zatkalik, J. and D. Sengupta, "A Preliminary Study of the Performance of Some Improved ATCRBS Antennas", Report No. 012539-502-M, University of Michigan Radiation Laboratory, Ann Arbor, February 7, 1974.

13. Zatkalik, J., D.L. Sengupta, and C-T Tai, "SLS Mode Performance of ATCRBS with Various Antennas", Report No. 012539-1-T, University of Michigan Radiation Laboratory, Ann Arbor, July 1974.

14. Drouilhet, P.R., Jr., "The Development of the ATC Radar Beacon System: Past, Present, and Future", IEEE Transactions on Communications, Vol. COM-21, No. 5, pp. 408-21, May 1973.

15. Ashley, A., C.F. Phillips, and A.A. Simohunas, "System Capability of Air Traffic Control Radar Beacon System", Report of the Department of Transportation Air Traffic Control Advisory Committee Vol. 2, pp. 287-305, December 1969.

16. "U.S. National Standard for the Mark X (SIF) Air Traffic Control Radar Beacon System (ATCRBS) Characteristics", FAA Order 1010.15A, Federal Aviation Administration, Washington, March 8, 1971.

17. Kerr, D.E. (ed.), Propagation of Short Radio Waves, McGraw-Hill Book Company, Inc., New York, 1951.

18. Reed, H.R. and C.M. Russell, Ultra High Frequency Propagation, Boston Technical Publishers, Inc., Lexington, Massachusetts, 1964.

19. Reintjes, J.F. and G.T. Coate, Principles of Radar, McGraw-Hill Book Company, Inc., New York, 1952.

20. Durlach, N.I., "Influence of the Earth's Surface on Radar", MIT Lincoln Laboratory Technical Report 373, January 18, 1965.

21. Durlach, N.I., A.M. Carpenter, and M.A. Herlin, "Curved-Earth Computations for Airborne Early Warning and Control", MIT Lincoln Laboratory Technical Report 194, January 13, 1959.

22. Hildebrand, F.B., Introduction to Numerical Analysis, McGraw-Hill Book Company, Inc., New York 1956.

23. "Preliminary Instruction Book, ATCBI SLS Omnidirectional Antenna Group", Report No. TI6360.8, Contract DOT-FA69-WA-2139, Radiation Systems, Inc., McLean, Virginia, May 19, 1969.

24. "Factory Test Data, ATCRBS Antenna Development Kit", Report 6237, Contract DOT-TSC-598, Hazeltine Corporation, Greenlawn, New York, April 24, 1974.

25. "ATCRBS Improvement Program, Test Data for ARSR-2 Modification Kit", Texas Instruments Incorporated, Dallas, Texas, Contract DOT-TSC-602 for Transportation Systems Center, Cambridge, Massachusetts, April 16, 1974.

26. "ATCRBS Improvement Program, Test Data for Omnidirectional Antenna (ARSR-2 Modification)", Texas Instruments Incorporated, Dallas, Texas, Contract DOT-TSC-602 for Transportation Systems Center, Cambridge, Massachusetts, April 15, 1974.

27. "ATCRBS Improvement Program, Test Data for the ATCRBS Reflector Antenna", Texas Instruments Incorporated, Dallas, Texas, Contract DOT-TSC-602 for Transportation Systems Center, Cambridge, Massachusetts, April 1974.

28. "ATCRBS Improvement Program, Test Data for Omnidirectional Antenna (Separate Rotator Installation)", Texas Instruments Incorporated, Dallas, Texas, Contract DOT-TSC-602 for Transportation Systems Center, Cambridge, Massachusetts, May 20, 1974.

29. "ATCRBS Array Antenna, Factory Test Plan & Test Data", Contract DOT-TSC-600, Westinghouse Electric Corporation, Baltimore, Maryland.

☆U.S. GOVERNMENT PRINTING OFFICE: 1976—A-0291/146